

Copyright Warning & Restrictions

The copyright law of the United States (Title 17, United States Code) governs the making of photocopies or other reproductions of copyrighted material.

Under certain conditions specified in the law, libraries and archives are authorized to furnish a photocopy or other reproduction. One of these specified conditions is that the photocopy or reproduction is not to be “used for any purpose other than private study, scholarship, or research.” If a user makes a request for, or later uses, a photocopy or reproduction for purposes in excess of “fair use” that user may be liable for copyright infringement,

This institution reserves the right to refuse to accept a copying order if, in its judgment, fulfillment of the order would involve violation of copyright law.

Please Note: The author retains the copyright while the New Jersey Institute of Technology reserves the right to distribute this thesis or dissertation

Printing note: If you do not wish to print this page, then select “Pages from: first page # to: last page #” on the print dialog screen

The Van Houten library has removed some of the personal information and all signatures from the approval page and biographical sketches of theses and dissertations in order to protect the identity of NJIT graduates and faculty.

ABSTRACT

PHYSICAL AND GEOTECHNICAL CHARACTERIZATION OF WATER TREATMENT PLANT RESIDUALS

by
Swamy C. Basim

The study of Water Treatment Plant (WTP) residuals is of recent origin and very little information is available in literature regarding these residuals. These waste materials have high solids contents, even in the mechanically dewatered condition, making it difficult to handle. These, along with stringent environmental regulations have forced the water utilities to look for new disposal options for these residuals. For this purpose as well as for evaluating suitable options for the beneficial reuse of residuals, it is essential to characterize WTP residuals.

As the dewatered residuals are plastic, the researcher may be prompted to treat these materials as clays. But, unlike clays, these residuals lose all their plasticity and behave like granular materials upon drying and weathering. Furthermore, available literature indicates that the compaction characteristics for these materials are different depending upon whether the test is carried out from the "wet to dry" condition or from "dry to wet" condition. Therefore, WTP residuals are different from clays, due to the presence of organics, and high concentrations of chemicals. It is postulated that the above changes in behavior of residuals are brought about by the change in structure, resulting in increased cementation and increase in grain size. This reinforces the need for characterizing these materials.

In this research, geotechnical tests were performed on six residual samples and geoenvironmental tests were carried out three on residuals to determine the causes and mechanisms responsible for the changes in behavior of residuals. Grain size analysis conducted by sieve, hydrometer analyses and particle size analyzer indicated that particle sizes increased substantially upon weathering and drying. Electron micrographs, elemental maps, X-Ray diffraction and X-Ray Fluorescence spectra were obtained. The results indicated that the particle size increase could be attributed to aggregation due to organic matter and cementation due to metal oxides such as calcium oxide. It was also observed that no leaching of metals occurred due to drying, freeze, and thaw effects.

**PHYSICAL AND GEOTECHNICAL CHARACTERIZATION OF WATER
TREATMENT PLANT RESIDUALS**

by
Swamy C. Basim

**A Dissertation
Submitted to the Faculty of
New Jersey Institute of technology
In partial Fulfillment of the Requirements for the Degree of
Doctor of Philosophy**

Department of Civil and Environmental Engineering

May 1999

Copyright© by Swamy C. Basim

ALL RIGHTS RESERVED

APPROVAL PAGE

**PHYSICAL AND GEOTECHNICAL CHARACTERIZATION OF WATER
TREATMENT PLANT RESIDUALS**

Swamy C. Basim

Dr. Dorairaja Raghu, Thesis Advisor Date
Professor of Civil and Environmental Engineering,
New Jersey Institute of Technology, Newark, NJ.

Dr. William Spillers, Committee Member Date
Professor of Civil and Environmental Engineering,
New Jersey Institute of Technology, Newark, NJ.

Dr. Raj P. Khera, Committee Member Date
Professor of Civil and Environmental Engineering,
New Jersey Institute of Technology, Newark, NJ.

Dr. Hsin-Neng Hsieh, Committee Member Date
Professor of Civil and Environmental Engineering,
New Jersey Institute of Technology, Newark, NJ.

Dr. Nuggehalli M. Ravindra, Committee Member Date
Professor of Physics,
New Jersey Institute of Technology, Newark, NJ.

BIOGRAPHICAL SKETCH

Author: Swamy C. Basim
Degree: Doctor of Philosophy
Date: May 1999

Undergraduate and Graduate Education:

- Doctor of Philosophy in Civil Engineering
New Jersey Institute of Technology, Newark, NJ, 1999.
- Master of Science Civil Engineering
Bangalore University, Bangalore, India 1981.
- Bachelor of Science in Civil Engineering
University of Mysore, Mysore, India 1975.

Major: Civil Engineering

Presentations and Publications:

1. Raghu, D., Hsieh, H.N., Basim, S.C., and Morgan, M., "Physical Characterization of Water Treatment Plant Residual and Top Soil Mixtures" *STP 1275-ASTM Publication code Number (PCN); 04-012750-38*. ASTM West Conshohocken, PA., 1997.
2. Raghu, D., Hsieh, H.N., Basim, S.C., and Tian, P., "Effects of Aging on the Properties of Water Treatment Plant Residuals"— *Proceedings of WEF/AWWA Joint Residuals/Biosolids conference*, Kansas City, MS., July 23-26, 1995.
3. Raghu, D. and Basim, S.C., "Use of Cupola Slag as Fill Material"— *Proceedings of the 10th International Conference on Solid Waste Management and Secondary Materials* Philadelphia, PA., Nov 1994.
4. Raj, P.P and Basim, S.C., "Stress-Strain Modulus of Compacted Silt"— *Proceedings of Indian Geotechnical Conference Vol. 1*, Roorkee, India, Dec 16-18 1995.

To the Memory of
My Brother Shri. B.G. Murthy and his Wife Smt. Pratibha
Who Reached the Heavenly Abode on December 10, 1995

ACKNOWLEDGEMENT

This research became possible only due to the constant inspiration and guidance of my advisor Dr Dorairaja Raghu. To be more precise, I got this wonderful opportunity to join NJIT and work on my Ph.D., only because of his earnest efforts despite many odds. I take this opportunity to record my sincere thanks and appreciation for his intelligible and excellent guidance in my research work.

All my committee members deserve my appreciation. Dr. Raj P. Khera encouraged me to expand my ken of Soil Behavior and other related subjects. His meticulous attention to minute details inspired me to do work as perfectly as possible to perfect my laboratory skills. I am highly thankful to him.

Ever since my association with NJIT, Dr. William Spillers was very considerate to me for all of my requests both academic and otherwise. I am very much grateful to him.

My acquaintance with Dr Hsieh dates back to January 1994 when I was working for AWWA sponsored project. I learned a great deal of environmental engineering from him. Also, during the course of this research work he provided useful comments. He was kind enough to extend my assistantship as my research took twice the time it should have taken. I will be failing in my duties if I do not acknowledge his help.

Despite his hectic schedule, Dr. Ravindra spent many hours with me and helped me in analyzing micrographs. I thank him profusely.

During this research, I have spent more than two years exclusively to study the fabric and microstructure of WTP residuals using different types of optical microscopes and environmental scanning electron microscope. Dr. Sudhi Mukherjee, Research Professor in Civil and Environmental engineering, sat with me months together ignoring

his priorities in front of microscopes to gather good images. I place on record my sincere thanks and appreciation of his help and kindness.

In deed I had a very good company and a great opportunity to work with Dr. H.K. Sehgal, Professor of Physics, Indian Institute of Technology, New-Delhi, India on the microscope during summer of 1997. I learned from him the physics behind scanning electron microscope to some depth. I sincerely acknowledge his help.

My friends Mr.Wiwat Kamolpornwijit, Ms Bumrongjaroen Walairat and Mr. Manaskon Rachakornkij (all soon to be doctors) happily extended their help while I was working with XRD, XRF and EDX. My friend Mr. Chandrakanth Patel, Laboratory Chemist of Geo-environmental laboratory, provided me unlimited entry to his laboratory. Mr. Clint Brockaway, helped me during TGA studies. Mr. Paras Trivedi offered me his constructive suggestions about my micrographs.

I thank Prof. Daunheimer; chairman, department of civil and environmental engineering, for all the support rendered to me during my stay at NJIT. My thanks are also due to Dr. Ronald Kane and Ms. Annette Damiano of Graduate Studies Office for helping me with format and corrections for this dissertation report.

I thank the authorities of Jersey City Department of Water, Jersey City, United Water Company, Hackensack, North Jersey District Water supply Commission, Wanaque, NJ, Pennsylvania American Water Company, Hershey, Pa, Sturgeon Point Water Treatment Plant, Derby, NY, Niagara River Water Treatment Plant, Tonawanda, NY and the Erie County Water Authority, Buffalo, NY, for providing me with residuals for this study.

Outside NJIT campus, I enjoyed unlimited help of all kinds and encouragement from my friends, Mr. Kartik Naik, Mr. David Cohen, Mr. Prabhakar, Dr. Mamatha Prabhakar, Dr. Nidugalle Gowda, Ms. Latha Gowda Dr. P. K. Swain, Mr. Ravi K. Iyengar, and many more. I take this opportunity to thank everyone.

Rather it is highly ineffable to explain the sacrifices made by my parents Sri. Basim Thimma Reddy and Smt. Kamamma to impart me with modern scientific education with moral and philosophical outlook. They are the constant source of inspiration and encouragement. I take this opportunity to place on record my sincere gratitude to them.

TABLE OF CONTENTS

Chapter	Page
1 INTRODUCTION, REVIEW OF LITERATURE AND PROPOSED RESEARCH	
1.1 Introduction.....	1
1.2 Composition and Structure of WTP Residuals.....	2
1.2.1 Water Phase of WTP Residuals.....	2
1.2.2 Solid Phase of the Residuals.....	4
1.3 Characteristics of Water Treatment Plant Residuals.....	7
1.3.1 Prior Studies Related to WTP Residual Characteristics	7
1.4 Prior Work Done at New Jersey Institute of Technology (NJIT), Newark, NJ.....	13
1.4.1 particle Size Distribution of Solids	13
1.4.2 Liquid Limit and Plastic Limit Tests.....	13
1.4.3 Specific Gravity of Solids.....	14
1.4.4 Compaction Tests	15
1.4.5 Unconfined Compression Tests.....	17
1.4.6 Effects of Aging and Weathering on the Properties of WTP Residuals.....	17
1.5 Proposed research.....	20
2 ORIGIN AND PRODUCTION OF RESIDUAL SAMPLES TESTED FOR THIS STUDY	
2.1 General.....	23
2.2 Treatment Plants Which Samples Were Collected.....	23

TABLE OF CONTENTS
(continued)

Chapter	Page
2.2.1 Ellwood City Water Treatment Plant, Ellwood City, Pennsylvania	23
2.2.2 Haworth Water Treatment Plant, Harrington Park, New Jersey.....	25
2.2.3 Jersey City Water Treatment Plant, Boonton, New Jersey	25
2.2.4 Strugeon Point Water treatment Plant Derby, New-York.....	29
2.2.5 Jerome D. Van de Water, Water treatment Plant, Tonawanda, New-York.....	29
2.2.6 Wanaque Water Treatment Plant, Wanaque, New Jersey.....	32
3 TESTING TECHNIQUES AND PROCEDURES	
3.1 Natural water Content.....	38
3.2 Specific Gravity of Solids Tests.....	38
3.3 Organic content Determination	39
3.4 particle Size analysis	39
3.4.1 particle Size Analyzer (PSA)	40
3.5 Compaction Tests (Wet to Dry).....	40
3.6 Unconfined compression Tests.....	41
3.7 Freeze-Thaw Tests.....	41
3.8 X-Ray diffraction (XRD) spectrometer	42
3.9 X-Ray Fluorescence (XRF) Spectrometer	42
3.10 Fabric Determination.....	43

TABLE OF CONTENTS
(continued)

Chapter	Page
4 RESULTS AND DISCUSSIONS	
4.1 Introduction.....	44
4.2 Natural Water Content.....	44
4.3 Organic Content	45
4.4 Specific Gravity of Solids	46
4.5 Atterberg Limits	49
4.6 Particle Size Distribution.....	51
4.7 Compaction Characteristics.....	61
4.8 Unconfined Compression and Direct Shear Tests	69
4.9 Freeze-Thaw Tests.....	74
4.10 Chemical Composition of WTP Residuals from XRF.....	75
4.11 X-Ray Diffraction Studies of the Residuals	84
4.12 Electron Micrographs	83
4.13 Energy Dispersive Spectrometer (EDS) Spectra.....	84
4.14 Elemental Mapping.....	93
4.15 Discussion on the Probable Causes and Mechanisms of Increase in Grain Size.....	93

TABLE OF CONTENTS
(continued)

Chapter	Page
5. CONCLUSIONS AND RECCOMENDATIONS FOR FURTHER STUDY	
5.1 Concusions	99
5.2 Suggestions for Further Study	100
REFERENCES	101

LIST OF TABLES

Table	Page
2.1 Information Summary of Water Treatment Facilities and Residual Samples	24
2.2 Impurities in Water Sources (yearly range).....	32
2.3 Water Treatment Processes, Chemicals added (yearly average value)	34
4.1 Natural Water Content of WTP residuals at different Drying Temperatures.....	45
4.2 Organic Content of the WTP Residuals at Different Drying Temperatures.....	46
4.3 Specific Gravity Values at Different Drying Conditions	49
4.4 Atterberg Limits and Indices for WTP Residuals	50
4.5 Grain Size Analysis Data for HWD, JCD and WQD at Different Conditions.....	53
4.6 Grain Size Analysis Data for ELD, STD and VDD at Different Conditions.....	54
4.7 Compaction Characteristics of WTP Residuals	61
4.8 Shear Strength Parameters as Obtained from Direct Shear Tests	71
4.9 Freeze-Thaw Test Results of Water Treatment Plant Residual Samples	75
4.10 Percentile Chemical Composition of WTP Residuals as determined by XRF	76
4.11 Minerals/Compounds as Identified by XRD.....	78

LIST OF FIGURES

Figure	Page
1.1 Comparison of Compaction Curves from Dry and Wet sides for residual RWA.....	16
1.2 Variation of Unconfined Compressive Strength for Residual RWA.....	18
2.1 Flow diagram of Ellwood City Water Treatment Plant, Ellwood City, PA	26
2.2 Flow Diagram of Haworth Water Treatment Plant at Harrington, NJ	27
2.3 Flow Diagram of Jersey City Water Treatment Plant at Boonton, NJ.....	28
2.4 Flow Diagram of Sturgeon Point Water Treatment Plant at Derby, NY	30
2.5 Flow Diagram of Jerome D. Van De Water, Water Treatment Plant, NY	31
2.6 Flow diagram of Water Treatment plant Water Supply Commission Wanaque, NJ....	33
4.1 Variation of Specific Gravity with Increased drying Temperatures.....	48
4.2 Grain Size Curve of Particles due to Weathering for Residual HWD	55
4.3 Grain size Curve of particles due to Weathering for Residual JCD.....	56
4.4 Grain Size Curve of Particles due to Weathering for Residual WQD	57
4.5 Grain size Curve of Particles due to Weathering for Residual ELD.....	58
4.6 Grain size Curve Particles due to Weathering for Residual STD	59
4.7 Grain size Curve of Particles due to Weathering for Residual STD.....	60
4.8 Variation of Undrained Shear Strength for Residual HWD	62
4.9 Variation of Undrained Shear Strength for Residual JCD	63
4.10 Variation of Undrained Shear for Residual WQD	64
4.11 Variation of Undrained Shear Strength for Residual ELD.....	65
4.12 Variation of Undrained Shear Strength for Residual STD	66

LIST OF FIGURES

Figure	Page
4.13 Variation of Undrained Shear Strength for Residual VDD	67
4.14 Shear Stress vs Horizontal Displacement Curves for the Residual JCD	72
4.15 Failure Envelope for Residual JCD	73
4.16 X-ray Diffractogram for residual JCD Prior to the Removal of Organics.....	79
4.17 X-ray Diffractogram for the Residual HWD after Drying at 105 ⁰ C	80
4.18 X-ray Diffractogram for the Residual JCD after Drying at 105 ⁰ C	81
4.19 X-ray Diffractogram for the Residual WQD after Drying at 105 ⁰ C	82
4.20 A Low Magnification Micrograph of the Residual HWD	85
4.21 Micrograph of the Residual HWD at a Magnification of 1100×	86
4.22 Micrograph of the Residual HWD at a Magnification of 2100×	87
4.23 A Low Magnification Micrograph of the Residual JCD	88
4.24 A Low Magnification Micrograph of the Residual WQD	89
4.25 EDS Spectra for the Residual HWD.....	90
4.26 EDS Spectra for the Residual JCD	91
4.27 EDS Spectra for the Residual JCD	92
4.28 Elemental Map for the WTP Residual HWD	95
4.29 Elemental Map for the WTP Residual JCDD	96
4.30 Elemental Map for the WTP Residual JCDD	97

LIST OF ACRONYMS, ABBREVIATIONS AND SYMBOLS

Å	Angstrom
ASTM	American Society for Testing and Materials
AWWA	American Water Works Association
AWWARF	American Water Works Association Research Foundation
C_c	Coefficient of Curvature, Compressibility Index
CEC	Cation Exchange Capacity
C_u	Color Unit
C_u	Coefficient of Uniformity
C_α	Coefficient of Secondary Consolidation
D_{10}	Diameter of the Particle Corresponding to 10% finer
D_{30}	Diameter of the Particle Corresponding to 30% finer
D_{50}	Diameter of the Particle Corresponding to 50% finer
D_{60}	Diameter of the Particle Corresponding to 60% finer
DDL	Diffused Double Layer
EDS	Energy Dispersive Spectroscopy
ELD	Dewatered sample from Ellwood City Water Treatment Plant in Ellwood City, Pennsylvania.
ESEM	Environmental Scanning Electron Microscope
HWD	Sample taken from Haworth Water Treatment Plant in Monmouth County, New Jersey
JCD	Sample taken from Jersey City Water Treatment Plant at Boonton, New Jersey
kN/m^2	Kilo-Newton per Square meter
kPa	Kilo-Pascal
LL	Liquid Limit
MDD	Maximum Dry Density
MH	Silts of High Compressibility
MX-15	Master Sizer 15 -X

LIST OF ACRONYMS, ABBREVIATIONS AND SYMBOLS
(continued)

NJDEP	New Jersey Department of Environmental Protection
NJIT	New Jersey Institute of Technology
NP	Non-Plastic
NTU	Nephelometric Turbidity Unit
OH	Organic Soil of High Compressibility
OMC	Optimum Moisture Content
PAC	Powdered Activated Carbon
pcf	Pounds per Cubic Foot
PI	Plasticity Index
PL	Plastic Limit
ppm	Parts per Million
PSA	Particle Size Analyzer
psi	Pounds per Square Inch
s	Solids Content
SC	Clayey Sand
SEM	Scanning Electron Microscope
SM	Silty Sand
SP	Poorly graded Sand
STD	Dewatered sample from Sturgeon point Water Treatment Plant
S_r	Degree of Saturation
S_u	Undrained shear Strength
TCLP	Toxicity Characteristics Leaching Procedure
tsf	Tons per Square Foot
USDA	United States Department of Agriculture
USEPA	United States Environmental Protection Agency
VDD	Dewatered Sample from Jerome D. Van de Water, Niagara River Water Treatment Plant Tonawanda, NY.
w	Water Content

LIST OF ACRONYMS, ABBREVIATIONS AND SYMBOLS
(continued)

WQD	Dewatered sample from Wanaque Water Treatment Plant at Wanaque, New Jersey
WTP	Water Treatment Plant
XAFS	X-Ray Absorption Fine Structure
XRD	X-Ray Diffraction
XRF	X-Ray Fluorescence
ZAVD	Zero Air Void Density

CHAPTER 1

INTRODUCTION, REVIEW OF LITERATURE AND PROPOSED RESEARCH

1.1. Introduction

This introductory chapter deals with the origin, composition, classification, disposal and the regulations governing Water Treatment Plant (WTP) residuals.

Water Treatment Plant residuals contain fine solid particles and organic materials removed from raw water during coagulation, softening, sedimentation and filter back washing processes at water treatment facilities. In addition, these residuals contain cations such as Calcium, Iron and Aluminum. These are introduced during the water treatment process by the addition of coagulants and conditioning agents. Depending on the type of coagulants added, the WTP residuals are classified into 3 main groups; namely lime, ferric, and alum residuals.

Various water treatment facilities of USA produce 200 to 300 million tons of residuals every year. These wastes contain 1 to 2% solids before dewatering. The solids contents of dewatered residuals is highly variable and it varies from plant to plant and one process of dewatering to another. Typical ranges of solids contents are from 10 to 30%. Due to the low solids contents, handling and disposal of these residuals pose significant problems. The stringent environmental regulations make it very difficult to deal with the issue of disposal of WTP residuals (Raghu and Hsieh 1997).

In the past, the disposal methods of WTP residuals have included direct discharge into sanitary sewers, waterways, land disposal, and ocean dumping with or without prior

dewatering and incineration. However, some of these alternatives are no longer feasible due to the current regulations that limit the direct discharge of water treatment plant residuals into watercourses such as rivers, streams and even lakes.

1.2. Composition and Structure of WTP Residuals

WTP residuals are two phase materials consisting of a solid phase and a liquid phase. In fresh residuals, liquid phase dominates the solid phase, consequently WTP residuals behave like viscous liquids. The solid phase of residuals is composed of inorganic soil solid particles, coagulants, and organic materials from the plant tissues. Sources of the soil particles and organic materials are the colloidal and suspended materials in raw water sources. The soil particles may be silt and or clay. The particles impart color and turbidity to the surface water. The liquid phase of residuals is water.

1.2.1 Water phase of WTP Residuals

Water in WTP residuals can be classified into four categories as discussed below (Knocke and Wakeland 1983, and Huang 1979):

1. Free water: Free water surrounds the flocs of residuals. This kind of water is capable of moving freely by gravity. Typically, WTP residual samples collected from lagoons contain large quantities of free water, and dewatered cake samples have very little free water.
2. Floc water: This kind of water is free water trapped within the voids of the floc structure and it travels within a floc. Dewatered residual cake contains mostly floc water. Unless the floc structure is destroyed, the floc water can not be

removed. Significant amount of energy may be required to remove floc water. This can be accomplished by processes such as heating, freeze and thaw, air drying and mechanical squeezing.

3. Capillary water: This is the water held tightly to the surfaces of particles by surface tension. These forces are believed to be short-ranged but very close to the particle surface resulting in the appearance of highly structured water molecules. In WTP residuals, this water can be within the flocs as well, as long as it is associated with a solid surface. The major difference between capillary water and floc water is that the latter is free to move within the floc and can be removed by mechanical dewatering. The capillary water is not free to move but adheres to solid surfaces. It can be removed by mechanical force if the flocs are broken up and the capillary water becomes free water.
4. Adsorbed (Bound) water: This kind of water is bound (adsorbed) within the molecular structure of colloidal solids. Water molecules are held together by hydrogen bonding. Due to the elliptical shape of these molecules, the centers of gravity of the positive and negative charges are not the same. So, the water molecules tend to assume a configuration such that their positively charged fractions are close to the negatively charged surfaces of the colloids present in the WTP residuals. These water molecules are adsorbed and so mechanical effects such as dewatering, evaporation, and normal drying processes can not remove them. A great deal of energy must be expended in breaking the bond between the water molecules and the negatively charged surfaces. Very high temperatures can accomplish this.

1.2.2 Solid Phase of WTP Residuals

Suspended inorganic solids are mainly clay-sized particles with a size ranging from 1nm to 1 μ m. They are fine crystal mineral sheets resulting from the weathering products of rocks. Minerals of the clay-sized fraction commonly include carbonate and sulfur minerals, layered silicates, and various oxides. These solids normally do not undergo any chemical reactions during water treatment processes (Bohn et al. 1985).

Clay minerals are very fine crystalline substances. Chemically they are hydrous aluminosilicates with some metallic ions. The presence of clay minerals in WTP residuals imparts plasticity, cohesion, swelling and shrinkage. Depending upon the type of clay mineral present, the cation exchange capacity (CEC) of the WTP residual also changes.

Other important constituents are free oxide minerals such as allophane. Allophane is a general name for amorphous aluminosilicate gels. Although the composition of allophane varies widely, it includes mostly hydrated Alumina (Al_2O_3), Silica (SiO_2), and Iron oxide (Fe_2O_3). Allophane may also have a high CEC and specific surface (Bohn et al. 1985). Layer silicates, allophane and chemical additives from water treatment process can play important role in affecting the properties of WTP residuals.

Organic materials are mainly colloidal polymers called humus produced by the degradation of non-humus materials undergoing enzymatic and chemical reactions. Organic matter in particulate media may be responsible for high plasticity, high shrinkage, high compressibility and low strength. Effects of organic carbon on plasticity properties of soils are now well known to engineers. A small increase in organic content of about 2 percent increases the plasticity of montmorrillonite by 20 percent (Odell et al.

1960). Soil organic matter is complex both physically and chemically and a variety of reactions and inter-reactions are possible (Oades 1989). Organic particles may range down to 0.1 micron in size and hence have high specific surfaces. The specific properties of the colloidal particles vary greatly depending upon parent material, climate, and stage of decomposition.

The humic fraction is negatively charged and has gel-like properties (Mitchell 1993, Marshall 1964). Organic particles may be strongly adsorbed on mineral surfaces and this adsorption modifies both properties of the minerals and the organic material itself. 20 to 70% of the total CEC of many soils is due to the organic matter present in them (Bohn et al. 1985). Decomposed organic matter, if present in large quantities, imparts to the soils dark grey to black color. At high moisture contents, decomposed organic matter may behave as a reversible swelling system. At some critical stages during drying, however, this reversibility ceases and this is often manifested by a large decrease in the Atterberg limits because of drying. Humus helps to stabilize the structure by forming structural units called aggregates, which are similar to flocs. It also increases the cation exchange capacity of the residual.

Soil organic matter consists not only of humic substance but also non-humic substances. The non-humic substances have recognizable physical and chemical properties and consist of carbohydrates, peptides, amino acids, fats, waxes, and low molecular weight acids. These compounds are easily attacked by soil microorganisms and persist in soil for only a brief period of times (Sparks. D.L., 1995)

During the water treatment process, hardness and color are usually removed by addition of lime and/or soda ash. Colloidal particles are removed from water by the

addition of coagulants, which induce flocculation. Some ions in the residual are retained in soils by cation and anion exchange, precipitation, and weak electrostatic attraction and as a complex with organic matter.

Alum, ferric chloride, ferric sulfate, and lime are mainly used as coagulants in water treatment process. Some water treatment plants use lime as conditioning agent in dewatering processes. These additives are used to promote colloidal aggregation by destroying the forces that stabilize colloidal particles. When these destabilized colloidal particles move toward each other and become attached during the sedimentation or dewatering process, flocculation occurs.

Clay colloidal impurities in receiving water usually carry negative charges. Since like charges repel, these similarly charged colloids are held apart from each other by their electric charges and thus are prevented from aggregating into larger particles. When coagulants are added (like alum or ferric sulfate, etc.), they will dissociate to yield Al^{3+} or Fe^{3+} ions. In turn, these ions hydrate to form a variety of aquametal complexes such as $\text{Al}(\text{OH})^{2+}$, $\text{Al}(\text{OH})_2^+$ and other poly-nuclear species such as aluminum hydroxide polymer ($\text{Al}_8(\text{OH})_{20}^{4+}$). These species are capable of being adsorbed at the surface of colloidal particles, reducing the surface potential. The negative charges of colloids are neutralized by a swarm of positive ions in the solution called diffused double layer (DDL), resulting in the destabilization of the colloidal particles. The DDL imparts a net positive charge at the edges of the colloidal particles. During processes such as flocculation, the charges at the edge participate to form an edge-to-face linkage between particles. The resulting structure is referred to as a floc-structure. The structure thus formed is sometimes called salt type floc-structure (Lambe and Whitman 1969).

1.3. Characteristics of WTP Residuals

Despite some common characteristics, WTP residuals behave significantly different from one treatment plant to another. Variations in properties have also been observed even in the residuals of the same plant. Characteristics of residuals depend mainly on the quality of water, treatment processes, chemicals added, and methods of dewatering. A detailed study of residuals and their characteristics is a prerequisite for engineers involved in safe and economical disposal of WTP residuals.

Generally, geotechnical behavior of WTP residual material is not only a function of the physical and chemical composition of its solid contents but also a function of the type, amount, and chemical nature of the pore fluids. As the structure and the solids, content of the WTP residual change, interactions between the solid and the liquid phases such as cementation takes place. This will affect the geotechnical properties such as compaction, shear strength and permeability.

Change in the water content (amount and distribution) of residual materials is the greatest single cause of variation in their geotechnical properties. It will not only alter the floc structure and the particle sizes of the solids but will also change the ion concentration and complex formation within the residuals.

1.3.1. Prior Studies Related to WTP Residual Characteristics

Research performed on WTP residuals, to date, indicate the drastic change in characteristics of WTP residuals from one treatment plant to another. Parameters such as, the quality of raw water, treatment processes, chemicals added, and methods of dewatering are found to have a significant effect on the characteristics of the WTP

residuals. The other possible factors that contribute to the variation in characteristics of residuals are the heterogeneity in the properties of soil in the catchment area of the water source and seasonal variation of water levels in the watercourses. A brief summary of some common characteristics of residuals presented in the literature is described below.

Elliott et al. (1990) conducted a study on the land application of WTP residuals. For the 20 WTP residuals tested, they found that the typical WTP residuals were predominantly inorganic. On an average, the residuals contained 3 percent by weight of organic carbon, which is stable and resistant to degradation. The nitrogen content is similar to that present in soil, which is 0.6 percent by weight. Trace metal concentrations in WTP residuals are between those of soils and sewage sludge. The total concentrations of the six metals (cadmium, copper, chromium, nickel, lead, and zinc) studied, varied considerably. Only two WTP residuals had total Ni levels close to the maximum recommended level (200 mg/kg) allowed in Pennsylvania for land application of waste materials. WTP residuals contain very low concentrations of phosphorus and large amounts of aluminum and iron hydroxide solids. The microbial toxicity of the residuals was very low except for two samples that had high concentrations of extractable Nickel and Cadmium.

In order to determine leaching of metals from coagulant residuals and their effect on water sources, George et al. (1991) conducted alum residual toxicity studies and found that toxicity occurs with both acidic and basic extracts and not with circumneutral extracts. They also reported that no chronic toxicity was measured with the alum residual extracts from the four water treatment plants tested. The data indicate that water utilities may adversely affect aquatic production by discharging alum residuals in acidic receiving

waters and soft surface waters with a hardness less than 40 mg CaCO₃/L. A pilot evaluation study for toxicity of WTP residuals was conducted by Cornwell et al. (1992). For the three residuals studied, they found that all three residuals were non-hazardous based on the results of Toxicity Characteristics Leaching Procedure (TCLP) tests. Some degree of leaching of arsenic, copper, iron, manganese, and zinc was observed from all residuals; however, the percentage of the total contaminants that leached was under 3 percent and often below 1 percent.

Historically, physical characteristics of WTP residuals have not been a major concern. This is because ultimate disposal practices did not have stringent strength requirements. Disposal of dewatered residual was typically governed by solids concentration (Cornwell et al. 1992). To establish design guidelines and criteria for residual handling, determination and understanding of the fundamental properties of these residuals are essential.

In one of the early studies on this subject, Raghu and Hsieh (1987a, 1987b) performed modified Proctor compaction tests on a lime/alum type residual and a lime type residual. Compaction curves exhibited typical one-hump shape. For the lime/alum residual, the optimum water content was about 65 percent and the maximum dry unit weight was about 51 pcf. The corresponding numbers for the lime residual were 28 percent and 84.5 pcf respectively. Cornwell et al. (1992) reported the results of standard Proctor compaction test on a coagulant residual that had been stored at a water plant for an extended time. The test results showed the typical one-hump compaction curve. Optimum moisture content and maximum dry unit weights were approximately 17 percent and 105 pcf, respectively. Wang et al. (1992a, 1992b) reported the engineering

behavior of one ferric and two alum coagulant WTP residuals. Test results indicate that the residuals were extremely plastic and highly compressible. The compaction curve for the iron type residual exhibited typical one-hump shape, whereas that for the alum residuals showed no peak. Wang et al. (1993) found that the compaction curve for alum type WTP residual was not that of the typical one-hump. Instead, it exhibited a monotonically decreasing pattern, the dry density decreased with increasing water content from a maximum near zero water content.

Raghu and Hsieh (1987a, 1987b) calculated the coefficients of permeability for two residuals from the results of one-dimensional consolidation tests. They found that the residuals were relatively impermeable and the ranges of permeability varied from 10^{-6} to 10^{-7} cm/s. Knocke and Wakeland (1983) investigated the compressibility of four residuals, --alum (low density), alum (high density), conditioned alum, and lime residuals. The average compression indices for the first three alum residuals ranged between 0.94 and 0.97, whereas the lime residual had a compressibility index of 0.79. These results indicate that the lime residual was considerably less compressible than the alum residual. Wang and Tseng (1993) reported the permeability characteristics of an alum water-treatment residual treated separately with a slaked lime and fly ash. They showed that, for both the treated and the untreated residuals, the permeability-versus-void ratio relationship was expressed as a power function as opposed to an exponential function. Under the same void ratio, the treated sample was found to be more permeable than the untreated sample.

Available information on the shearing strength characteristics of WTP residuals concentrates mainly on the undrained strength. Raghu and Hsieh (1987a) conducted

unconfined compression and direct shear tests on lime residuals. They have reported an unconfined compressive strength of 9.6 psi at a dry density of 84.5 pcf and moisture content of 28 percent. The direct shear tests made at the same density and water content gave an angle of internal friction of 28 degrees and cohesion of 2.5 psi.

Cornwell and Koppers (1990) determined the shearing strength of WTP residuals obtained from 14 utilities at solid contents ranging from 20 to 50 percent using a laboratory vane shear apparatus. They have observed a very inconsistent variation of shear strength with respect to solids content. The vane shear strength was found to vary from 2 kPa to 40 kPa for solids for solids contents ranging from 20 to 50 percent. They also found that 72% of the samples failed to satisfy the minimum required shear strength of 10 kPa, to be placed in landfills.

Novak and Calkins (1975) after studying the shearing strength of five soft residuals using a torvane recommended a minimum undrained strength of 0.04 tsf for easy handling of residuals. This minimum shear strength is about 2.5 times lower than 10 kPa (0.104 tsf) currently used in Germany and Netherlands for determining the acceptability of WTP residuals for disposal in a landfill (Cornwell and Koppers 1990). Using both a torvane and a viscometer, Huang (1979) presented a relationship between the undrained shear strength and solids concentration for two residuals. He observed that the undrained strength increased with increase in solids content.

Knocke and Wakeland (1983) found that WTP residuals exhibit marked increase in strength due to thixotropic hardening. However, very little information on the thixotropic behavior of WTP residual is currently available. Alvi and Lewis (1986) suggested that in residuals, the attractive forces due to cementation dominate over gravity forces.

Wang et al. (1992) tested one iron and two alum coagulant WTP residuals and found that the samples were highly sensitive and thixotropic. For the same moisture contents, ferric residuals had higher shear strength than alum residual samples.

Wang et al. (1993) found that mixing of alum residuals with certain additives increases the shear strength considerably. The undrained shear strength of untreated residual was low. Both the untreated and the treated residuals were sensitive and highly thixotropic.

The major constituent of any of the WTP residuals is water. In the case of lime residuals, the dewatering characteristics are related to the calcium and magnesium molar ratio. A residual with a calcium and magnesium ratio less than two will be difficult to dewater AWWA (1981). Studies have also shown that the calcium carbonate formed during the chemical reaction also affects the residual thickening and dewatering (Judkin and Wynne (1983).

Softening and coagulation of residuals tend to be thixotropic and the coagulated residual is generally gelatinous AWWA (1978). In the case of alum residual, the chemically bound water is about 40 percent of the total water content and therefore, it will be difficult to dewater a residual in the form of chemical hydroxide to greater than 60 percent solids concentration with a mechanical device. In practice, dewatering is limited to 45 to 50 percent solids concentration. With the passage of time, because of the alternate freezing and thawing, and wet and dry environment, concentration of solids increases up to 90 percent.

Ferrell et al. (1970) reported on the design of facilities for dewatering alum residuals by natural freezing. Logsdon and Edgerley (1971) studied the relationship

between dewatering and rate of freezing. They observed that residuals could be frozen effectively in thin layers. Vesilind et al. (1990) presented a conceptual model for freezing of WTP residuals that explained the improvement of dewaterability of WTP residuals by freezing.

1.4. Prior Work Done at New Jersey Institute of Technology (NJIT), Newark, NJ

In the research project sponsored by American Water Works Association Research Foundation (AAWARF), Raghu and Hsieh (1997) of NJIT have investigated the geotechnical properties of residuals from 10 water treatment plants. The results of these investigations are explained below.

1.4.1 Particle Size Distribution of Solids

Since 95% of residual solids passed No. 200 mesh, particle size distribution was determined by hydrometer analysis. Hydrometer tests were performed using wet residual in the slurry form and air-dried pulverized residual. It was observed that there was a noticeable difference in the grain size distribution curves indicating larger grain sizes when air-dried residuals were used. In certain cases, zone settling occurred making it impossible to determine the grain size distribution. Raghu et al. (1995) found that the residuals lost all their plasticity and became non-plastic after weathering.

1.4.2 Liquid Limit and Plastic Limit Tests

The liquid limit and plastic limit tests are helpful to classify and characterize the residuals. The residual samples studied during this course of research had higher liquid

and plastic limits than natural clays (in some cases the liquid limits and plasticity indices were as high as 600 and 230, respectively). The residual samples with high initial water contents had high liquid and plastic limits. Samples of residuals with low initial water contents had low values for these limits.

The natural water content (initial water contents in tests) of one of the samples was equal to its liquid limit. This sample was in a cake form with natural water content of 330% (initial water contents in tests) and possessed thixotropic properties. It is believed that in its natural state, this sample possessed a flocculated structure with significant amounts of trapped water. Upon squeezing, the floc water escaped and slurry was formed. Without water being added, the sample lost its shear strength. This residual behaved like a sensitive fine-grained soil, which loses strength upon remolding.

1.4.3 Specific Gravity of Solids

Specific gravity is a fundamental property. It provides vital clues about the physical characteristics of materials and their mineral chemistry. Presence of organic matter decreases the specific gravity and the presence of heavy metals increases the specific gravity. This may be due to the reduction of volume and water content by shearing. Raghu and Hsieh (1997) found that the values of specific gravity for most of the residuals varied from 1.87 to 2.3 and only in one out of ten samples, the specific gravity was 2.71. That particular residual was found to contain Iron.

1.4.4 Compaction Tests

Raghu and Hsieh (1997) studied the compaction characteristics of 10 WTP residuals by both dry to wet and by wet to dry methods. Typical compaction curves plotted as percent solids content vs. dry unit weight are shown in Figure 1.1.

In dry to wet tests, the values of maximum dry unit weight ranged from 6.0 to 14.64 kN/m³ corresponding to optimum solids contents of 50 to 80%. The relationship between solids content (s) and water content (w) was given by the following formula.

$$s = \frac{1}{1 + w} \quad (1.1)$$

The compaction curves for the dry to wet as shown Figure 1.1 were of one hump form with a significant peak. In all the cases, the compaction curves for all residuals were similar to those of mixed soils. This pattern was also observed for water treatment residual samples by other researchers (Wang et al. 1992).

In wet to dry method, the representative sample of residuals earmarked for compaction test was compacted by drying the residuals at room temperature. Raghu and Hsieh (1997) noticed that the residuals behaved differently at the same moisture content in wet to dry tests than those in dry to wet tests. The compaction curves were of odd shape without a definite peak. Further the values of maximum dry unit weights were lower than those obtained from dry to wet tests. These trends are clearly observed in Figure 1.1. Raghu and Hsieh (1997) attribute this strange pattern to the floc structure of WTP residuals and the process of cementation.

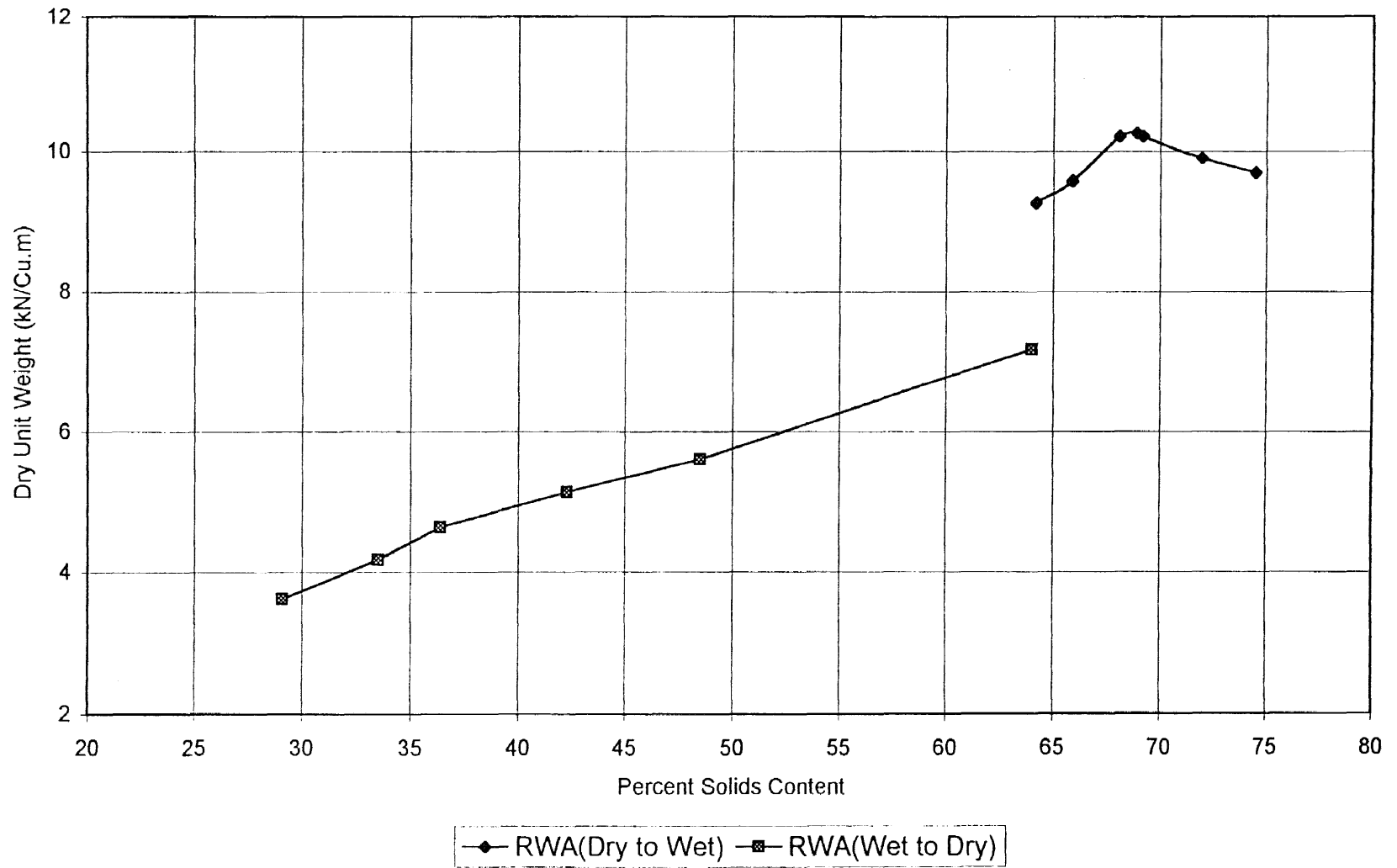


Figure 1.1 Comparison of Compaction Curves from Dry and Wet Sides for Residual RWA (after Raghu and Hsieh 1997)

During drying, the floc water was gradually removed from floc spaces. Edge-to-face bonding is gradually lost and voids collapse. The flocs are held together to form a new inter-particle bonding. Finally, floc structure gets destroyed while the particle size increases leaving behind a dry sandy material. Raghu and Hsieh (1997) also observed that when the dried samples of residuals were soaked in water for a week, water failed to break the strong adhesion due to inter-particle bonding. Therefore the original floc structure can not be recreated and the particle size distributions of the samples will resemble those of silts or sands.

1.4.5 Unconfined Compression Tests

Raghu and Hsieh (1997) determined the unconfined compressive strength of WTP residuals with increasing solids content. The unconfined compressive strength vs. percent solids content as reported by them for one residual is given in Figure 1.2. They observed that the unconfined compressive strength increased with increasing solids content up to a certain point and it decreased with further increase in solids content.

1.4.6 Effects of Aging and Weathering on the Properties of WTP Residuals:

While working on the AWWA sponsored project "Development of Criteria for WTP Residual monofills", the author noticed marked changes in the basic characteristics of residuals upon aging and weathering. For this study, the fresh residual samples were collected from a water treatment plant from New Castle, Pennsylvania. The aged and weathered samples were obtained at different time intervals from a monofill made out of the same residuals. The following observations were made.

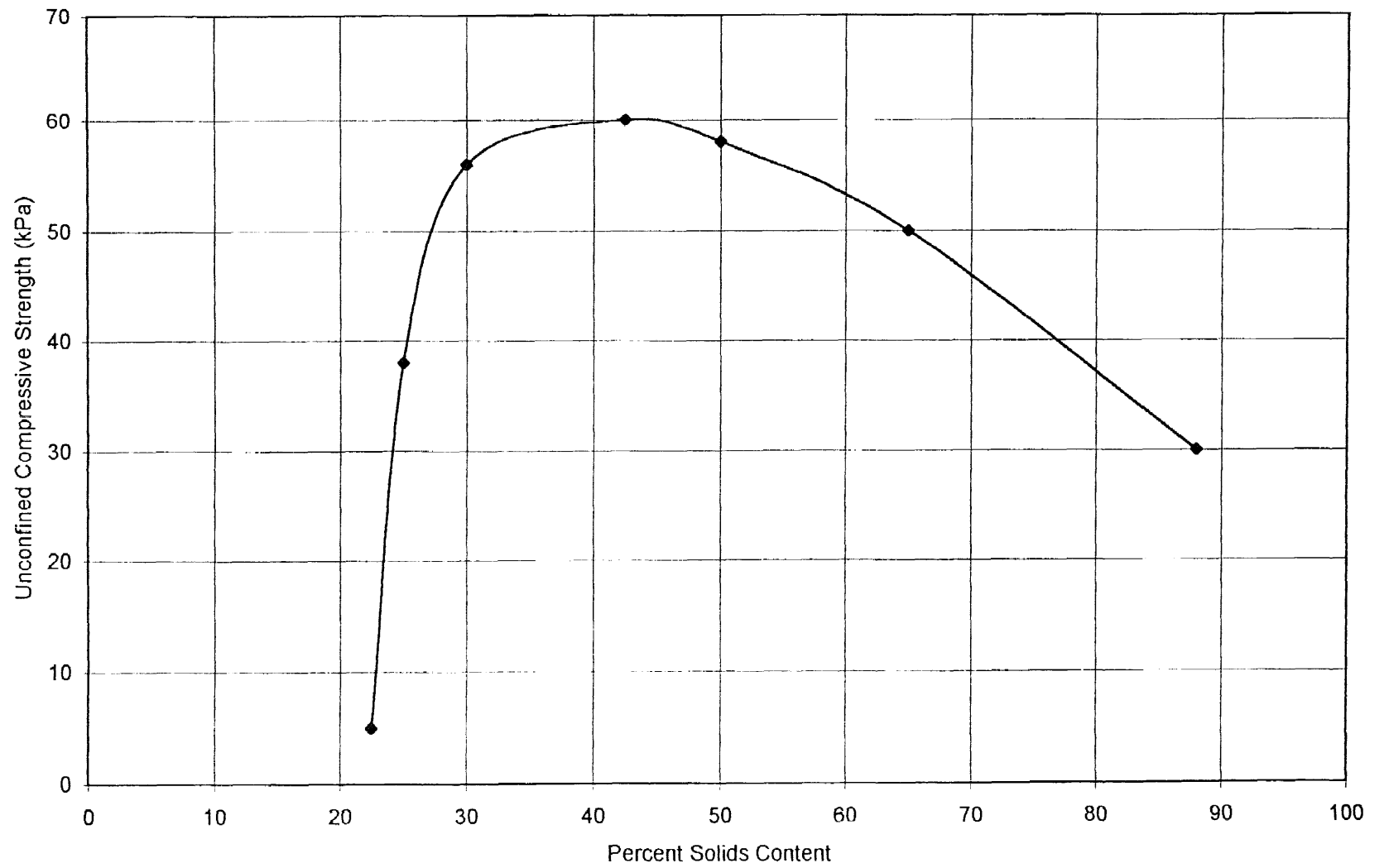


Figure 1.2 Variation of Unconfined Compressive Strength with Solids Content for Residual RWA (after Raghu and Hsieh 1997)

1. Fresh WTP residuals had very high plasticity. The values of liquid limit and plasticity index for residuals in their fresh state was found to vary from 280 to 425 and 82 to 225 respectively. These values were comparable to those of clay mineral montmorillonite. However, unlike clay minerals and clayey soils, the WTP residuals subjected to weathering lost not only plasticity but also affinity to water. The values of liquid limit dropped to 55 and lower. Further, as plastic limit could not be determined in this state, as they became non-plastic. It is believed that in addition to air drying, freeze-thaw cycles tend to expel trapped water resulting in the rearrangement of the floc structure causing the suppression of the diffused double layer. The suppression of the double layer leads to the cementation of the particles and increases the particle size. This was corroborated from the results of grain-size analyses on weathered samples.

2. Water content-dry unit weight relationships for the fresh and aged samples also revealed marked differences. In their fresh state, compaction of residuals was difficult and compaction curve obtained was close to zero air voids curve. Further, compaction tests performed from wet to dry state showed high optimum moisture content (OMC) and low maximum dry unit weight for fresh residuals. However, tests performed on weathered residuals yielded lower optimum moisture contents and relatively higher dry unit weights than fresh residuals. This further confirmed that the residuals transform into granular material after weathering.

3. Results of direct shear tests showed increase in angle of friction for the residuals upon weathering.

4. From the results of one-dimensional consolidation tests, it was observed (Raghu and Hsieh, 1997) that the compression index (C_c) and the coefficient of secondary

consolidation (C_α) decreased and the coefficient of permeability increased due to aging and weathering.

1.5. Proposed Research

Although the research work on geotechnical characteristics of WTP residuals (Raghu and Hsieh 1987) began a decade ago, a critical mass of knowledge in this area is not available presently. Physical and geotechnical behavior of WTP residuals is not understood completely. Therefore, this proposed research is aimed at characterizing the geotechnical behavior of WTP residuals.

In the preceding sections, results of prior work done at NJIT on characterizing WTP residuals were discussed. One of the significant findings of that work was that the residual materials behaved, differently under the same water contents in the wet to dry tests than in dry to wet tests.

Compaction characteristics from dry to wet tests, show a one hump pattern, whereas the compaction curves in wet to dry tests were odd shaped without any definite peak. The latter pattern is unlikely for mixed soils and is only possible for highly compressive cohesive soils with liquid limits greater than 70 (Das 1994). The hump pattern does occur for all mixed soils. These trends indicate that the residuals undergo irreversible changes in structure resulting in reduction of cohesion upon drying.

In order to explain the characteristics of residuals, the researcher may be tempted to compare the residuals with clays due to the high plasticity of the residuals. Clays are the plastic fines possessing cohesion or cohesive strength, which increases with decrease in water content. They have very low permeability, are difficult to compact when wet and

are impossible to drain by ordinary means. Compacted clays are usually resistant to erosion and piping, and are not normally susceptible to frost heave. Expansion and shrinkage accompany changes in water content in clays. Properties of clays are influenced by, size shape and mineralogical composition.

WTP residuals are also made up of clay, silt and sometimes-fine sand particles with higher concentrations of cations and organic matter. The values of compacted density for WTP residuals are much lower than clays. Residuals are susceptible to frost action. Unlike clays, the behavior of residuals is different in wet to dry conditions and dry to wet conditions. Hence, the WTP residuals do not behave like clays.

Since no explanation for the irreversible changes occurring in WTP residuals due to loss of water is available in literature, the following hypothesis has been proposed. It is believed that with the egress of water, the concentration of cations increases resulting in the depression of the double layer and an increase in net repulsive forces. As the particles get closer to each other, the cations in solution, come out of solution and cause cementation. This increases particle size, which in turn causes reduction in double layer and increase in permeability. Due to this, more water is removed. As this process continues, so does the cementation phenomenon.

The purpose of this doctoral research is to investigate the behavior of residuals and to verify and confirm our hypothesis regarding the mechanisms that alters basic nature of residuals from cohesive to cohesionless upon drying. Results of this study can be utilized to predict the long-term behavior of the residuals in monofills and to determine beneficial uses of this waste material. Geotechnical tests will be conducted on WTP residual samples in fresh, dry and freeze-thawed conditions to determine the index properties,

specific gravity of solids, compaction and shear strength characteristics. X-ray diffraction (XRD) and X-ray fluorescence (XRF) analyses will be conducted to determine the chemical composition. Microstructures of these residuals will be investigated using environmental scanning electron microscope (ESEM) and energy dispersive spectrometer (EDS). Electron micrographs, elemental maps and EDS spectra will be obtained from the aforementioned tests. Based on these results, conclusions will be drawn for the changes in behavior of residuals from fresh state to dry and freeze-thawed states.

CHAPTER 2

ORIGIN AND PRODUCTION OF RESIDUAL SAMPLES TESTED FOR THIS STUDY

2.1 General

Samples of WTP residuals for this study were collected from six treatment facilities whose locations are listed in Table 2.1. This table also presents information describing the designations used in this study for residual samples, the types of WTP residuals and water sources.

Samples were collected directly from the drying beds and dewatering machines, since the purpose of this research was to investigate the dried/dewatered residuals which are ready to be disposed off. The respective utility personnel shipped STD and VDD samples to New Jersey Institute of Technology (NJIT). They were properly labeled and placed in the coolers with freeze packs. Appropriate procedures were followed during transportation, storage, and preparation for testing so that samples would not be disturbed or cross contaminated (USEPA 1986)

2.2 Treatment Plants from which Samples were Collected

2.2.1 Ellwood City Water Treatment Plant, Ellwood City, Pennsylvania

The water source for this plant is Slippery Rock Creek. Figure 2.1 displays the flow diagram for this plant. Average water production is 8 mgd ($3 \times 10^4 \text{ M}^3/\text{d}$). Impurities in water are turbidity, taste and odor, iron, and hardness (Table 2.2). Water treatment processes include coagulation with lime, sometimes oxidation with KMnO_4 , pre-settling,

sedimentation, filtration and chlorination. Ferric Chloride and cationic polymer are used as coagulants. Backwash water from dual media gravity filtration and sedimentation residuals is directly sent to lagoons. Then they are moved to a drying bed and transported to a monofill after drying.

Table 2.1 Information summary of water treatment plant facilities and residual samples

Residual Designation	Residual Type	Location	Water source
ELD	Lime	Ellwood City Water Treatment Plant, Ellwood City, PA	Slippery Rock Creek
HWD	Alum	Haworth Water Treatment plant at Harrington Park, NJ	Hackensack River
JCD	Lime	Jersey City Water Treatment plant at Boonton, NJ	Rockaway River and Boonton Reservoir
STD	Polymer	Sturgeon Point Water Treatment Plant, Derby, NY	Lake Erie
VDD	Alum	Jerome D. Van de Water, Water Treatment Plant, Tonawanda, NY	Niagara River
WQD	Polymer	Wanaque Water Treatment Plant at Wanaque, NJ	Wanaque reservoir

2.2.2 Haworth Water Treatment Plant at Harrington Park, New Jersey

Haworth Water Treatment Plant (Figure 2.2) has a peak capacity of 160 mgd (6.1×10^5 M³/day) at two treatment plants and an average capacity of 103 mgd (3.9×10^5 M³/day). The surface water from Hackensack River and Pascack Brook is stored in the reservoir, and is then pumped into an ozone contactor. Water is then subjected to flotation/skimmer, dual media filtration, and finally it flows into the distribution system after disinfection. The impurities in raw water include hardness and color (Table 2.2). Alum is used as coagulant in the coagulation process (Table 2.3). Activated carbon is used occasionally. Ozone is used as the primary disinfectant. The backwash water from dual media filters is pumped into the lagoons and is transported to the drying bed after thickening. The residual sample was collected from the drying bed.

2.2.3 Jersey City Water Treatment Plant at Boonton, New Jersey

Water treated in Jersey City Water Treatment Plant (Figure 2.3) is collected from the Rockaway River and Boonton Reservoir. This plant produces 47 to 80 mgd (1.7 to 3.0×10^5 m³/day) of water. Impurities in raw water include turbidity, color, iron, and hardness (Table 2.2). Treatment processes consist of rapid mix coagulation, flocculation, filtration and chlorination. Lime, alum, and polymers are used as coagulants. WTP residuals, produced from coagulation and filtration, are conditioned by adding 59 percent of lime and dewatered with plate frame filter press (table 2.3). The amount of residual cake generated in this plant is approximately 8,000 lb/day (3,616 kg/day). The dewatered residual has a solids content of about 25-35 percent.

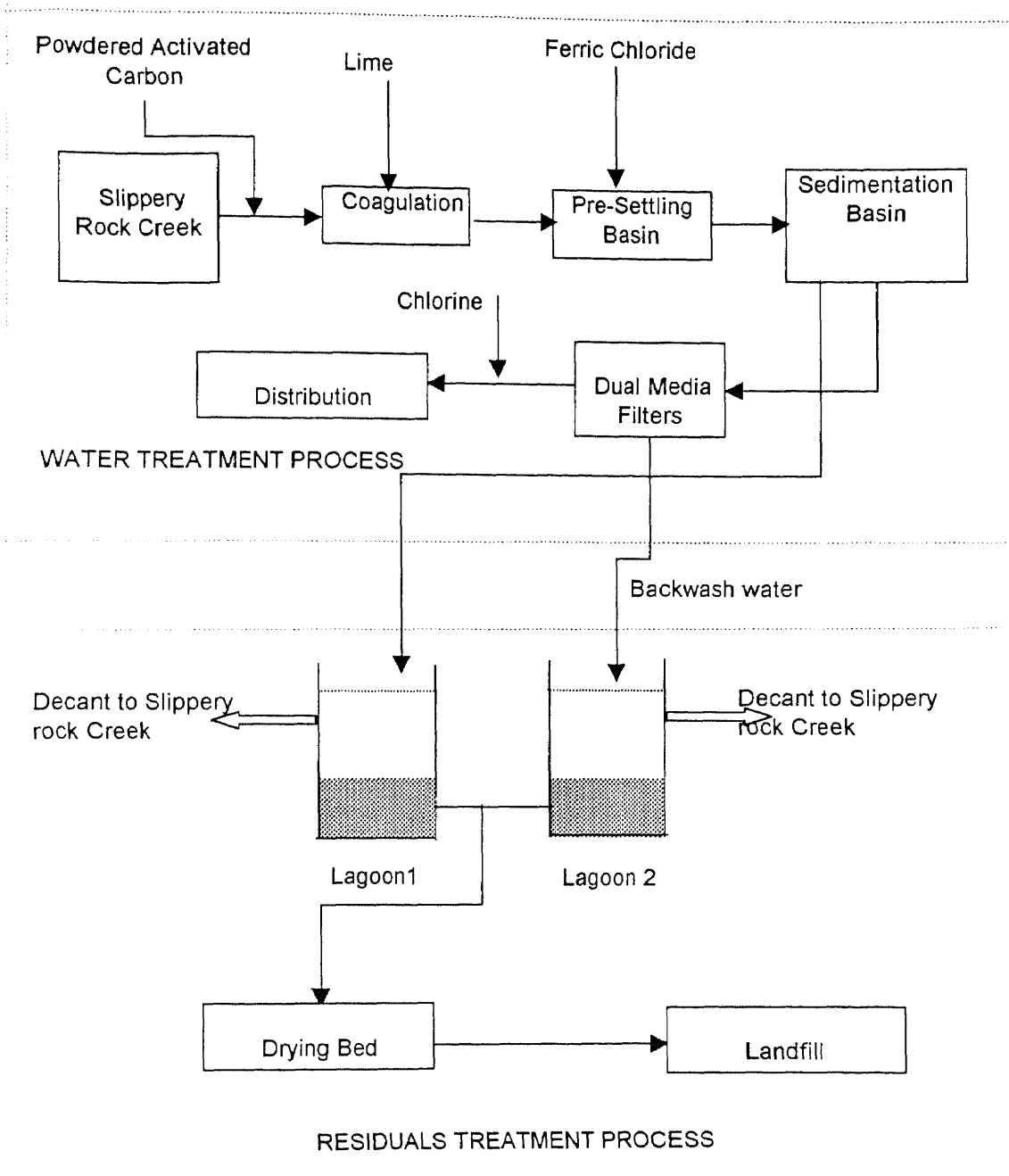


Figure 2.1 Flow Diagram of Ellwood City Water Treatment Plant of Pennsylvania American Water Company Western Division in Ellwood City, PA.

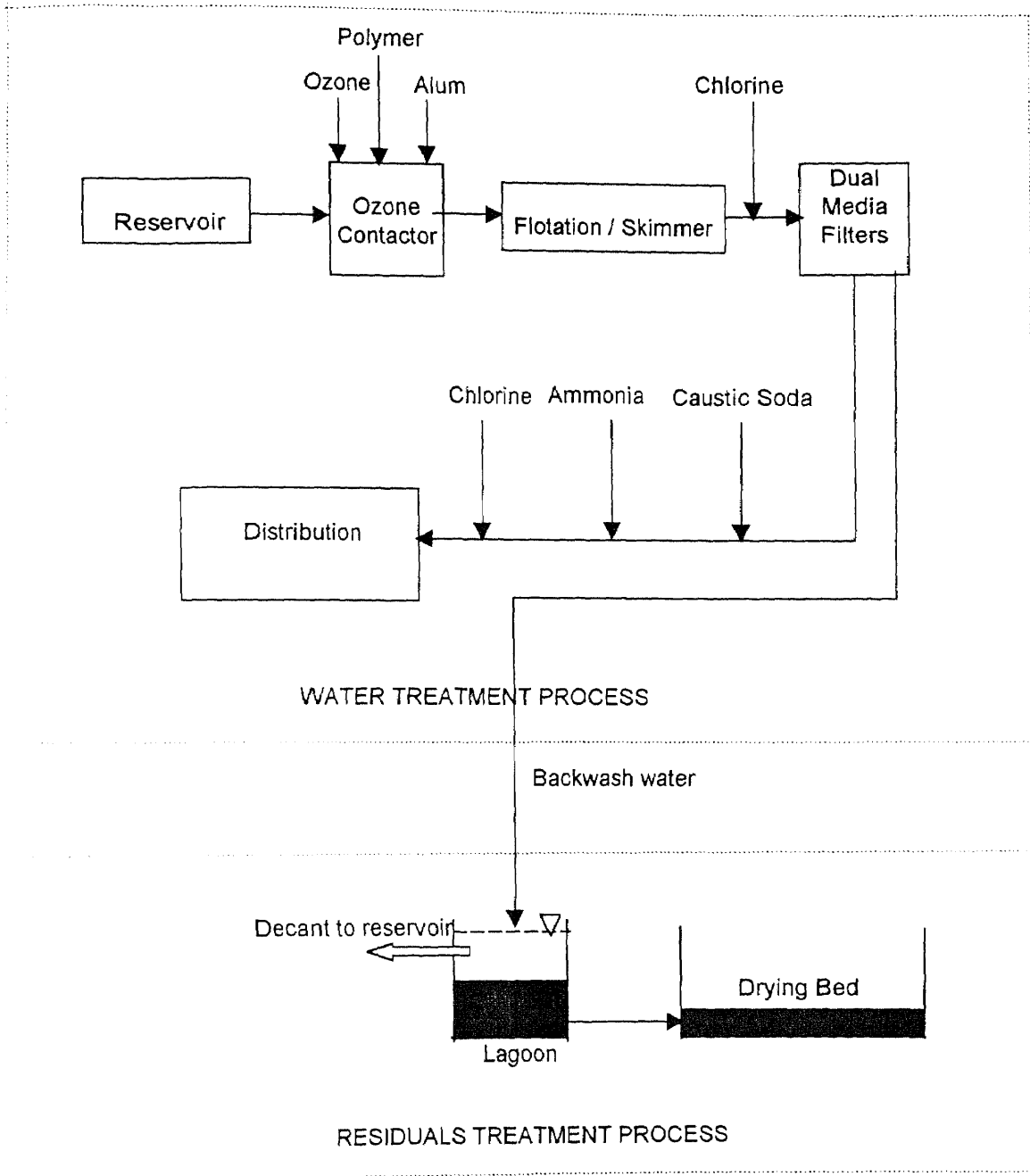


Figure 2.2 Flow Diagram of Haworth Water Treatment Plant at Harrington Park NJ.

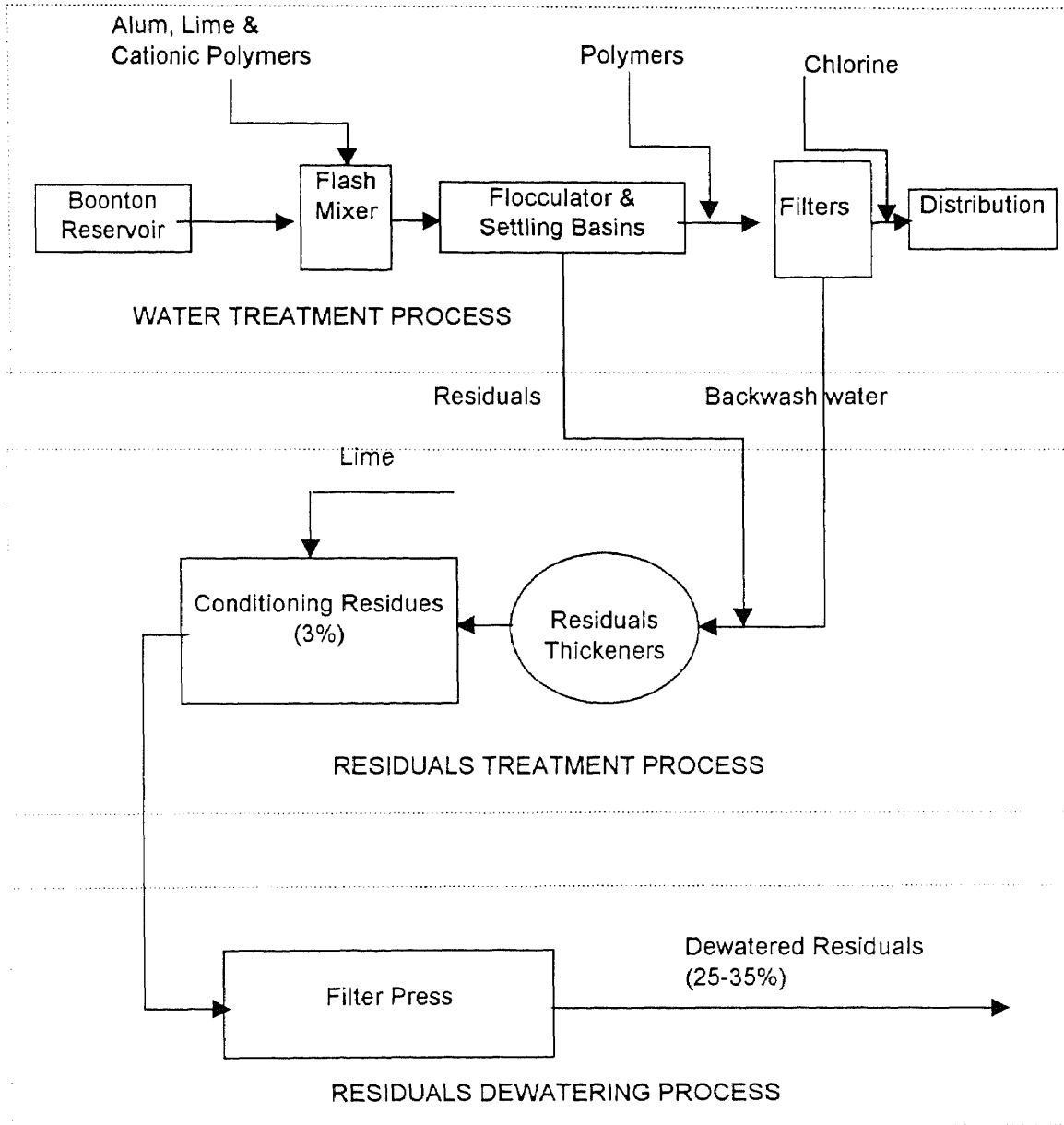


Figure 2.3 Flow Diagram of Jersey City Water Treatment Plant at Boonton, NJ.

2.2.4 Sturgeon Point Water Treatment Plant, Derby, New York

The flow diagram of Sturgeon Point Water Treatment Plant, shown in Figure 2.4. This plant has a maximum production capacity of 90 mgd ($3.4 \times 10^5 \text{ M}^3/\text{d}$). Raw water from Lake Erie is pumped into rapid mixing tanks where dispersion of pretreatment chemicals (powder activated carbon and chlorine) is accomplished. Chemically treated water from the mixing tanks flows by gravity to coagulation tanks for flocculation and sedimentation. From here, water flows to mixed-media filters. Filtered water is treated with chlorine, caustic soda and fluorine and stored on-site in a clearwell from where it is pumped into the distribution system. Filtered residuals from the coagulation basins and filter backwash waste water flow to thickener/clarifier tanks. Decant water from this tank is blended with raw water. Thickened residuals are led into lagoons. Dewatered residuals from the lagoons are taken to retention area for disposal.

2.2.5 Jerome D. Van de Water, Water Treatment Plant, Tonawanda, New York

Flow diagram of Jerome D. Van de Water, Water Treatment plant is shown in Figure 2.5. The current rated capacity is 49 mgd ($1.9 \times 10^5 \text{ M}^3/\text{d}$). Raw water is mixed with alum in the rapid mixer and flows to flocculation and sedimentation basins. Then chlorine is added and the water is sent to mixed-media filters. The water is then mixed with caustic soda, fluosilicic acid and chlorine and conveyed to the distribution system. Filter backwash water is pumped into equalization tanks. Wastewater from coagulation basins and the equalization basins is thickened utilizing sludge thickener and decant tank. Thickened residual is conditioned in a conditioning tank and dewatered using pressure filtration and then disposed.

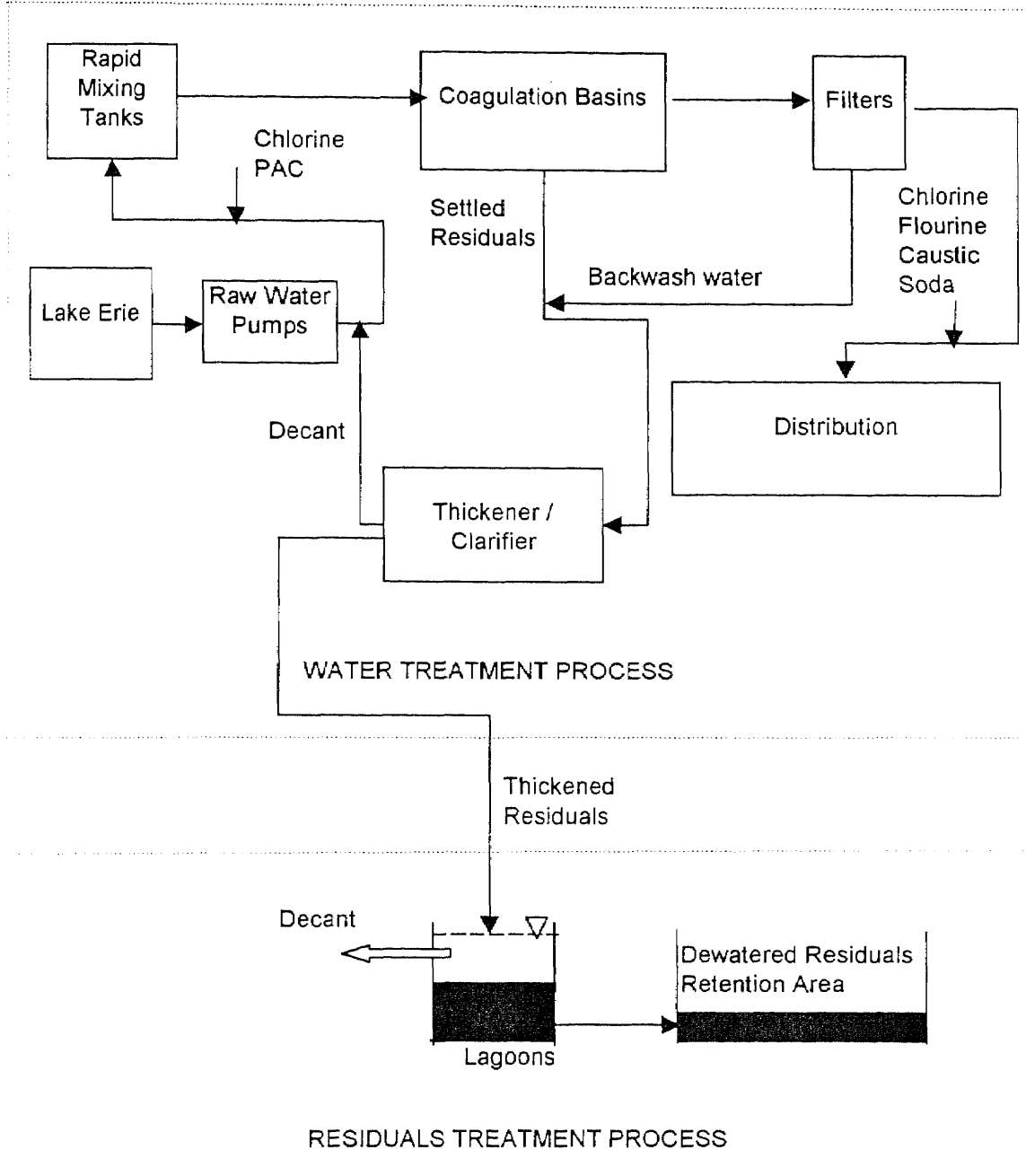


Figure 2.4 Flow Diagram of Sturgeon Point Water Treatment Plant at Derby NY.

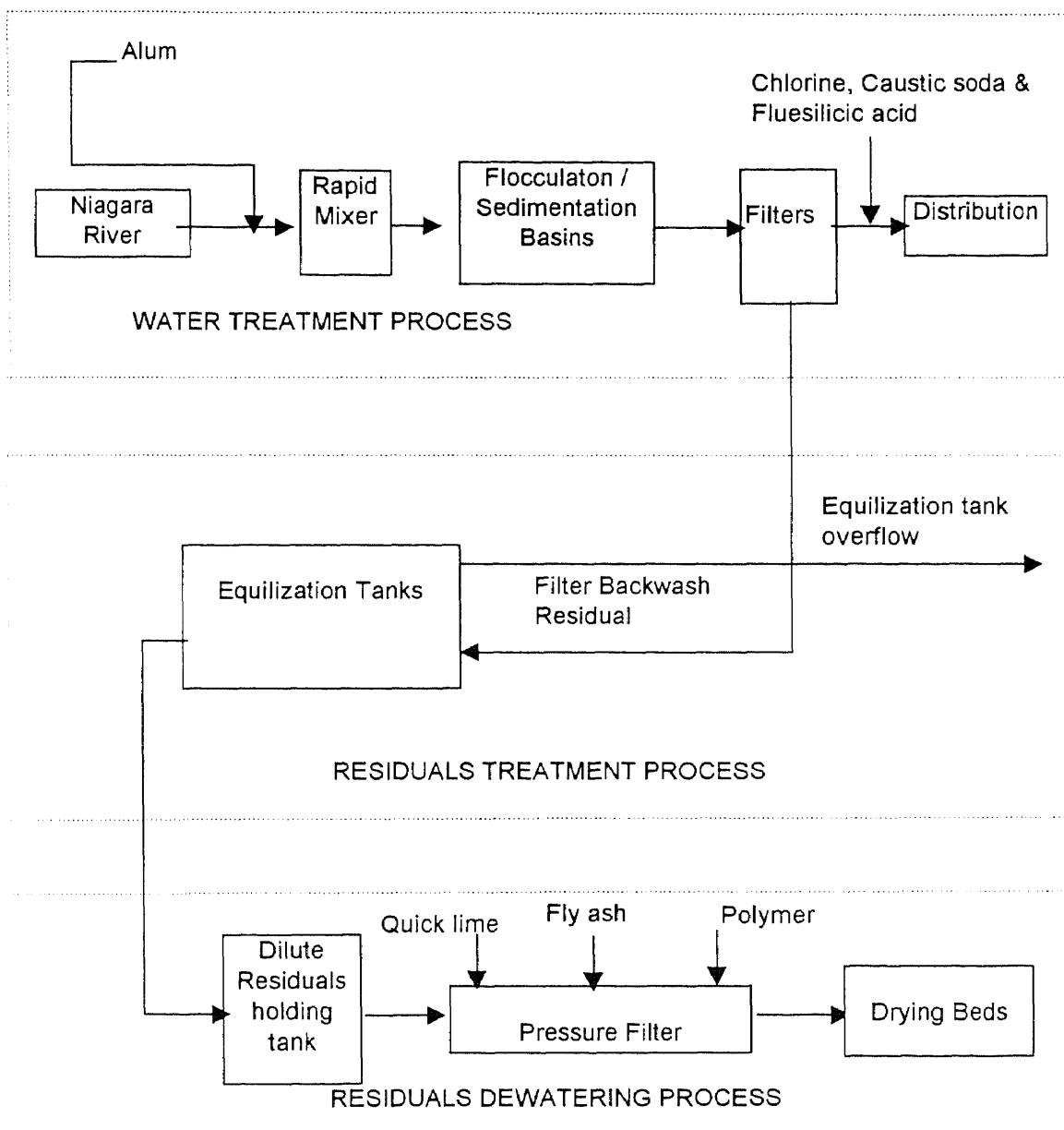


Figure 2.5 Flow Diagram of Jerome D. Van de Water, Water Treatment Plant at Tonawanda, NY.

2.2.6 Wanaque Water Treatment Plant at Wanaque, New Jersey

The flow in the Wanaque water treatment plant (Figure 2.6) varies from 40 to 140 mgd (1.5 to 5.3×10^5 M³/day), and the average capacity is 105 mgd (4.0×10^5 M³/day). Water is stored in Wanaque Reservoir before treatment. Impurities in raw water mainly consist of turbidity, color, iron and manganese (Table 2.2). The water treatment process involves pretreatment (premix basins and reaction basins), coagulation, sedimentation, and filtration. Alum and polymer are used as coagulants (Table 2.3). WTP residuals, produced from settling basins and filters, flow to lagoons and have an average solids content of 0.25 to 1.0 percent. The residuals were dewatered with a belt press-dewatering machine to a concentration of 14 percent solids content and then air dried in a drying bed.

Table 2.2 Impurities in water sources (yearly range)

Sample	Turbidity (NTU)	Color (CU)	Iron (ppm)	Manganese (ppm)	Hardness (mg/l)
ELD	2 - 100		0.5	0.06	150
HWD	3	25			120
JCD	0.5-6	10-30	0.1	<0.02	40-70
WQD	0.75-2.5	0-20	0.05-0.16	0.01-0.06	170-230
STD	1 - 500	0-20	10	8-10	118-122
VDD	1 - 500	0-20	15	8-10	118-122

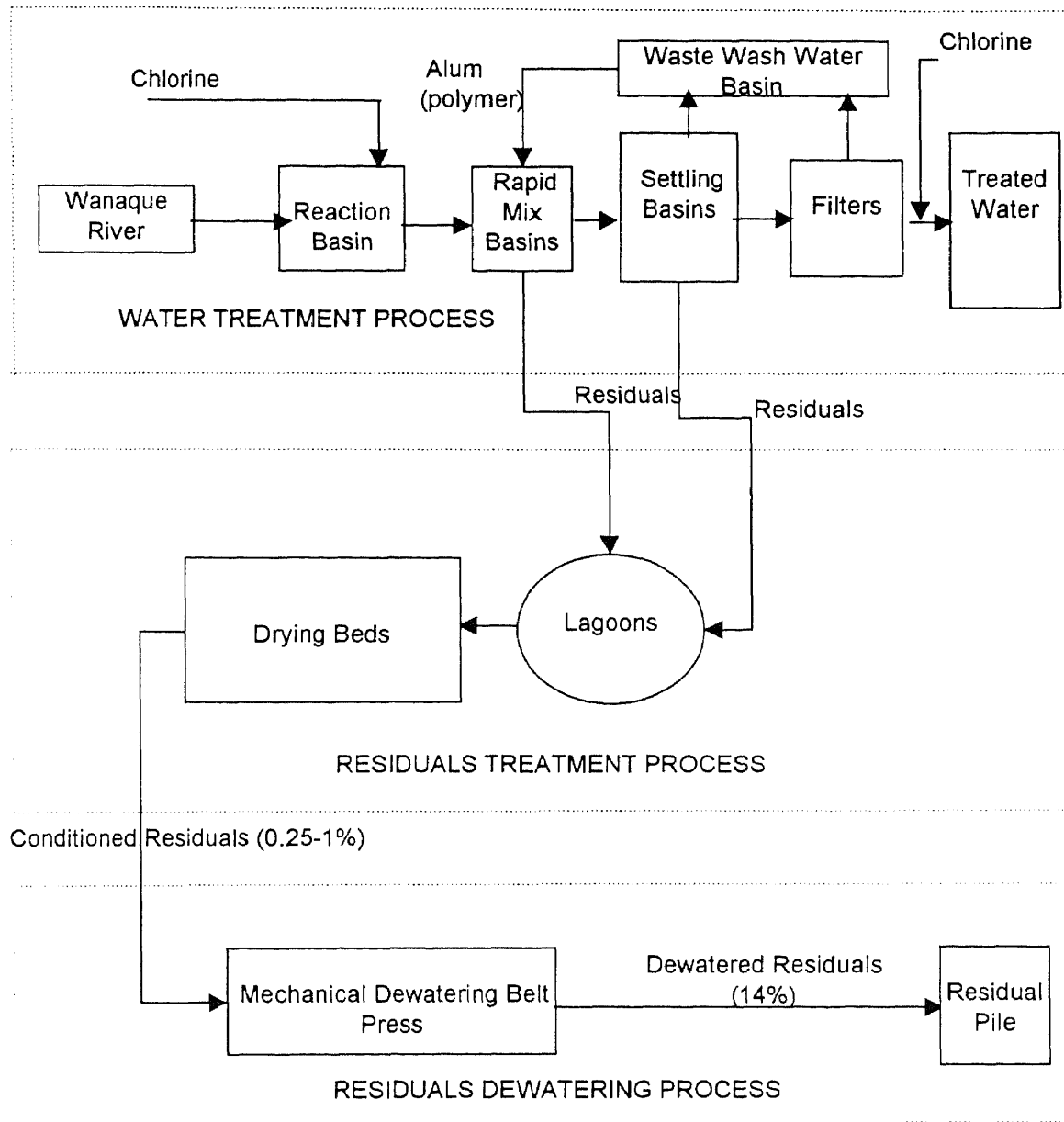


Figure 2.6 Flow Diagram of Water Treatment Plant of North Jersey District Water Supply Commission in Wanaque, N.J.

Table 2.3 Water treatment processes, chemicals added (yearly average value)

Sample	Treatment Process	Lime (ppm)	Ferric Chloride (ppm)	Alum (ppm)	Coagulants and other chemicals (ppm)
ELD	Pre-settling, coagulation, sedimentation, filtration, and chlorination	coagulant	20	-	Powder activated carbon
HWD	Ozone contactor, Flotation skimmer, media filtration, and disinfection	-	-	5	Cationic polymer (0.5-1)
JCD	Rapidmix, flocculation, sedimentation, filtration and chlorination	1-3	-	3-6	Cationic polymer (0.5-1)
WQD	Pretreatment, coagulation, sedimentation, filtration and chlorination	-	-	10-12	Polymer, KMnO ₄ , Activated Carbon, and poly aluminum chloride

Table 2.3 (continued)

Sample	Treatment Process	Lime (ppm)	Ferric Chloride (ppm)	Alum (ppm)	Coagulants and other chemicals (ppm)
STD	Rapid mix, flocculation, sedimentation, filtration and chlorination	-	-	-	Activated carbon, chlorine, fluorine, NaOH (3.5 ppm), Poly aluminum chloride (3.5-14 ppm)
VDD	Rapid mix, flocculation, sedimentation, filtration and chlorination	-	-	-	Alum, NaOH, chlorine, and fluosilicic acid

The information presented here will be helpful in analyzing and interpreting the geotechnical and geoenvironmental test data presented in this research.

CHAPTER 3

TESTING TECHNIQUES AND PROCEDURES

This chapter deals with the testing techniques adopted to characterize the residuals considered for this study. Tests conducted include physical and geotechnical tests, X-ray diffraction (XRD) to determine the inorganic mineralogical composition, X-ray fluorescence (XRF) to determine the elemental chemical composition. Environmental Scanning Electron Microscope (ESEM) and Energy Dispersive Spectrometer (EDS) were used to study the microstructure, the distribution of elements on the surface (elemental mapping) and the mineral composition.

The XRD analysis was carried out by using Philips PW 3040-MPD X'PERT machine. The XRF study was made by using Philips PW 2400 Spectrometer. In the study of fabric of residuals, Electroscan ESEM 2020 was used. Dispersive X-ray scanning was studied using Kevex Super Dry EDX. Malvern's MasterSizer X was used to measure the grain size analysis. In all these cases testing procedure was followed in accordance with the manufacturers' manual.

Barring a few, most of the geotechnical tests listed below were conducted in accordance with American Society of Testing and Materials (ASTM) standards and the reader is referred to ASTM (1997) for detailed discussions of the test procedures. In some cases where the ASTM procedures were not available, the tests were carried out in accordance with reference cited. In some cases the test procedures were modified from ASTM standards and/or formulated to suit the requirements of testing of residuals.

For all geotechnical tests, quartering was performed to obtain the required quantity of representative samples. All tests were repeated at least three times and the average values were reported. Following is the list of all the tests conducted on residuals.

- | | | |
|-----|----------------------------------|------------------------|
| 1. | Natural moisture content | ASTM D 2216 (modified) |
| 2. | Specific gravity tests | ASTM D 854 |
| 3. | Organic content determination | ASTM D 2974 |
| 4. | Grain size analysis | ASTM D 421 and 422 |
| 5. | Atterberg limits (dry to wet) | |
| 6. | Atterberg limits (wet to dry) | ASTM D 4318 |
| 7. | Compaction tests (dry to wet) | ASTM D 698 |
| 8. | Compaction tests (wet to dry) | |
| 9. | Unconfined compression tests | ASTM D 2166 |
| 10. | Direct Shear tests | ASTM D 3080 |
| 11. | Freeze and thaw tests | ASTM D 560 |
| 12. | X-ray diffraction analysis | Manufacturer's Manual |
| 13. | X-ray fluorescence spectroscopy | Manufacturer's Manual |
| 14. | Study of the fabric | |
| | (a) Scanning electron microscope | Manufacturer's Manual |
| | (b) Image mapping by Energy | |
| | (c) Dispersive X-ray scanning | Manufacturer's Manual |

3.1. Natural Water Content

Water present in the pores is in the form of gravitational water, capillary water, and adsorbed water; it can also be present as chemically bounded water within the crystalline lattice of clay particles (Wilun. Z, and Starzewski. K 1972)

On heating up to 150⁰ C, free water, capillary water, and some of the weakly held water on the perfect crystal faces is lost. On further heating from 150⁰ C to 400⁰ C, water, which is strongly held by the free ions at the points of imperfections in the crystalline lattices and at the edges of the clay crystals, is evaporated. Only on heating to temperatures higher than 400⁰ C does the chemically bounded water in the form of hydroxides, contained within the crystalline lattices of clay minerals, begin to evaporate. Because a given soil loses different quantities of water, depending on the temperature, in engineering analysis of soils, a temperature range of 105-110⁰ C has been adopted. However, for organic soils drying temperatures of 105 - 110⁰ C drives out significant amounts of organic matter (Singh. A 1975). As the residuals were suspected to possess organic matter their water content was determined at 60⁰ C. Drying of residuals at 60⁰ C requires a prolonged drying period of about 48 hours.

3.2 Specific Gravity of Solids Tests

For inorganic soils, specific gravity values ranges from 2.6 to 2.8. Organic soils and residuals have low specific gravity values. In this test, removal of air is the critical factor. ASTM recommends air removal either by heating the contents of the pycnometer in a temperature bath for about 15 minutes or by applying a vacuum. As heating may result in loss of volatile solids and organic matter, air was removed by the application of vacuum

to the sample. For all the residuals considered in this study, the specific gravity tests were carried out on freeze/thaw sample and samples dried at 60⁰, 105⁰, 250⁰ and 550⁰ C.

3.3 Organic Content Determination

The total organic/carbon content consists of first drying in a constant temperature oven at 105⁰ C for 24 hours. This dried mass is further dried in a muffle furnace at 550 – 600⁰ C for about 2 hours. The ratio of loss in weight to the weight of the dry sample dried at 105⁰ C is called the total organic/carbon content. ASTM recommends a drying temperature of 105⁰ C for inorganic soils to remove water. As the residuals were suspected as highly organic, they were first dried at 60⁰ C to remove water. The organic/carbon contents were also determined at drying temperatures of 105 and 250⁰ C.

3.4 Particle Size Analysis

Particle size distribution of solids in residuals can be quantitatively determined by conducting sieve analysis for the coarse portion and by hydrometer analysis for fine portion of the particles. Depending upon the particulate media and the extent of particle size distribution required, particle size analysis may involve both sieving and hydrometer analysis or it may be restricted to either one of them. As the residuals contain sand, silt and clay size particles combined sieve and sedimentation analyses were performed. The representative samples used for these tests were prepared by quartering. PSA required a very small quantity of sample of about 5 grams in the form of suspension. This representative sample was taken after homogenizing the entire residual. In order to get the consistent and reliable data the grain size distribution was repeated for six times.

3.4.1 Particle Size Analyzer (PSA)

Particle size distribution for fine-grained particles such as WTP residuals is usually performed by hydrometer analysis. Xia (1994), Raghu and Hsieh (1997) reported that hydrometer tests could not be performed for some residuals due to zone settling. In such circumstances, laser beam techniques to measure particle size distribution can be employed.

The sample preparation stage is particularly important to obtain accurate and reproducible results. The sample should be preferably in the form of suspensions in a liquid media. Fresh, air-dried, and freeze-thawed residual samples tested for this study were mixed with water and suspensions were prepared. These suspensions were used in the PSA to determine the particle size distribution. The tendency for the particles to stick together and form flocs is prevented by mechanical action of stirring and ultrasound using Master Sizer X-15 (MSX 15) sampling unit.

3.5 Compaction tests (Wet to Dry)

This method of test is a deviation from the standard test procedure. This method consists in running the test from wet side than from the dry side. The residuals were allowed to dry slowly under at room temperature. Compaction characteristics were studied as and when they were ready to be compacted. This method took about ten days to complete one compaction test.

3.6 Unconfined Compression Tests

Unconfined compressive strength of WTP residuals were determined corresponding to dry unit weights and water contents of both the wet to dry and dry to wet compaction methods. Cylindrical specimens were obtained by pushing Harvard miniature compaction molds of diameter 33 mm and length 71 mm pushed into the compacted residuals.

3.7 Freeze-Thaw Tests

If a WTP residual is placed in landfills, it may be subjected to cycles of freezing and thawing. In order to determine the stability of the residuals under these conditions, freeze and thaw tests were conducted. Cylindrical specimens of 33 mm in diameter and length 71 mm long were prepared from each residual sample at its original (natural) condition. The specimens were prepared by compacting the residuals in a Harvard miniature compaction mould by spring calibrated 20-pounds tamping rod in five layers and each receiving 25 blows. The molding water contents and the corresponding values of density at which the test specimens were prepared are given in Table 4.9. If the samples were very wet and could not be compacted in the condition in which they were received, they were air-dried under room conditions. When the samples were in a condition to be molded, they were prepared for testing. In such case, the molding water contents were not the same as natural moisture contents. Then the specimens were stored in the freezer at a temperature of $-5 \pm 0.5^\circ\text{C}$ for 24 hours. After this, the samples were allowed to thaw under room temperature of $24 \pm 2^\circ\text{C}$ conditions for 24 hours. This 24 hours cycle of alternate freezing and thawing was repeated 12 times for each specimen.

3.8 X-ray Diffraction (XRD) Spectrometer

X-ray diffraction studies for WTP residuals can be employed to detect the presence of crystalline clay minerals that may be present. For this research work, Philips X'PERT MPD X-ray Diffractometer was used. A 486 personal computer with X'MANAGER software is used in controlling the instrument, acquiring data, analyzing data and making reports.

Sample preparation: The sample preparation is an important step in XRD analysis. It is recommended that all samples to be analyzed using XRD should not contain more than 5% organic matter and they should pass 75 micron mesh. As WTP residuals were rich in organic matter, it became necessary to remove them by drying the sample at 105-degree Celsius for about 24 hours. The residuals are then pulverized using mortar and pestle and the material passing No.200 sieve was used in XRD analysis. The percentages passing for residuals HWD, JCD and WQD were respectively 42%, 35% and 22% respectively.

3.9 X-ray Fluorescence (XRF) Spectrometer

Elemental compositions of WTP residuals in different states were determined by using X-ray Fluorescence Spectrometry. For this study, Philips PW2400 wavelength dispersive X-ray Fluorescence Spectrometer (XRF) with a Semi-Q software was utilized.

Sample preparation: For quantitative analysis, sample matrix effects should be taken into account while preparing the sample. The sample should be homogeneous and representative with respect particle size and distribution. The clear advantage of XRF is that the samples can be reused repeatedly or be used with other instruments for

confirmation or for more detailed analyses. During the course of this study wet and dry powder samples were used. The representative samples were first homogenized by mixing thoroughly using a spatula and it was reduced to the required size by quartering. In addition to quartering and homogenization, dry samples were prepared by passing the dry residuals by sieving through 200 mesh. The material passing 200 mesh is used for the analysis.

3.10 Fabric Determination

Both direct and indirect methods are available to study the fabric and fabric features of fine-grained materials. Mitchell (1993) presents many methods of fabric measurement. Of these methods, electron microscopy offers the advantage of direct unambiguous information about the specific fabric features. For this research, observations of microstructure of WTP residuals were performed by Environmental Scanning Electron Microscope (ESEM) Electroscan ESEM 2020. Samples were subjected to freeze and thaw using the cold stage system.

Sample Preparation: Representative samples were prepared by homogenization, making sure that the particle sizes and shapes were not altered. The sample was mounted on a specimen stub, coated with the adhesive carbon solvent and observed in ESEM. It was ensured that the specimen was unaffected by the adhesive solvent and the coating method did not damage the surface.

CHAPTER 4

RESULTS AND DISCUSSIONS

4.1 Introduction

This chapter deals with the results and discussions of the physical and geotechnical characteristics of the residuals considered for this study. The discussions include the effects of drying and freezing and subsequent thawing. It is to be noted here that the residuals HWD, WQD and VDD are alum residuals, JCD is a lime residual and ELD is a ferric residual. The residual STD is rich in carbon as the treatment plant uses activated carbon to remove organic matter in raw water. All tests were conducted on three samples of each residual and the average values are reported.

4.2 Natural Water Content

The water contents for all the residuals were determined by drying in air at controlled temperature of 20 degree Celsius, at 60 degree Celsius and at 105 degree Celsius in a constant temperature oven. As it can be seen from the Table 4.1, there is a marked difference in water contents indicating significant loss of organic matter when heated to 105 degree Celsius. Hence, for all subsequent geotechnical tests, water contents were determined upon drying at 60 degree Celsius till constant weight was attained. In most cases, the time required was about 48 hours. The natural water contents, when dried at 105 degree Celsius, varied from 115% for the residual JCD to 602% for the residual WQD. These values of high initial water contents can be attributed to the presence of organic matter, as their moisture retention capability is very high.

Data presented in Table 4.2 will corroborate this fact. For example, the residual WQD whose organic content is 48.58% has high moisture content of 569% when dried at 60⁰ C.

Table 4.1 Natural Water Contents of WTP Residuals at Different Drying Temperature

Residual Type	Natural Water Content (%)		
	Air Drying at 20 ⁰ C	Drying at 60 ⁰ C	Drying at 105 ⁰ C
HWD	272	286	314
JCD	301	316	329
WQD	512	569	602
ELD	370	402	426
STD	186	197	242
VDD	187	215	254

4.3 Organic Content

The organic contents of all the residuals considered for this study were determined for both the dry and freeze-thaw conditions. Weight losses with reference to the weight of sample dried at 60⁰ C were determined by drying the material to 105⁰ C, 250⁰ C and 550⁰ C. Though the loss in weight corresponding to drying temperatures of 105⁰ C and 250⁰ C is partly due to the loss in water in addition to the oxidation of organic matter, it is premised here that the loss is mainly due to organic matter, as it is impossible to apportion the weight loss between organic matter and vaporization of water.

Table 4.2 presents the percentage organic contents of all the residuals. It can be seen that all the residual samples were rich in organic matter. The residuals WQD and

HWD possess very high organic fractions of 48.58% 41.85% respectively. The effect of freezing and thawing on organic matter was also studied by determining organic content of residuals which have been subjected to 12 cycles of alternate freezing and thawing. These values are presented in the extreme right column of table 4.2. The variations in organic contents for all the residuals from air-dried to freeze-thaw conditions is less than 2%. For all practical purposes, this variation is negligible. Hence it can be inferred that freeze and thaw conditions do not change the organic contents of residuals.

Table 4.2 Organic Contents of the WTP Residuals at Different Drying Temperatures

Residual Type	Loss in Weight Presumed to be Organic Content (%)			
	Drying (105 ⁰ C)	Drying (250 ⁰ C)	Drying (550 ⁰ C)	Drying at 550 ⁰ C (Freeze/Thawed Sample)
HWD	3.44	15.26	41.85	40.25
JCD	4.60	14.58	34.50	32.59
WQD	10.25	18.23	48.58	48.23
ELD	8.92	15.75	36.71	35.54
STD	8.52	17.26	39.22	37.21
VDD	7.98	14.52	36.58	35.15

4.4 Specific Gravity of Solids

Specific gravity of solids for all the residuals was determined utilizing residuals dried at different temperatures and for freeze-thawed samples. The ash was removed by washing and filtering the dried samples. The results obtained and presented in Figure 4.1 and

Table 4.3 show that with the increase in drying temperatures the specific gravity values increase. This indirectly suggests that, as in most of the organic soils, organic phase (indicated by the weight losses) of WTP residuals is responsible for low values of specific gravity. .But, upon heating, the specific gravity of solids increases. For instance, the specific gravity of the residual JCD that had a total organic content of 34.5% was 2.11 before the oxidation of organic matter. However, upon heating and drying at 550⁰ C, the specific gravity rose to 2.75. This means that there is an increase of 30.3% in the values of specific gravity. As it can be seen from Table 4.3 after the oxidation of organic matter, all residuals experienced an increase in specific gravity values and the range of increase varied from 28.7 to 53.6%.

As the sample loses weight upon heating to high temperature, two things happen. Organic contents are reduced. The oxides such as Calcium oxide, Iron oxide and alumina come out of solution and cement the grains of solids in the residuals. The reduction in the organic matter and the change in chemical composition due to cementation by metal oxides cause increase in the specific gravity of solids of the WTP residuals. Further discussion on the cementation phenomenon will be presented at the end of this chapter.

By comparing the specific gravity, values for freeze-thaw and dried samples at 60⁰ C again we can reconfirm that freeze and thaw do not bring about any change in organic matter. For instance, the residual JCD possessed a specific gravity value of 2.11 both during freeze-thaw and drying at 60⁰ C. The same trend has been observed for all the other five residuals

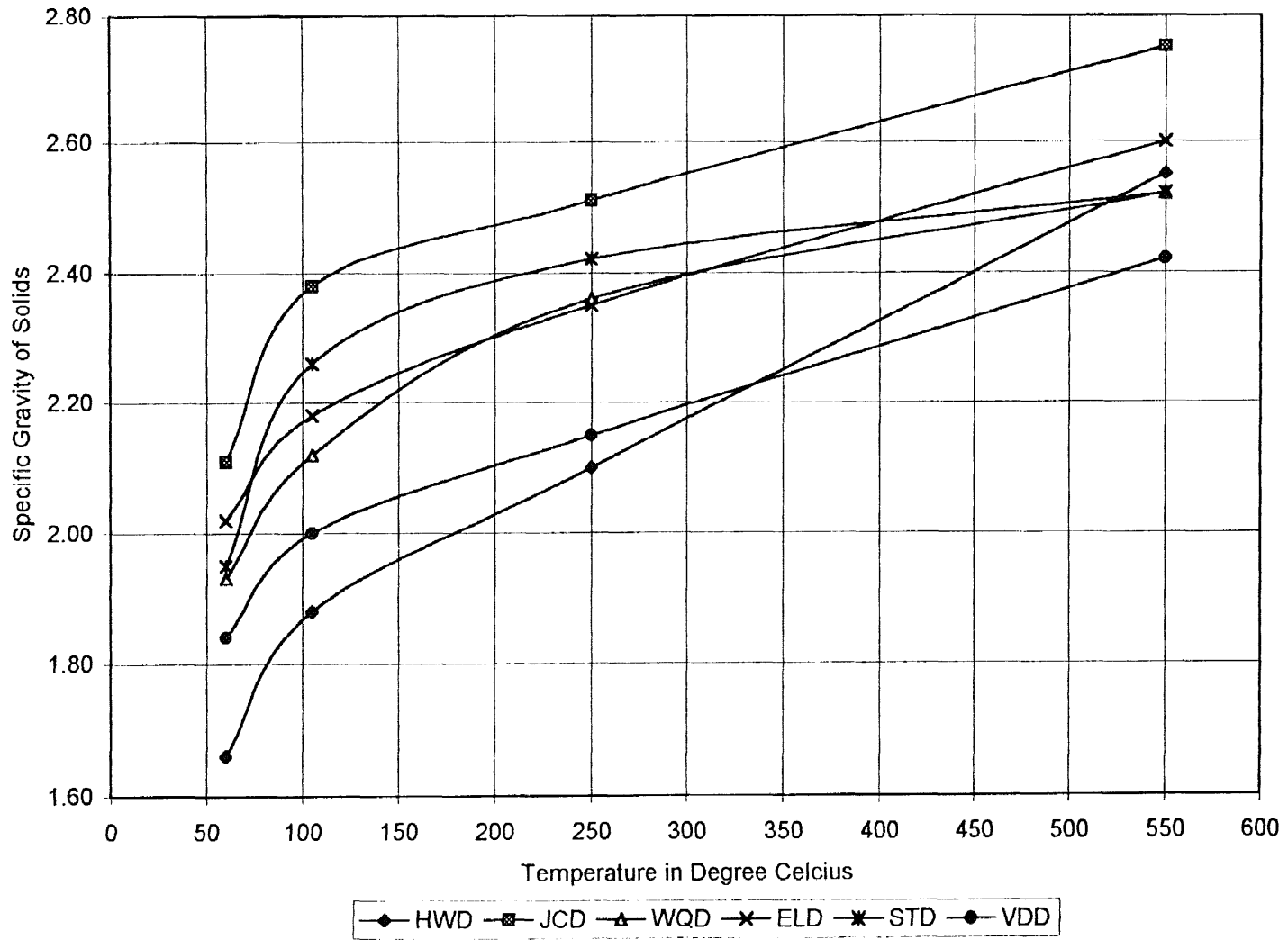


Figure 4.1 Variation of Specific Gravity with Increased drying Temperatures

Table 4.3 Specific gravity values at different drying conditions.

Residual sample	Freeze/Thaw weathered	Dried at 60 ⁰ C	Dried at 105 ⁰ C	Dried at 250 ⁰ C	Dried at 550 ⁰ C	Percent Increase from 60 ⁰ to 550 ⁰ C
HWD	1.75	1.66	1.88	2.10	2.55	53.6
JCD	2.11	2.11	2.38	2.51	2.75	30.33
WQD	1.92	1.93	2.12	2.36	2.52	30.56
ELD	2.02	2.02	2.18	2.35	2.60	28.70
STD	1.95	1.95	2.26	2.42	2.52	29.20
VDD	1.83	1.84	2.00	2.15	2.42	31.52

4.5 Atterberg Limits

The properties of interest are liquid limit, plastic limit and plasticity index. These characteristics are not only important in classification and identification but also in predicting engineering behavior such as strength and compressibility. These limits and indices were determined on samples at their natural water contents, air-dried, and freeze-thaw conditions respectively. The results are tabulated in the Table 4.4.

By studying the results presented in Table 4.4, one will underscore the drastic reduction in the plasticity characteristics of the residuals due to drying, freezing and subsequent thawing. In the fresh state, all of these residuals were soft and plastic with very high liquid limits and plasticity indices. The alternate freezing and thawing conditions rendered all residuals non-plastic. However after air-drying all of the residuals except ELD became non-plastic. In the dry to wet tests on air-dried samples,

this residual had plasticity index of 82, that is much lower than that for fresh residual in wet to dry state. This indicates that freezing and thawing is more effective in transforming a plastic residual to a non-plastic material especially for the residuals such as ELD.

Table 4.4 Atterberg Limits and Indices for WTP Residuals.

Residual	Liquid limit			Plastic limit			Plasticity Index		
	Wet to Dry	Dry to wet	Freeze-Thaw	Wet to Dry	Dry to wet	Freeze-Thaw	Wet to Dry	Dry to wet	Freeze-Thaw
HWD	371	107	110	228	NP	NP	144	NP	NP
JCD	329	37	42	200	NP	NP	129	NP	NP
WQD	690	151	165	20	NP	NP	670	NP	NP
ELD	330	125	70	212	43	NP	118	82	NP
STD	161	55	53	57	49	NP	104	6	NP
VDD	206	118	110	115	NP	NP	91	NP	NP

Note: NP indicates Non-plastic.

The residual WQD had a very high liquid limit of 690, and plastic limit of 20 possessed a very high plasticity with a plasticity index of 670. But the same residual lost all of its plasticity upon drying and freezing and thawing. The values of liquid limit corresponding to these two conditions are 151 and 165 respectively and in both the cases plastic limit could not be determined. This transformation might be due to the

suppression of double layer, which increased the growth of particles by flocculation and cementation. Further, the loss of plasticity is found to be irreversible as the residuals lost affinity to water. This means that the water treatment plant residuals will not rehydrate when water is added. More discussion on the causes and mechanisms responsible for the loss of plasticity will be presented in later sections of this chapter.

4.6 Particle Size Distribution

Particle size distributions for all the residuals were determined by the sieve analysis, hydrometer analyses and Particle Size analyzer (PSA). In their fresh states, combined sieve and sedimentation analyses were carried out on residuals JCD, ELD, STD and VDD. Hydrometer and PSA tests were employed to determine grain size distribution of fresh residual HWD. However in the case of fresh residual WQD, hydrometer test was not successful since the sample formed a gel. The grain size distribution of that residual was determined by PSA. For sample JCD in the fresh state, grain size distribution by PSA was not possible, since the sampling chamber choked up, probably due to the high calcium compounds present in that sample. For dry and freeze and thaw samples, the grain size distribution was determined by combined sieve and hydrometer and PSA methods.

Figures 4.2 to 4.7 present the grain distribution of the six residuals considered for this study under fresh, dried and freeze-thawed conditions respectively. The parameters required for classification, --the uniformity coefficient, coefficient of curvature, sand, silt and clay fractions have been shown in Tables 4.5 and 4.6 respectively. The specific surfaces for all the residuals corresponding to the average size (D_{50}) were calculated,

assuming the solid particles were to be perfectly spherical. The residuals were classified according to the unified classification system and the group names and the group symbols are also included in Tables 4.5 and 4.6.

An examination of the results presented in the Table 4.5 and 4.6 and the grain size distribution curves shown in Figures 4.2 to 4.7 clearly indicates the increases in sizes of particles of residuals, due to drying and freezing and thawing. Initially in fresh state, all these residuals were predominantly fine-grained. Upon drying, and freezing and thawing, increase in the sizes of particles took place, making the residuals coarse-grained materials. The values specific surface, defined as the ratio of surface area to weight, dropped significantly for all the residuals. Increase in particle size is more pronounced in the residual JCD, where the value of specific surface decreased from 23800 cm²/g in the fresh state to 476 cm²/g for weathered sample due to freezing and thawing. Discussion for the possible causes will be presented later in this chapter.

The grain size distribution of residual HWD in its fresh state as obtained by hydrometer gives smaller sizes of the particles than that of PSA. This may be due to the fact that no dispersing agent solution was used in PSA and some particles might have flocculated. Also, it has to be pointed out here that both PSA and hydrometer techniques do not make absolute determinations of particle size. In PSA, particle size is measured from the diffraction patterns created by the laser beam on the sample. The hydrometer technique is based on the measurement of settling velocities.

Table 4.5-Grain Size Distribution Analysis Data for HWD, JCD and WQD at Different Conditions.

Residual	HWD			JCD			WQD		
	Fresh	Dry	Freeze/ Thaw	Fresh	Dry	Freeze/ Thaw	Fresh	Dry	Freeze/ Thaw
% fines	86	48	35	100	30	24	65	27	34
% sand	14	52	65	---	70	76	35	73	66
D ₁₀ (mm)	0.004	0.006	0.006	0.0008	0.014	0.014	0.0065	0.027	0.013
D ₃₀ (mm)	0.012	0.024	0.06	0.0034	0.08	0.1	0.023	0.16	0.065
D ₅₀ (mm)	0.04	0.4	1.4	0.006	0.28	0.3	0.05	0.4	0.29
D ₆₀ (mm)	0.024	0.24	0.8	0.008	0.5	0.38	0.07	0.6	0.4
C _u	6	40	133.3	10	35.7	27.14	10.77	22.22	30.77
C _c	1.5	0.4	0.75	1.8	0.9	1.88	116	1.58	0.82
Specific surface (cm ² /g)*	2820	282	81	23800	510	476	2544	318	439
Group Symbol	OH	SM	SM	OH	SM	SM	OH	SM	SM
Group name	Organic silt	Silty Sand	Silty Sand	Organic Silt	Silty Sand	Silty Sand	Sandy Organic Clay	Silty Sand	Silty Sand

*The specific surfaces are calculated by assuming the particles are as perfect spheres and the average size

D₅₀ is used in these calculations.

Table 4.6-Grain Size Distribution Analysis Data for Residuals ELD, STD and VDD at Different Conditions.

Residual	ELD			STD			VDD		
	Fresh	Dry	Freeze/ Thaw	Fresh	Dry	Freeze/ Thaw	Fresh	Dry	Freeze/ Thaw
% fines	62	10	15	77	50	60	72	52	55
% sand	38	90	85	23	50	40	28	48	45
D ₁₀ (mm)	0.006	0.075	0.056	0.0028	0.007	0.003	0.0026	0.01	0.01
D ₃₀ (mm)	0.022	0.10	0.13	0.01	0.037	0.026	0.01	0.033	0.032
D ₅₀ (mm)	0.048	0.18	0.14	0.025	0.08	0.062	0.028	0.085	0.065
D ₆₀ (mm)	0.07	0.23	0.17	0.04	0.15	0.092	0.04	0.15	0.09
C _u	11.7	3.1	3.0	14.3	21.4	30.7	15.4	15	9.0
C _c	1.15	0.58	1.78	0.89	1.30	2.45	0.96	0.73	1.14
Specific surface (cm ² /g)*	2525	673	866	5424	1695	2187	4286	1412	1846
Group Symbol	OH	SP-SC	SM	OH	SP& OH	SM	OH	OH	OH
Group Name	Organic Silt	Silty Clay	Silty Sand	Organic Silt	Poorly graded sand and Organi c Silt	Silty Sand	Organic Silt	Sandy Organic Silt	Sandy Organic Silt

* The specific surfaces are calculated by assuming the particles are as perfect spheres and the average size

D₅₀ is used in these calculations.

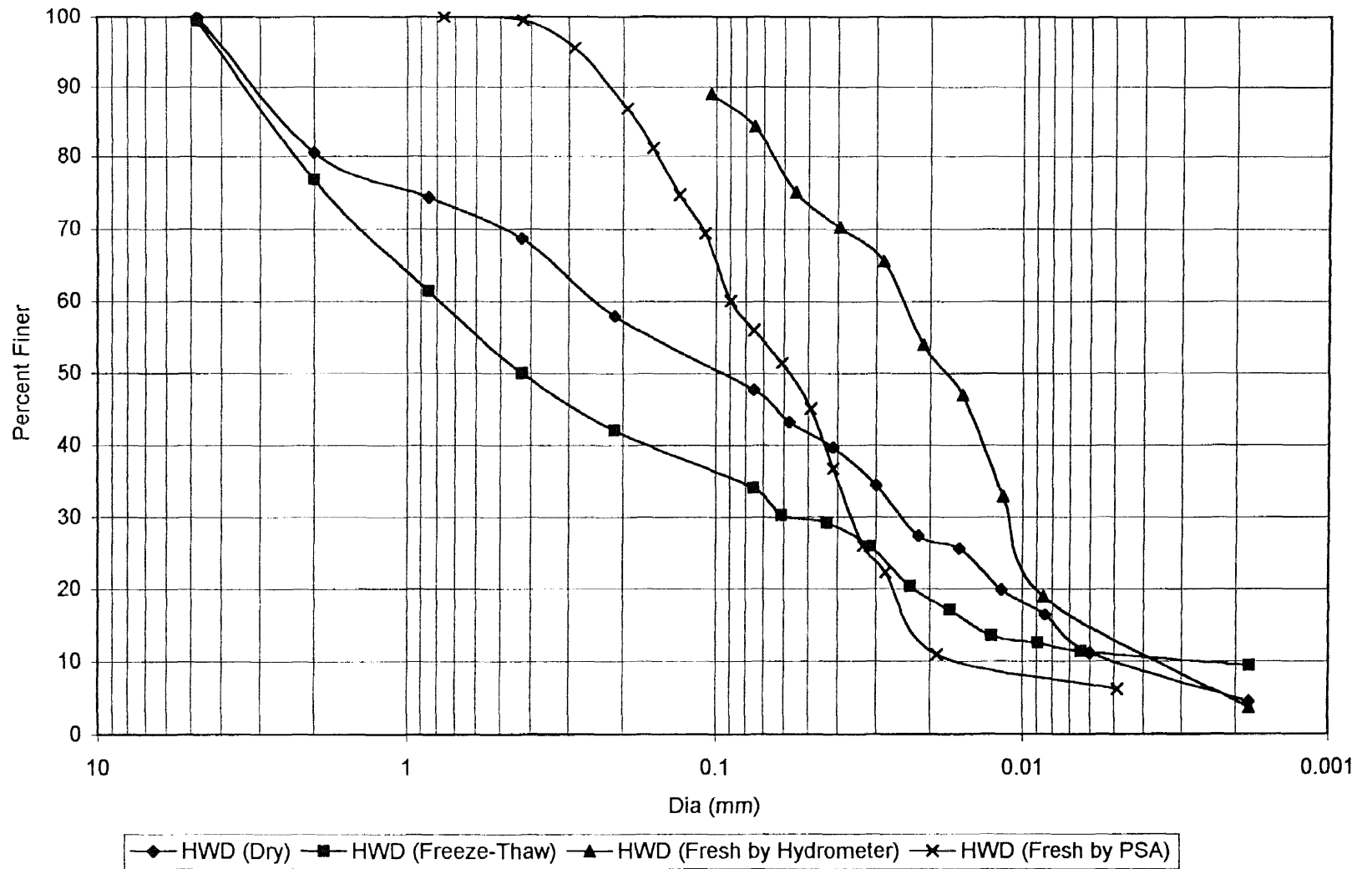


Figure 4.2 Grain Size Curve Depicting Increase in Size of Particles due to Weathering for Residual HWD

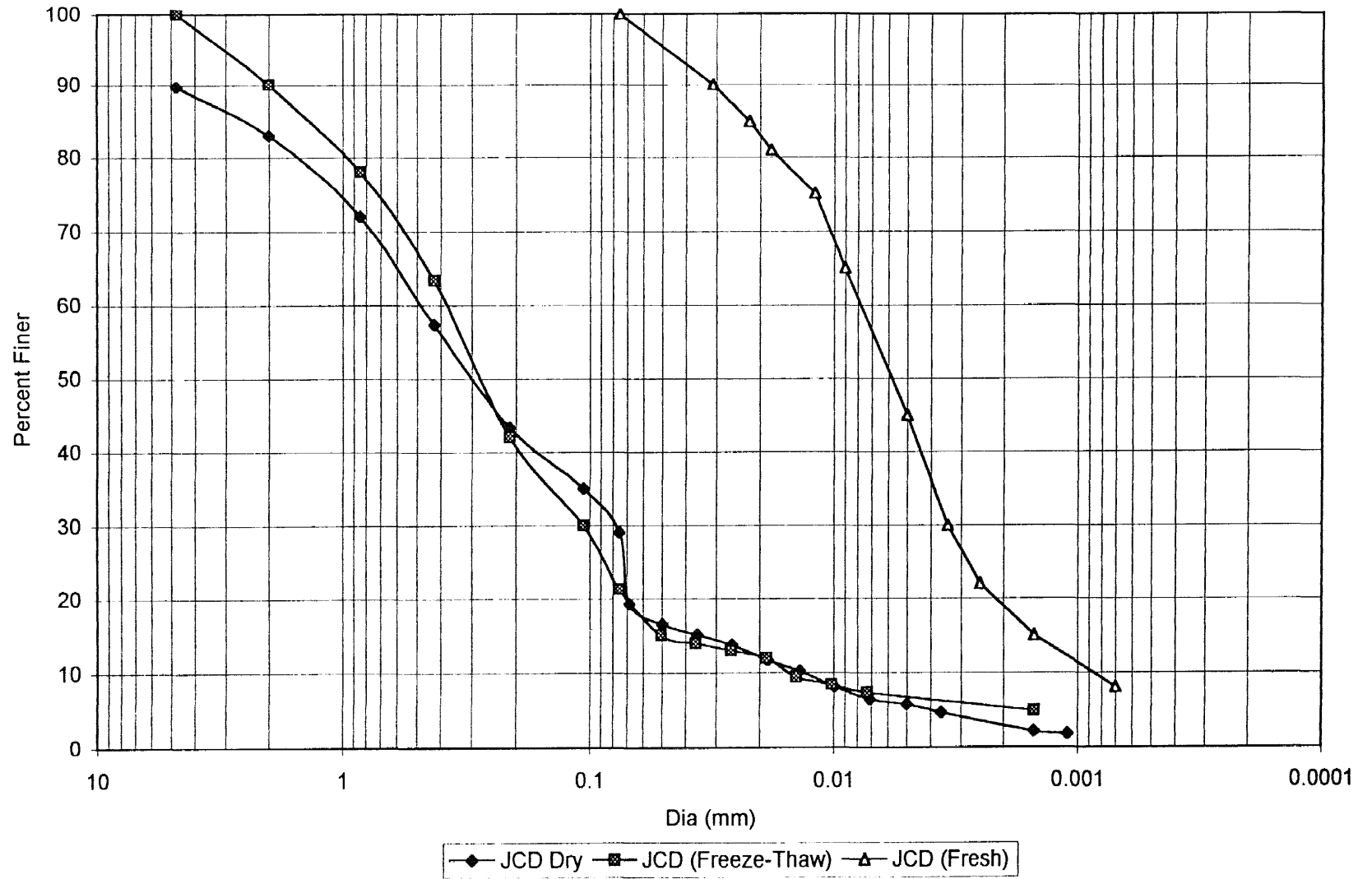


Figure 4.3 Grain Size Curve Depicting Increase in Size of Particles due to Weathering for Residual JCD

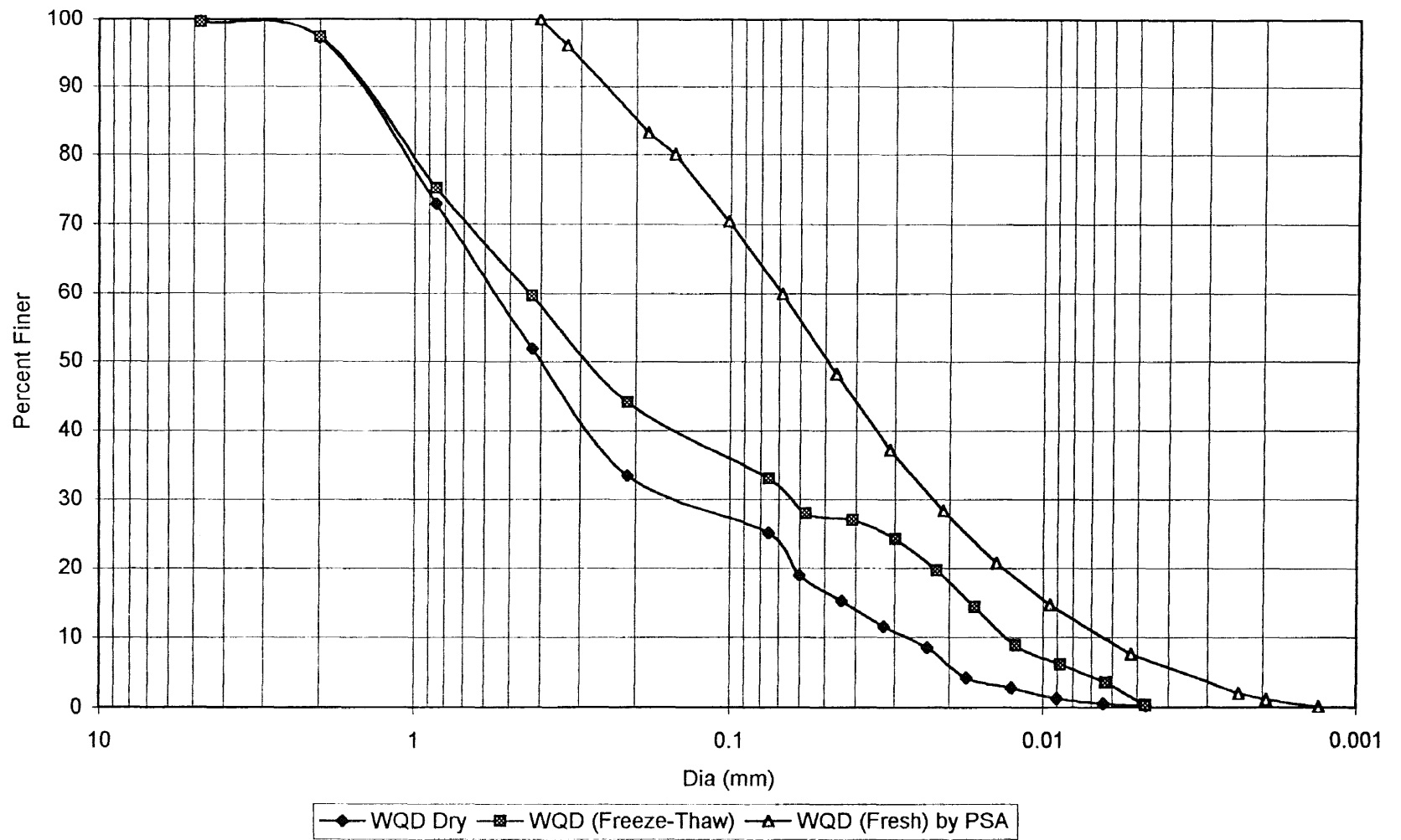


Figure 4.4 Grain Size Curve Depicting Increase in Size of Particles due to Weathering for Residual WQD

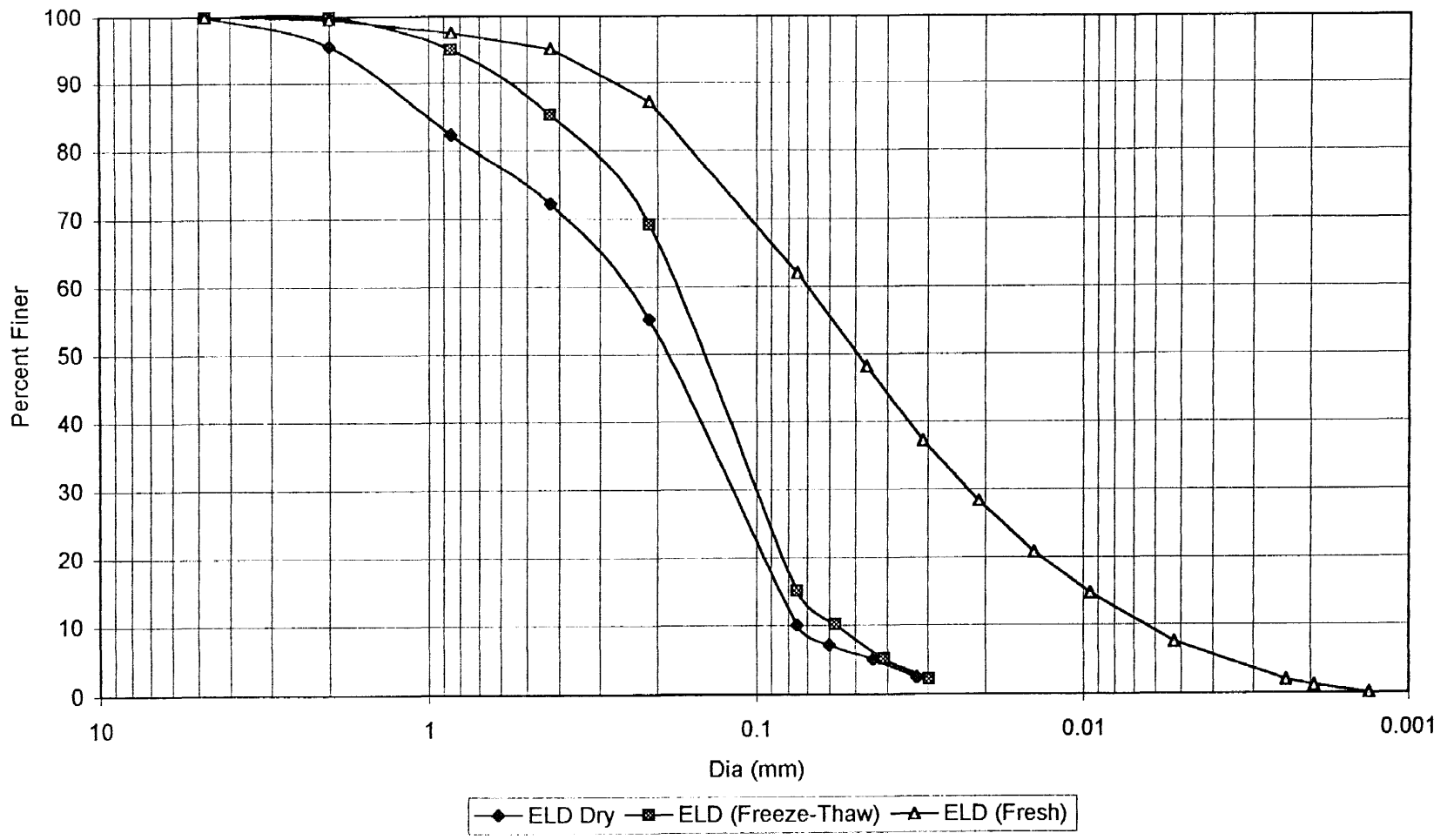


Figure 4.5 Grain Size Curve Depicting Increase in Size of Particles due to Weathering for Residual ELD

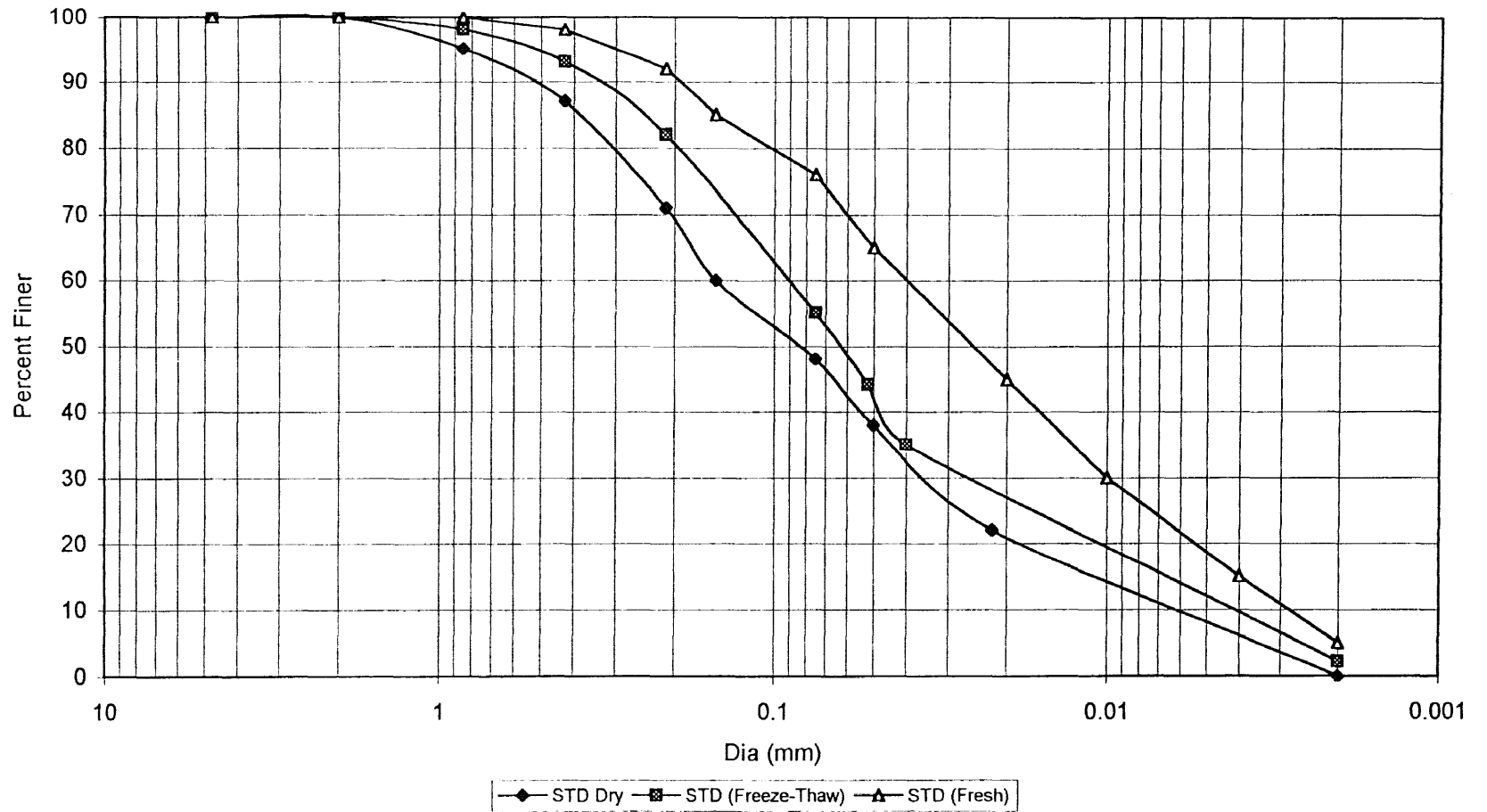


Figure 4.6 Grain Size Curve Depicting Increase in Size of Particles due to Weathering for Residual STD

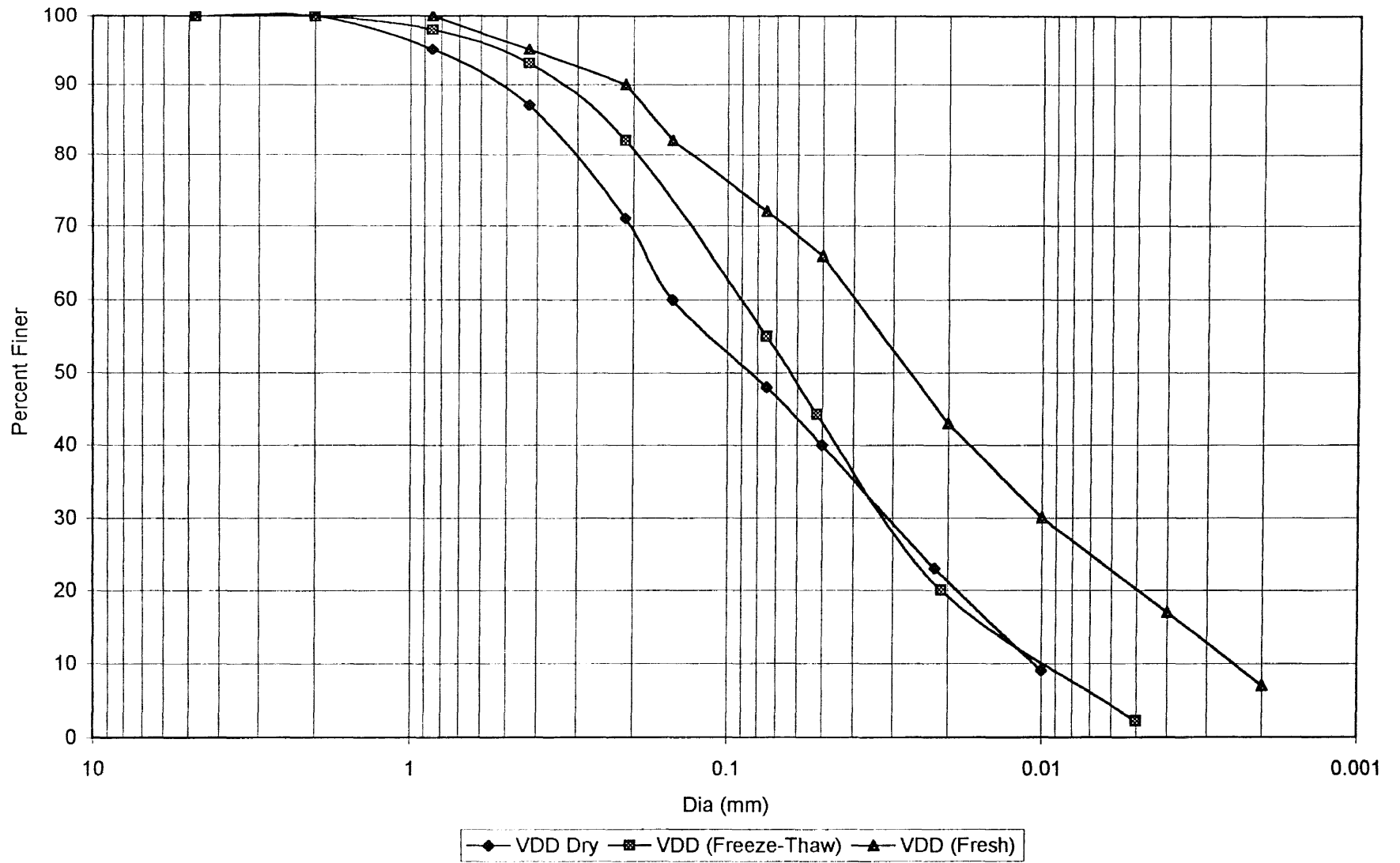


Figure 4.7 Grain Size Curve Depicting Increase in Size of Particles due to Weathering for Residual VDD

4.7 Compaction Characteristics

The compaction characteristics for the residuals were determined by performing standard proctor tests. These tests were carried out both on the fresh residuals, by decreasing water content (wet to dry) and by increasing water content (dry to wet). Figure 4.8 to 4.13 show plots of dry density with water content. Table 4.7 summarizes the values of maximum dry unit weights and the corresponding optimum moisture contents and the degree of saturation for all the residuals obtained from these tests.

Table 4.7 Compaction Characteristics of WTP Residuals.

Residual Type	Dry to Wet			Wet to Dry		
	OMC(%)	Maximum Unit Weight (kN/m ³)	S _r (%)	OMC(%)	Maximum Unit Weight (kN/m ³)	S _r (%)
HWD	75	7.22	90.86	130	4.08	69.51
JCD	27	13.88	94.44	57	9.10	86.79
WQD	25	13.35	95.28	110	5.90	92.49
ELD	80	7.53	95.00	86	6.98	91.00
STD	35	12.16	96.20	46	10.30	90.23
VDD	62	8.58	96.45	94	6.30	89.20

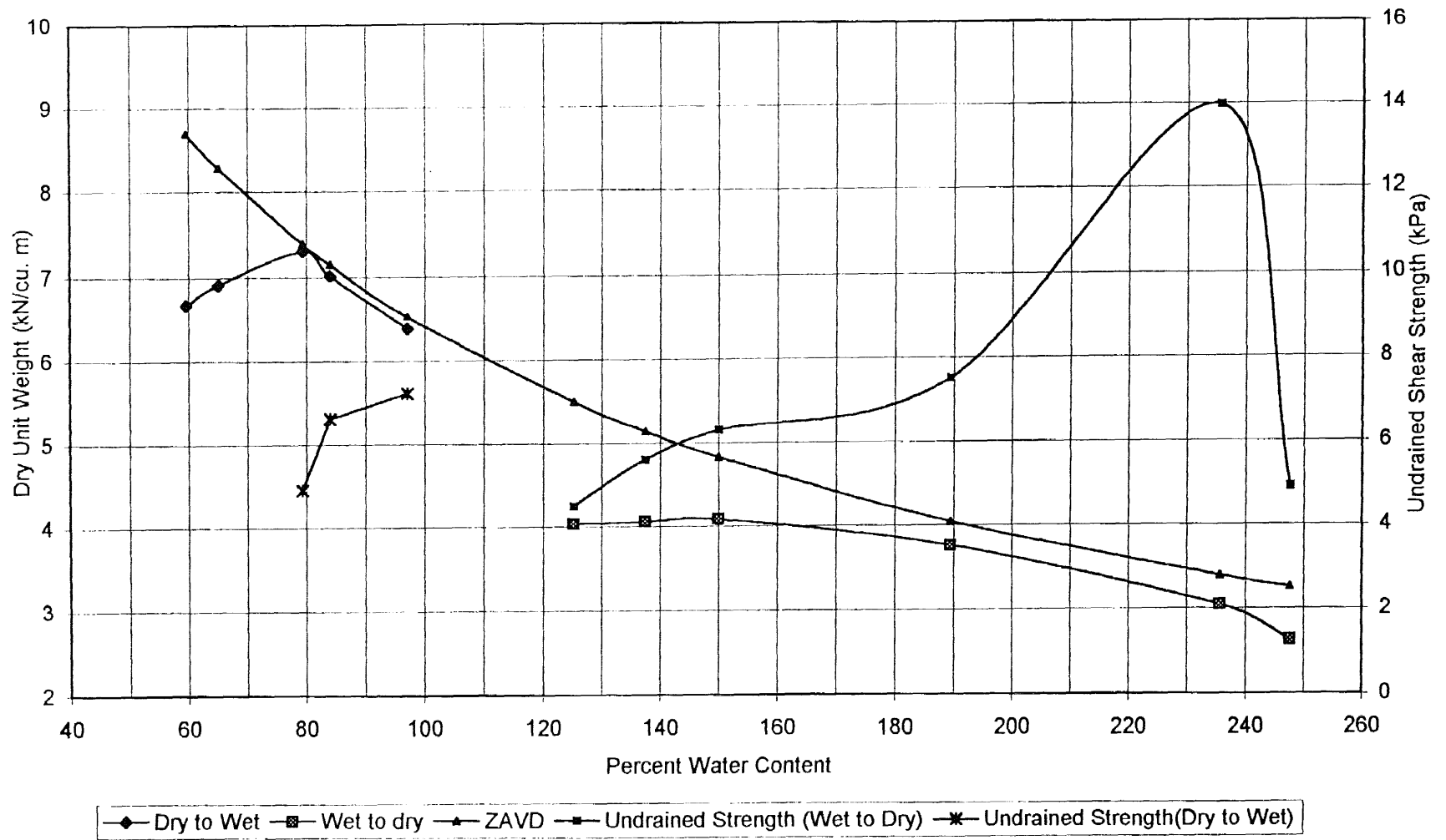


Figure 4.8 Variation of Undrained Shear Strength with Water Content and Dry Unit Weight for Residual HWD

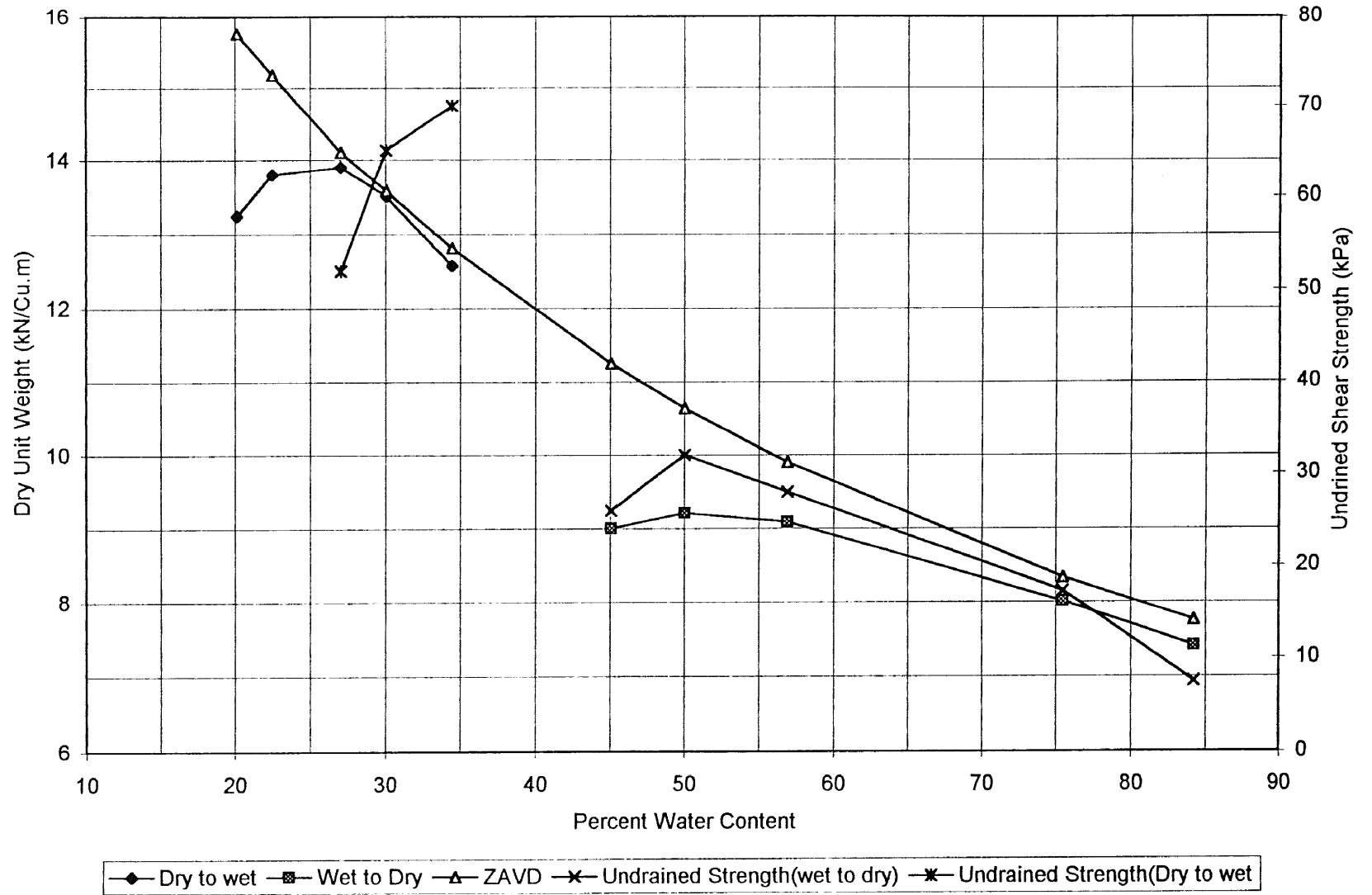


Figure 4.9 Variation of Undrained Shear Strength with Water Content and Dry Unit Weight for Residual JCD

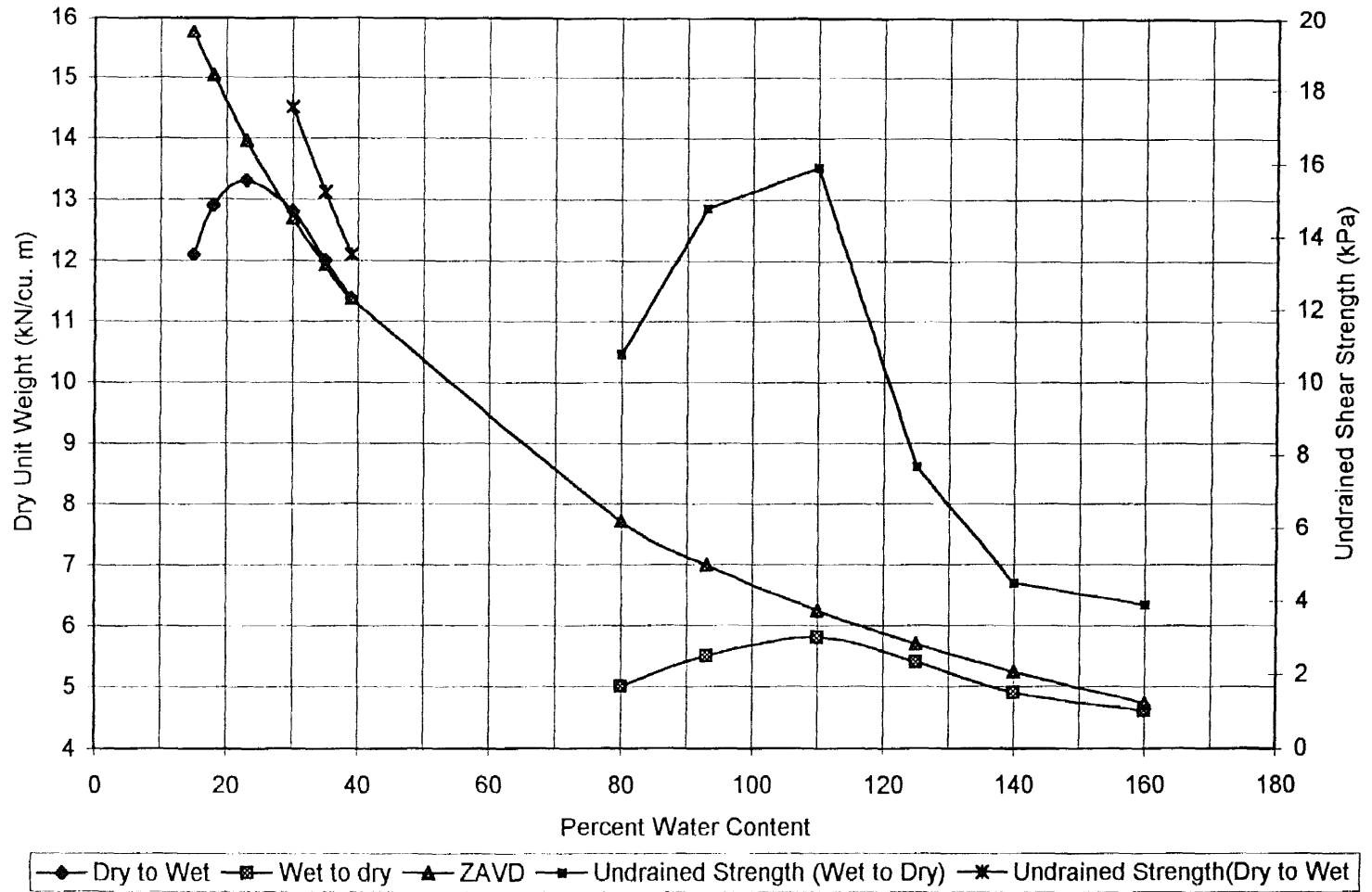


Figure 4.10 Variation of Undrained Shear Strength with Water Content and Dry Unit Weight for Residual WQD

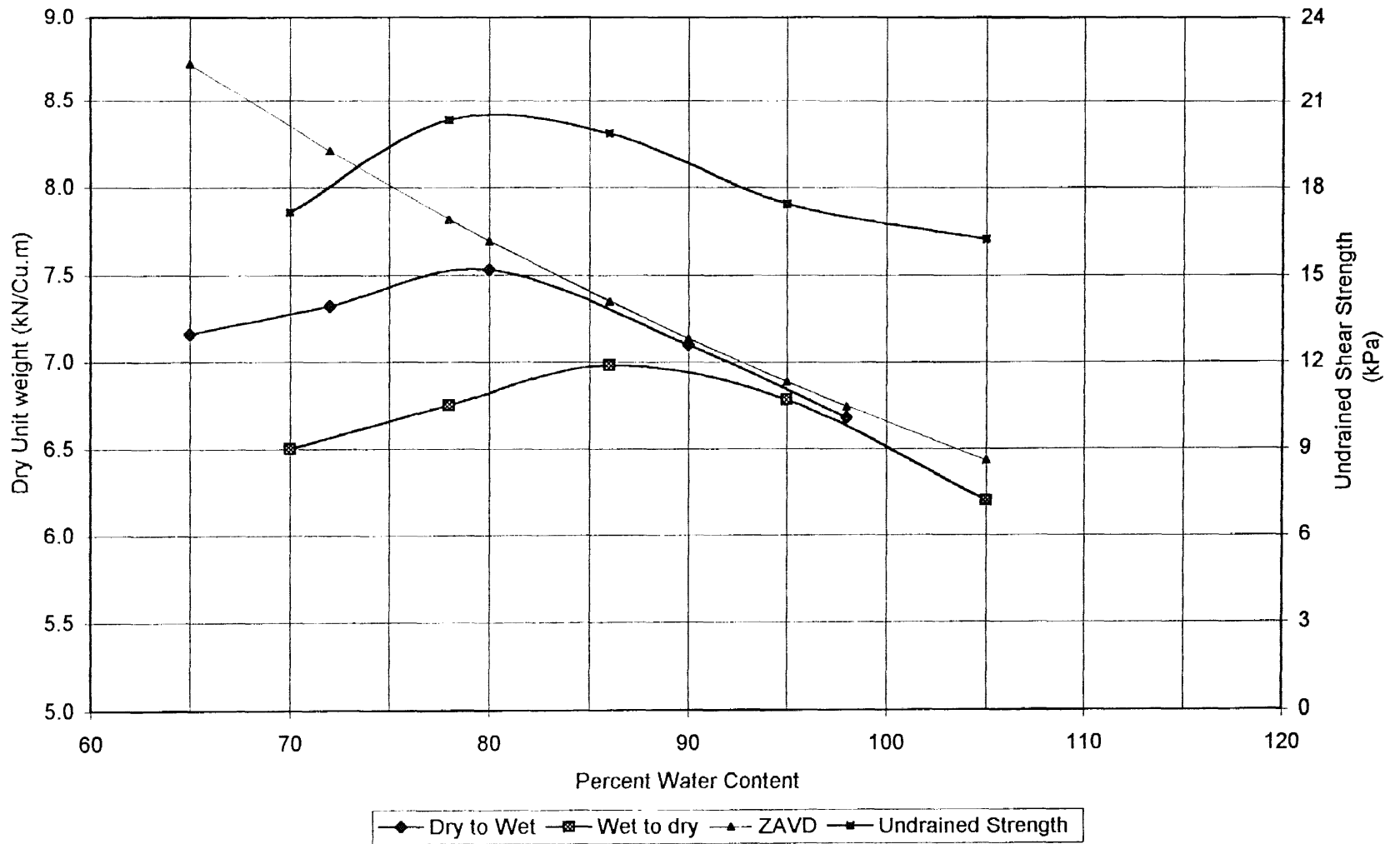


Figure 4.11 Variation of Undrained Shear Strength with Water Content and Dry Unit Weight for Residual ELD

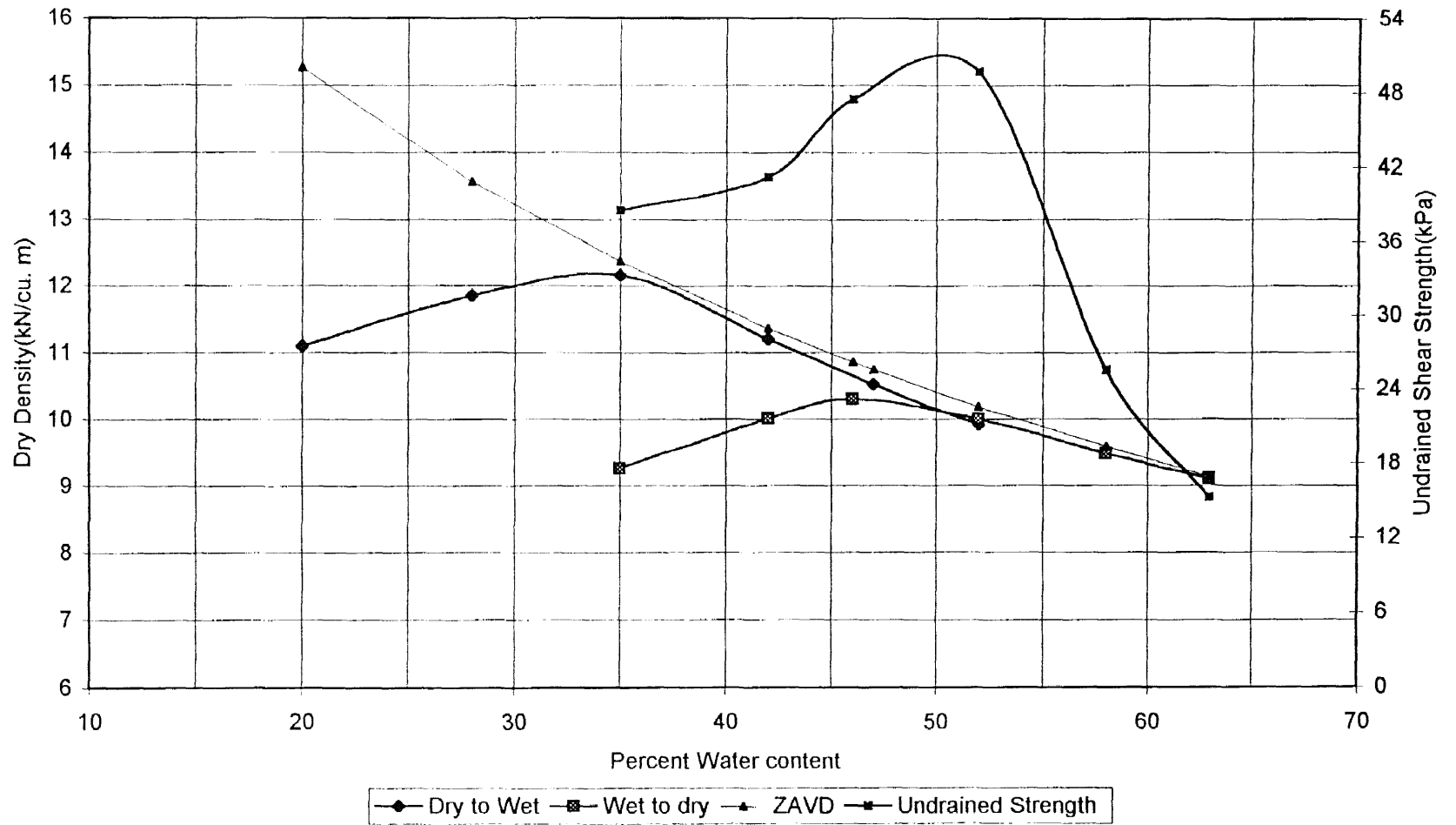


Figure 4.12 Variation of Undrained Shear Strength with Water Content and Dry Unit Weight for Residual STD

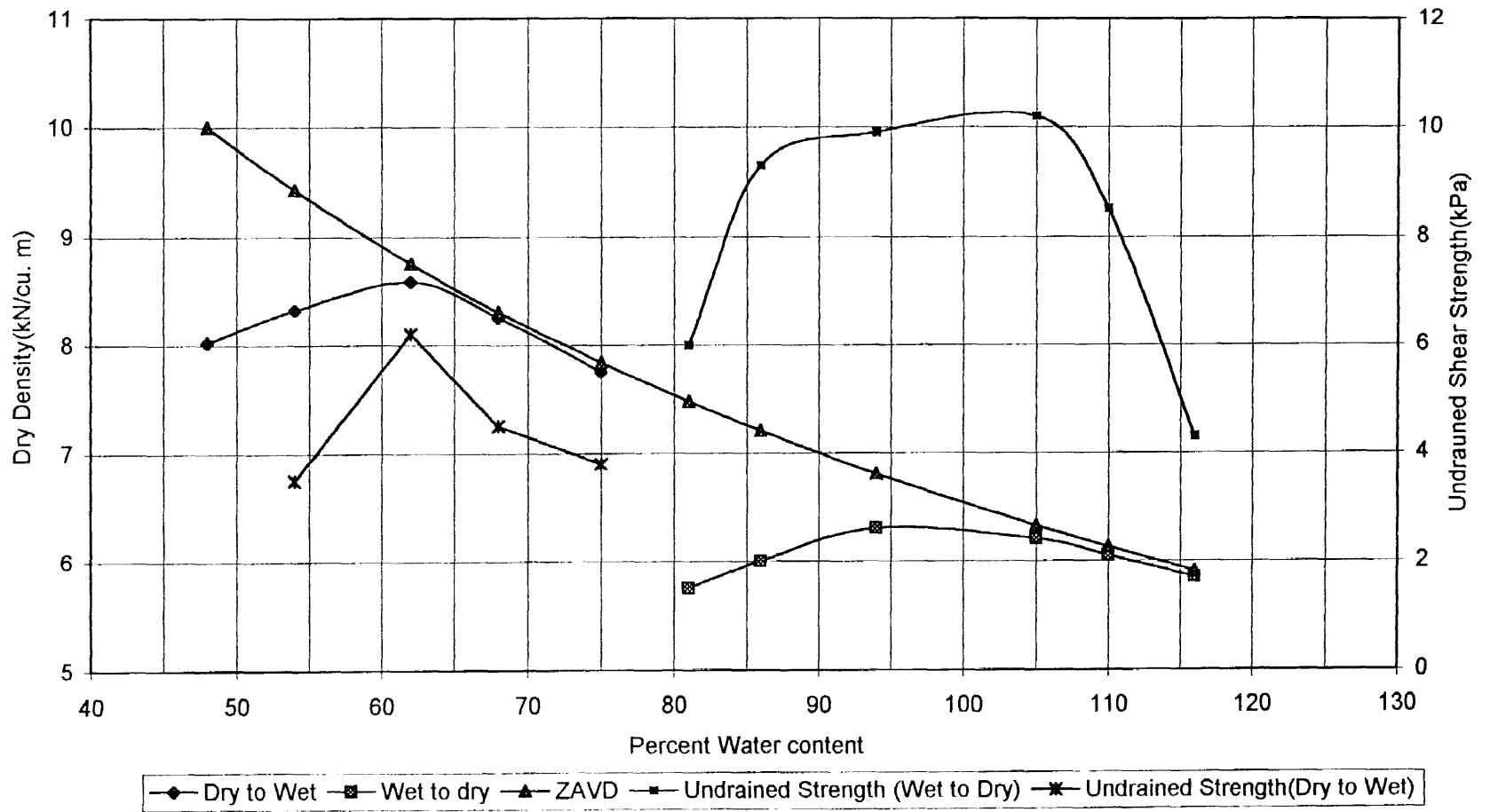


Figure 4.13 Variation of Undrained Shear Strength with Water Content and Dry Unit Weight for Residual VDD

From Figures 4.8 to 4.13 and the results presented in Table 4.7, the following observations are made:

1. For all residuals, maximum dry unit weight was greater and the OMC was lower for tests conducted under dry to wet conditions than those under wet to dry conditions did.
2. Degree of saturation values at OMC in dry to wet tests were higher than those from wet to dry tests, though values obtained for OMC were very high in wet to dry tests.

Reduction in OMC and increase in maximum dry unit weight can be attributed to the increase in particle sizes of the residuals upon drying. For all particulate materials with very fine particles, the specific surface is high and the water requirement for lubrication of all the surfaces of particles is also high. Hence, in case of WTP residuals, high values of OMC and low values of maximum dry unit weight are possible in the wet to dry tests.

The significant drop in the values of OMC and the raise in maximum dry unit weights in the dry to wet compaction tests reconfirmed the inference drawn from the results of the Atterberg limit tests that WTP residuals have transformed into coarse-grained materials. It is well known that coarse-grained soils require less water for complete saturation than that required for fine-grained materials. For example, well-graded sands (SW) can attain a maximum dry unit weight of about 19 kN/m^3 at optimum moisture content of about 13%. Silts of high compressibility (MH) can have a maximum dry unit weight of 13 kN/m^3 at an optimum moisture content of about 30%. Likewise as indicated in Table 4.7, WTP residuals possess higher optimum moisture contents in the

wet to dry tests and lower maximum dry unit weights than those in dry to wet tests. Further the degree of saturation is lower in the wet to dry state than those in the dry to wet state.

4.8 Unconfined Compression and Direct Shear Tests

Unconfined compression tests were conducted at the water contents and dry unit weights obtained from compaction tests. Cylindrical specimens of diameter 3.3 cms and length 7.04 cms were obtained by pushing Harvard miniature compaction molds into the compacted residual samples in Proctor molds. Specimens so retrieved were tested to failure at a strain rate of 5% per minute in the unconfined compression machine to prevent the loss of moisture content. Three trial tests were run corresponding to each water content and density to obtain average values.

Most of the specimens tested for unconfined strength at conditions corresponding to “wet to dry” compaction tests exhibited bulging at failure. Failure planes, in wet condition became noticeable after the samples were air-dried for about two days. These planes were inclined approximately at an angle of 45 degree with the major principal plane. Therefore the angle of friction was assumed to be zero. However, in the case of specimens tested for unconfined strength in the dry to wet procedure of compaction exhibited brittle failure and the inclination of failure planes to the major principal planes ranged from 50 to 65 degrees. The undrained shear strength (S_u) was calculated for all the cases as half the unconfined compressive strength.

The undrained shear strength (S_u) as obtained from unconfined compression tests corresponding to the dry unit weights and water contents of dry to wet and wet to dry compaction tests are shown in Figures 4.8 to 4.13.

From these graphs, the following trends were observed

1. In dry to wet conditions, S_u decreased with increasing moisture content and decreasing dry density for all residuals except for HWD and JCD. However, S_u for these two residuals increased with increase in moisture contents. This may be due to increased effective stress due to capillary action
2. In wet to dry tests, S_u increased with increase in moisture content upto a certain point and decreased with the further increase in moisture content. For instance, the residual HWD had an undrained strength of about 4.5 kPa at a water content of 122%. With increase in water content, S_u increased to a peak value of 14kPa at a water content of 235%, then S_u decreased to about 5 kPa at a water content of 248%%.

Shear strength parameters of the residuals for water contents corresponding to dry to wet method of compaction were also determined by direct shear tests. Table 4.8 presents the shear strength parameters of WTP residuals. The shear stress vs. horizontal displacement plot and failure envelope for the residual JCD at a water content of 27% and a dry unit weight of 13.9kN/m^3 are presented in Figures 4.14 and 4.15 respectively.

Table 4.8 Shear Strength Parameters Obtained from Direct Shear Tests

Residual Type	Water Content (%)	Dry Unit Weight (kN/m ³)	Cohesion (kPa)	Angle of Internal Friction (Degrees)
HWD	79	7.3	2.20	32
	84	7.0	3.5	29
	97	6.4	4.5	25
JCD	27	13.9	38.0	35
	30	13.5	41.0	31
	35	12.6	43.0	28
WQD	30	12.8	7.0	33
	35	12.0	7.5	29
	39	11.4	7.5	27
ELD	65	7.16	16.5	25
	72	7.32	18.1	20
	80	7.53	20.0	16
STD	20	11.1	--	34
	28	11.9	17.53	28
	35	12.2	38.52	20
VDD	54	8.3	2.25	26
	62	8.6	3.57	22
	68	8.3	4.9	18

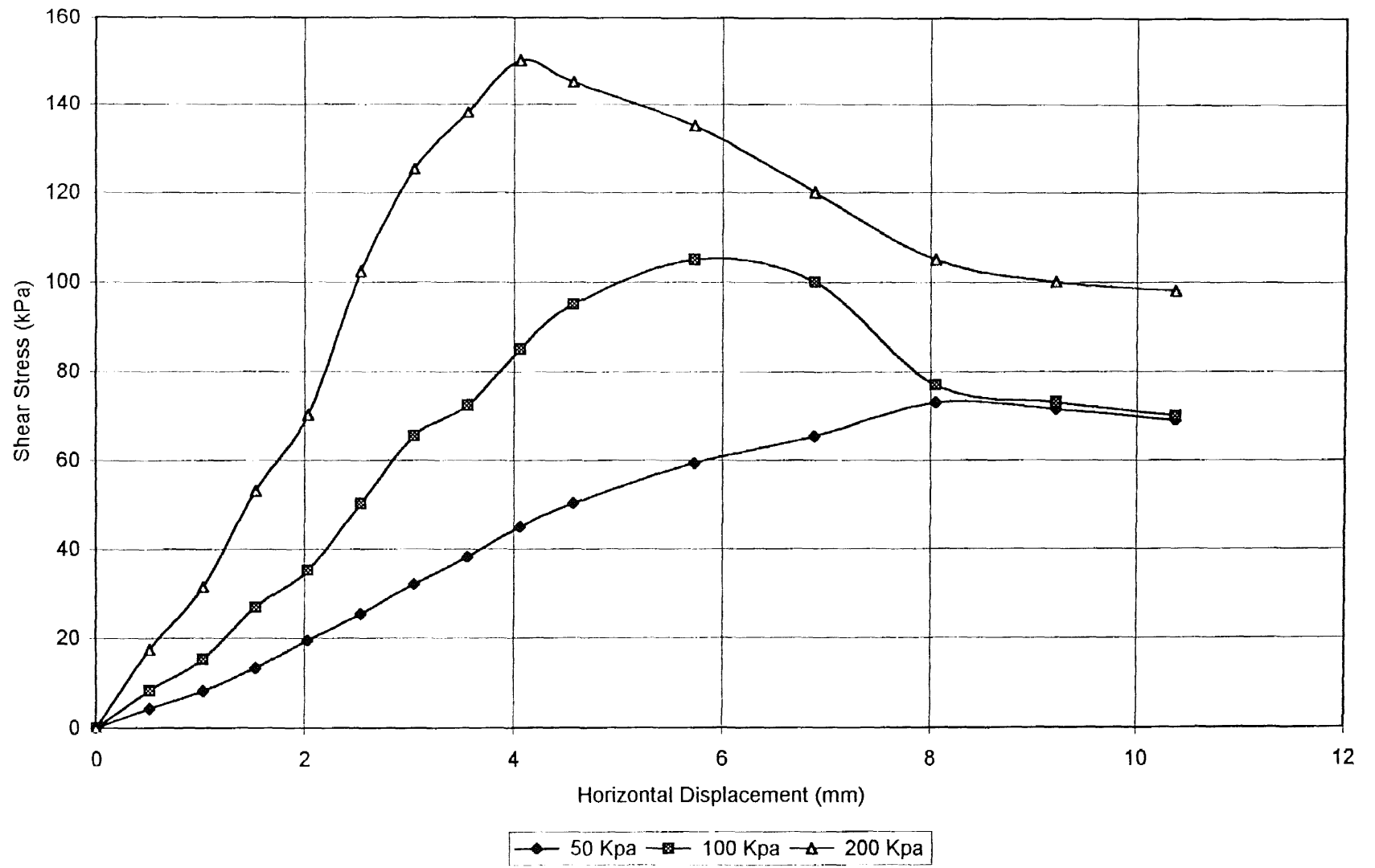


Figure 4.14 Shear Stress vs Horizontal Displacement Curves for the Residual JCD.

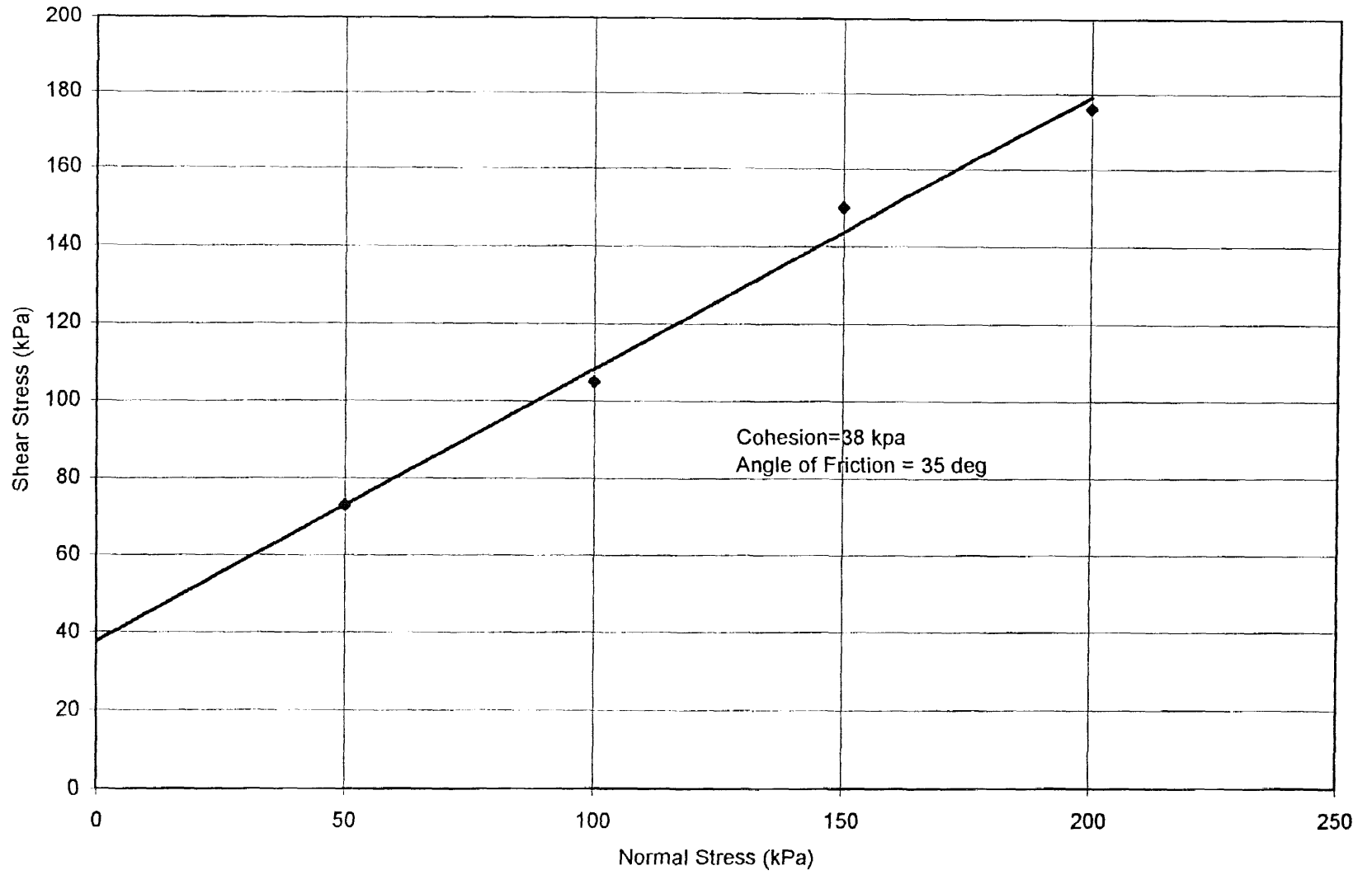


Figure 4.15 Failure Envelope for Residual JCD.

4.9 Freeze-Thaw Tests

Weight losses of the samples at the end of 12 cycles are presented in Table 4.9. In addition, cracks formed on the surface of most samples. Finally, the surface of the material became dry, loose, crispy, and even sprawled off. Cylindrical specimens of residuals that have experienced large reductions in volume and weight crumbled to many pieces.

It can be inferred that the initial water content influenced the weight loss after twelve cycles. Residual specimens with high initial water contents experienced high losses in weight while low weight losses were observed for samples with low initial water contents. For example, the residual WQD with the molding water content of 569% experienced a weight loss of 82.6%, whereas the residual JCD with the molding water content of 72% experienced the weight loss of 40.5%. This indicates that the major cause of weight loss during freeze/thaw was the moisture loss caused by evaporation.

When a residual is being frozen and or being dried, inorganics will come out of the solution. These substances may cause cementation and increase in particle size. Freezing of water is always associated with increase in volume and the overall increase is about 9% (Mitchell 1993). Volume expansion caused by freezing of water will cause some of the unfrozen water in the residual to squeeze out due to increased permeability. This increased permeability may also be due to increased grain size caused by cementation. These phenomena cause both volume and weight reduction of residuals. Since the cylindrical specimens of residuals in our study cracked and crumbled the volume changes could not be measured. But the percentage weight loss based on the total initial weight were recorded in Table 4.9

Table 4.9 Freeze-thaw test results of water treatment plant residual samples

Residual Type	Molding Water Content(%)	Molding Dry Unit weight(kN/m ³)	Solids Content (%)	Weight loss (%) Based on total weight
HWD	286	2.50	25.9	72.5
JCD	72	8.4	58.1	40.5
WQD	569	1.58	14.9	82.6
ELD	402	2.17	19.9	78.5
STD	197	4.07	33.7	69.5
VDD	215	3.73	68.5	68.5

4.10 Chemical Composition of WTP Residuals from XRF

The chemicals added to thicken and condition the residuals brings about changes in their chemistry. In order to determine the effects of normal air drying, freezing, and thawing conditions on the chemical composition of the residuals, representative samples were analyzed using wavelength X-ray fluorescence spectrometry (XRF). Table 4.10 shows average percentile concentration of compounds present in the residuals HWD, JCD and WQD in their fresh, air dried, and freeze/thaw conditions as determined by XRF.

From the data presented in Table 4.10, it can be noted that there is no significant variation in the chemical compositions of residuals in their fresh, air dried and freeze-thaw conditions with the exception of iron oxide. It is believed that iron oxide, upon release from solution, may have formed different complex compounds with organic matter, which may not have been detected by XRF tests. Calcium and aluminum

compounds together with organic matter which are thought to be responsible for cementation and grain growth remain unaltered after drying and weathering due to freeze-thaw. Thus, it can be inferred that air-drying and freeze/thaw processes do not leach metals appreciably. In such cases, the metal ions have to remain within the floc structure of the residual, which causes cementation and the increase in particle size.

Table 4.10. Percentile Chemical Composition of WTP Residuals as Determined by XRF

Residual	HWD			JCD			WQD		
	Fresh	Air-Dry	Freeze/Thaw	Fresh	Air-Dry	Freeze/Thaw	Fresh	Air-Dry	Freeze/Thaw
MgO	0.85	0.88	0.92	0.54	0.52	0.542	0.25	0.22	0.23
Al ₂ O ₃	15.18	16.99	17.829	8.66	7.49	8.649	25.43	28.46	23.65
SiO ₂	9.98	10.37	10.749	7.41	9.20	6.80	8.09	9.15	9.06
P ₂ O ₅	1.13	0.97	0.974	0.22	0.24	0.19	0.96	0.81	0.58
SO ₃	2.30	1.72	1.047	0.73	0.85	0.69	2.41	2.15	1.52
K	0.87	0.73	0.44	0.44	0.48	0.33	0.07	0.17	0.09
CaO	8.07	7.00	7.04	39.64	38.05	30.95	1.92	1.43	0.90
TiO ₂	0.52	0.36	0.19	0.33	0.39	0.25	0.03	0.08	0.07
MnO ₂	3.83	1.77	1.94	0.50	0.21	0.28	5.77	4.64	3.23
Fe ₂ O ₃	14.04	5.69	4.86	6.61	4.41	3.80	5.47	3.64	2.88
CuO	1.39	0.33	0.30	0.03	0.02	0.03	0.05	0.03	0.02
ZnO	0.09	0.03	0.028	0.04	0.02	0.02	0.05	0.03	0.02
PbO	0.18	0.03	0.028	traces	traces	0.011	traces	0.01	traces

It is to be noted here that the compounds and their concentrations shown in Table 4.10 are merely indicative of the elements are present. In residuals, except silica, all

compounds occur either in the form of hydroxide and carbonates but not as oxides. Thus the data obtained from the software of XRF and presented in Table 4.10 only gives the clue as to what inorganic compounds are present in the residuals.

From the results presented in Table 4.10, it can be inferred the chemical composition of WTP residuals unaltered after drying and subjected to freezing and subsequent thawing. Further it can be seen that alumina contents in the residuals WQD and HWD are about 17% and 27% indicating that the treatment uses alum as a conditioner. The residual JCD has very high concentration of Calcium of about 31% indicating that the treatment plant utilizes very high dosage of lime as coagulant in the treatment of water and as a conditioner to thicken the residual.

4.11 X - Ray Diffraction Studies of the Residuals

XRD analyses on the residuals were carried out to determine qualitatively as to whether the WTP residuals contained any clay minerals or not. Tests were carried out first without removing organic matter and then by removing organic matter. Presence of organic matter produced broad X-ray diffraction peaks, increased the background and inhibited dispersal of other minerals as evidenced in the diffractogram of the residual sample JCD presented in Figure 4.16. As the residuals were rich in organic matter, low temperature ashing technique was used to remove organic matter (Moore and Reynolds, 1996).

With the set up of XRD used for this study, quantitative analysis was not possible and the results are only qualitative. Figures 4.17, 4.18 and 4.19 show the X-ray diffraction patterns for the three residuals (HWD, JCD and WQD) considered for this

study. Peaks of these patterns matched with the peaks of the minerals/compounds shown in Table 4.11. By studying the results presented in Table 4.10 and 4.11, both XRF and XRD have identified silica in the three residuals chosen for the study. XRF results indicate the presence of alumina (Al_2O_3) in all the three residuals HWD, JCD and WQD. XRD detected alumina only in HWD and WQD. Alumina has also been detected in XRF.

Table 4.11 Minerals/compounds as identified by XRD

Sl No	Mineral/Compound	HWD	JCD	WQD
1	Quartz (SiO_2)	Present	Present	Present
2	Graphite(C)	Present	Present	Present
3	Alumina (Al_2O_3)	Present	---	Present
4	Ringwoodite (Mg,Fe) 2SiO_4	---	---	Present
5	Rhodochrosite (MnCO_3)	----	---	Present
6	Calcite (CaCO_3)	----	Present	----
7	Hercynite (FeAl_2O_4)	----	Present	----

XRD detected a non-clay mineral *hercynite* (FeAl_2O_4) in the residual JCD. This was not observed from the results of XRF. Calcium was detected in XRF analyses in the form of oxide in all the three residuals. XRD showed the presence of calcium in the form of calcium carbonate in the residual JCD. Some of the differences in results between XRD and XRF analyses may be due that drying the sample at 105°C will not remove organics fully. It was also found that none of these residuals contain clay minerals and hence plasticity of residuals is only due to the organic matter.

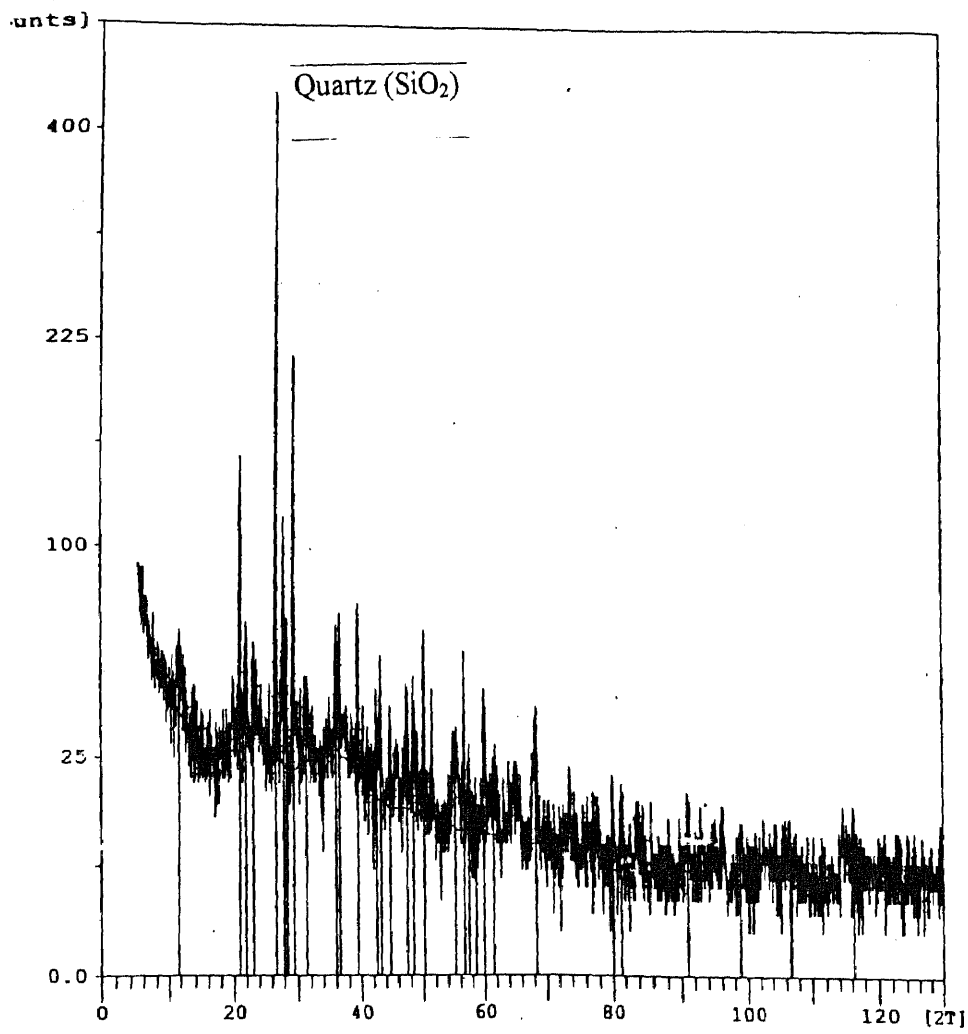


Figure 4.16 X-ray Diffractogram for Residual JCD Prior to the Removal of Organics

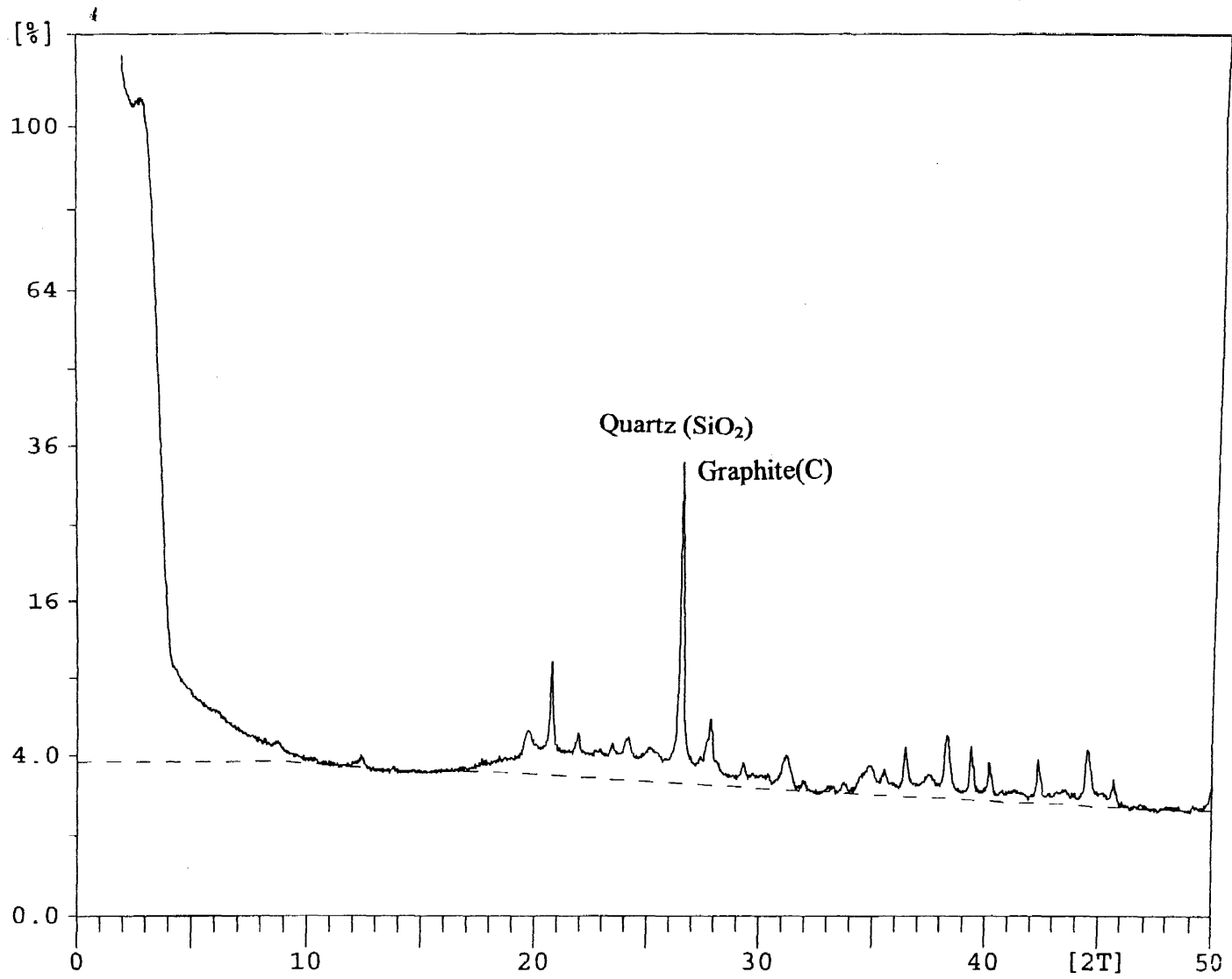


Figure 4.17 X- ray Diffractogram for Residual HWD after Drying at 105° C.

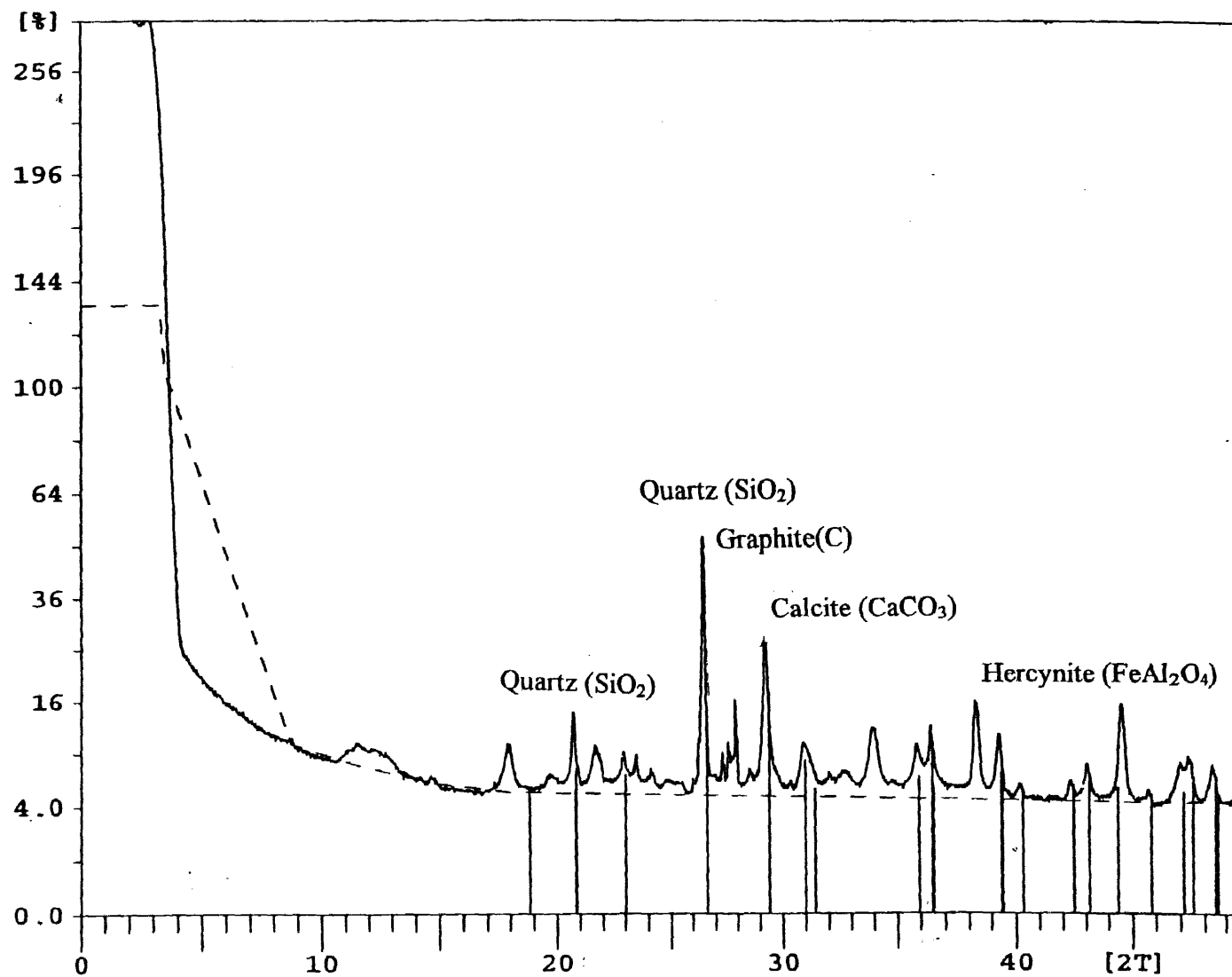


Figure 4.18 X-ray Diffractogram for Residual JCD after Drying at 105°C .

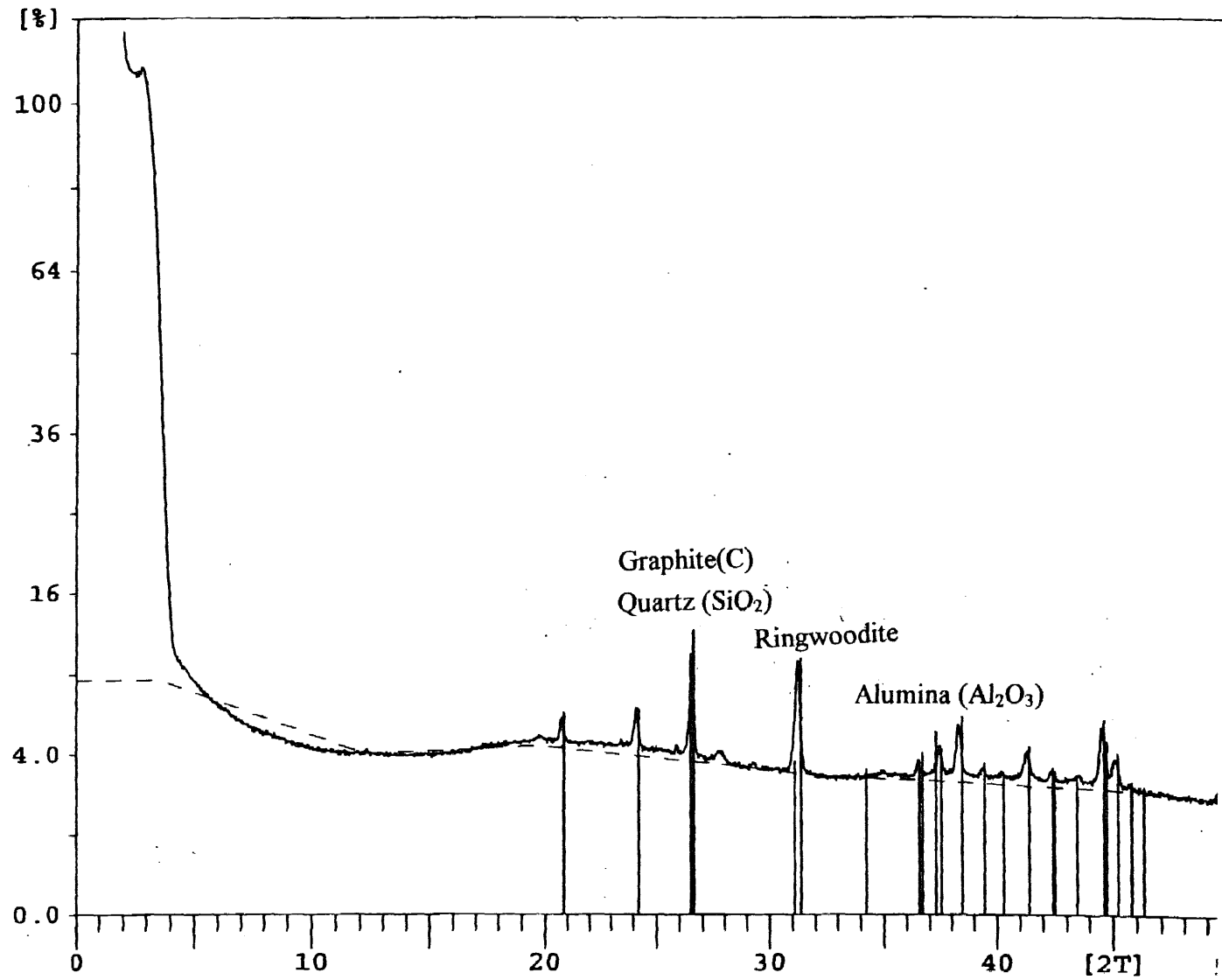


Figure 4.19 X-ray Diffractogram for Residual WQD after Drying at 105^o C.

4.12 Electron Micrographs

In order to understand the mechanisms of increase in particle size in residuals due to drying and freeze-thaw, electron micrographs of residuals were obtained. ESEM is particularly useful in materials analysis for the examination of surfaces. By supplementing this technique with compositional analysis as determined by EDX, XRD and XRF, interpretations about the microstructure were made.

Figure 4.20 is a low magnification scanning electron micrograph of the sample HWD in its frozen condition. Three distinct areas can be identified here. For the sake of convenience, these have been labeled as “A”, “B” and “C”. In region “A”, ordered structures resembling long chains can be seen. A number of organic compounds used as soil conditioners are mostly long chain compounds that attach themselves to the exchange sites and thus link together many small particles. (Kohnke, 1968). This results in increased grain sizes. In region “B”, structures with long range order resembling that of an amorphous phase is visible. The XRF and XRD analyses conducted on residuals revealed the presence of several metal oxides such CaO , Al_2O_3 , Fe_2O_3 and SiO_2 that are amorphous in nature and the results are consistent. The area in region “C” represents droplets of water arising from frozen state of the sample as has been confirmed by the supplementing techniques.

Figure 4.21 is the micrographs of the same sample HWD. This has been taken with a magnification of 1100 \times . The tubular structures believed to be organic matter are observed again. (Region “A”). Presence of these structures became more clear in Figure 4.22 as this micrograph has been captured with high magnification of 2100 \times .

Figure 4.23 shows a typical micrograph for the residual JCD. Unlike in the residual HWD, tubular structures are not present. Three distinct zones have been identified and they have been marked as “F”, “G”, and “O”.

The regions “F” are clusters of dense metallic precipitates as confirmed from the supplementing experimental techniques. The region “G” is also part of the residuals with lesser concentration of metallic precipitates. “O” is the region where higher concentrations of organic matter are observed. JCD sample has a very high concentration of calcium oxide and hence the presence of regions “F” and “G” can be explained.

A typical micrograph for the residual WQD is presented in figure 4.22. Five distinct regions have been identified. They are labeled as “A”, “B”, “C”, “O” and “V”. In zone “A”, long tubular structures were noticed. “B” is the region concentrated by amorphous like materials as confirmed by other experimental techniques. The droplets of water are labeled as “C”. The zone “V” represents voids. These voids are present in any soil-like materials. In this case, they may be due to the escape of water from the pores.

4.13 Energy Dispersive Spectrometer (EDS) Spectra

EDS spectra for residual samples, HWD JCD and WQD are presented in Figures 4.25, 4.26, and 4.27 respectively. These spectra confirm the results of XRF and XRD analyses and reinforce our interpretations of electron micrographs. For example, the large peaks of calcium for the sample JCD are consistent with the large calcium content of this sample obtained from XRF analyses. Quantitative analysis by using EDS gave the percentile composition of calcium, aluminum, silica and iron in the residual JCD as 24.42, 10.24, 12.23 and 6.12 respectively. These results are consistent with those

obtained from XRF. Results of chemical composition obtained by XRF are more representative than those obtained by EDS. EDS provides us with the concentrations of elements on the surface. Hence, the EDS spectra obtained are used only for the purposes of verifying the results of XRF analyses.

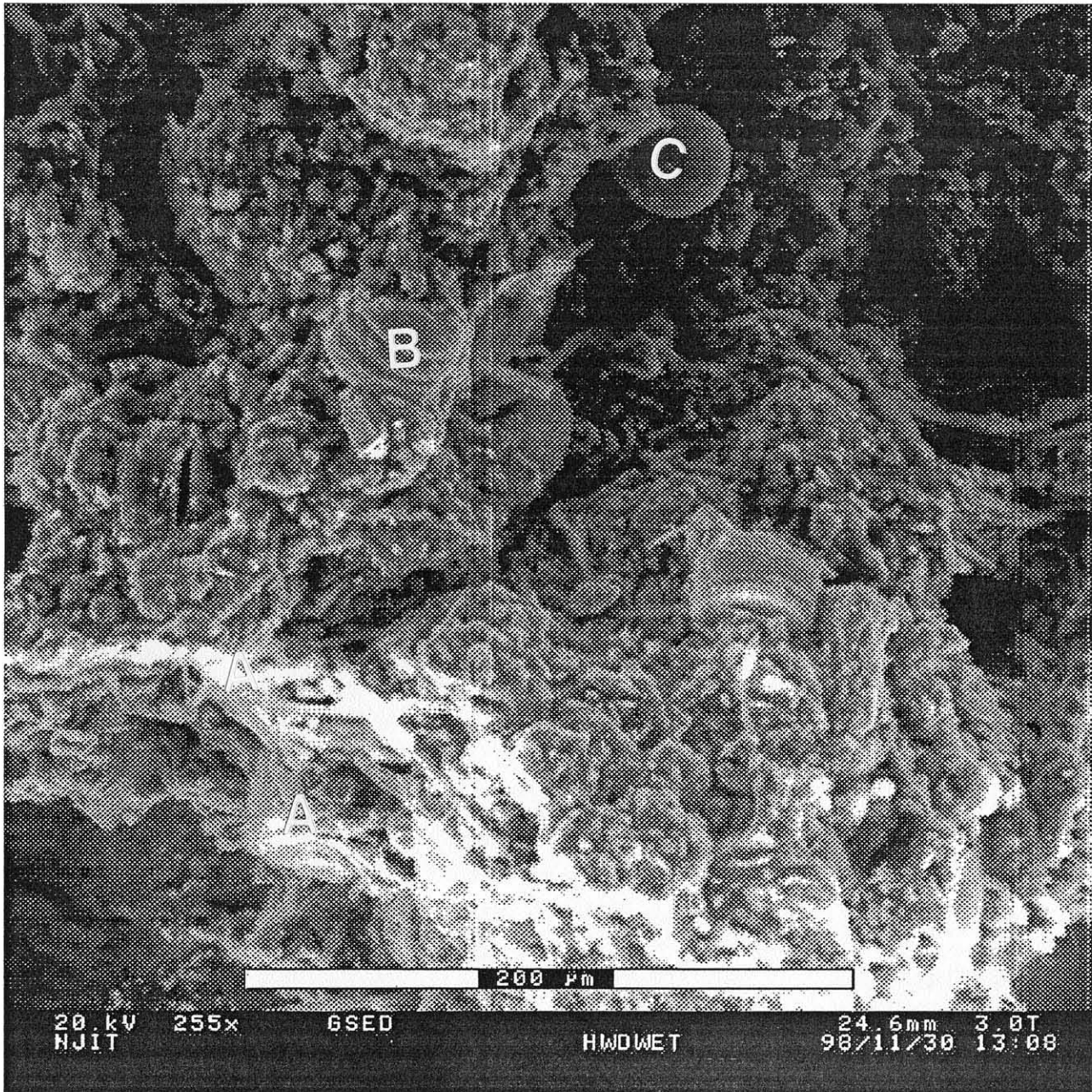


Figure 4.20 A Low Magnification Micrograph of the Residual HWD

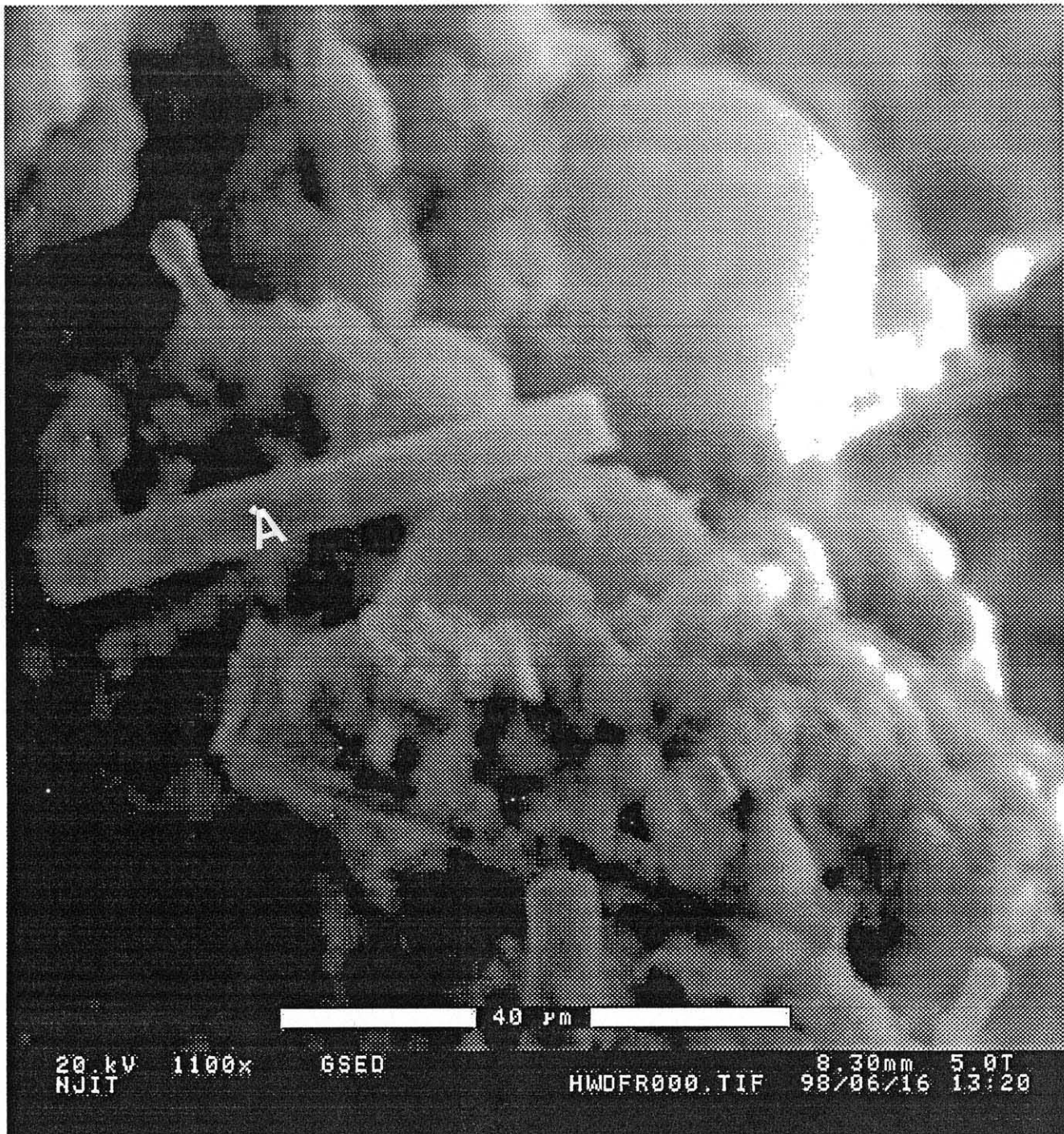


Figure 4.21 Micrograph of the Residual HWD at a Magnification of 1100x.



Figure 4.22 Micrograph of the Residual HWD at a Magnification of 2100X

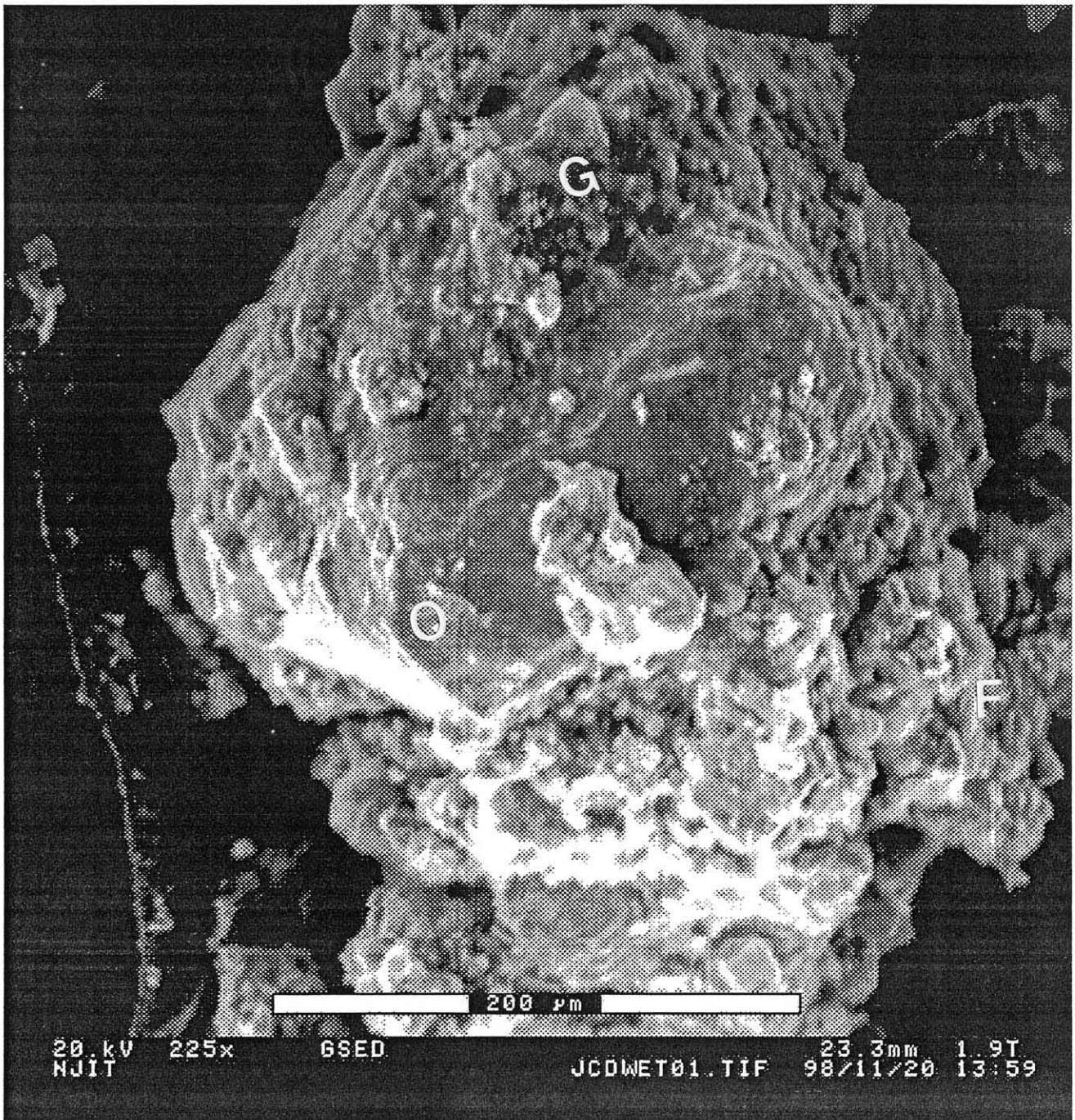


Figure 4.23 A Low Magnification Micrograph of the Residual JCD.

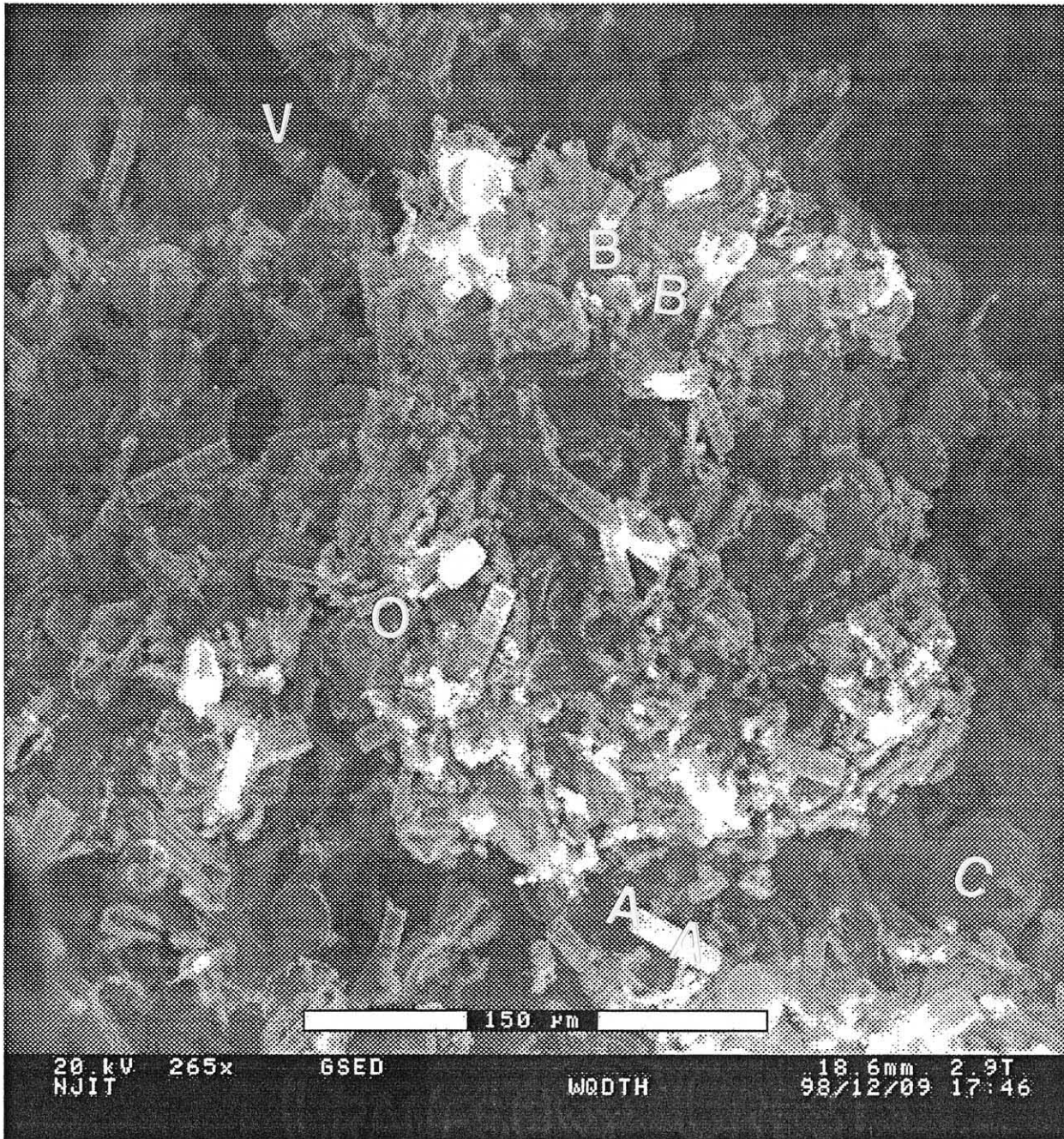


Figure 4.24 A Low Magnification Micrograph of the Residual WQD.

Spectrum: CE702BRASS

Range:20 keV

Total Counts=7828, Linear, Auto-VS=216

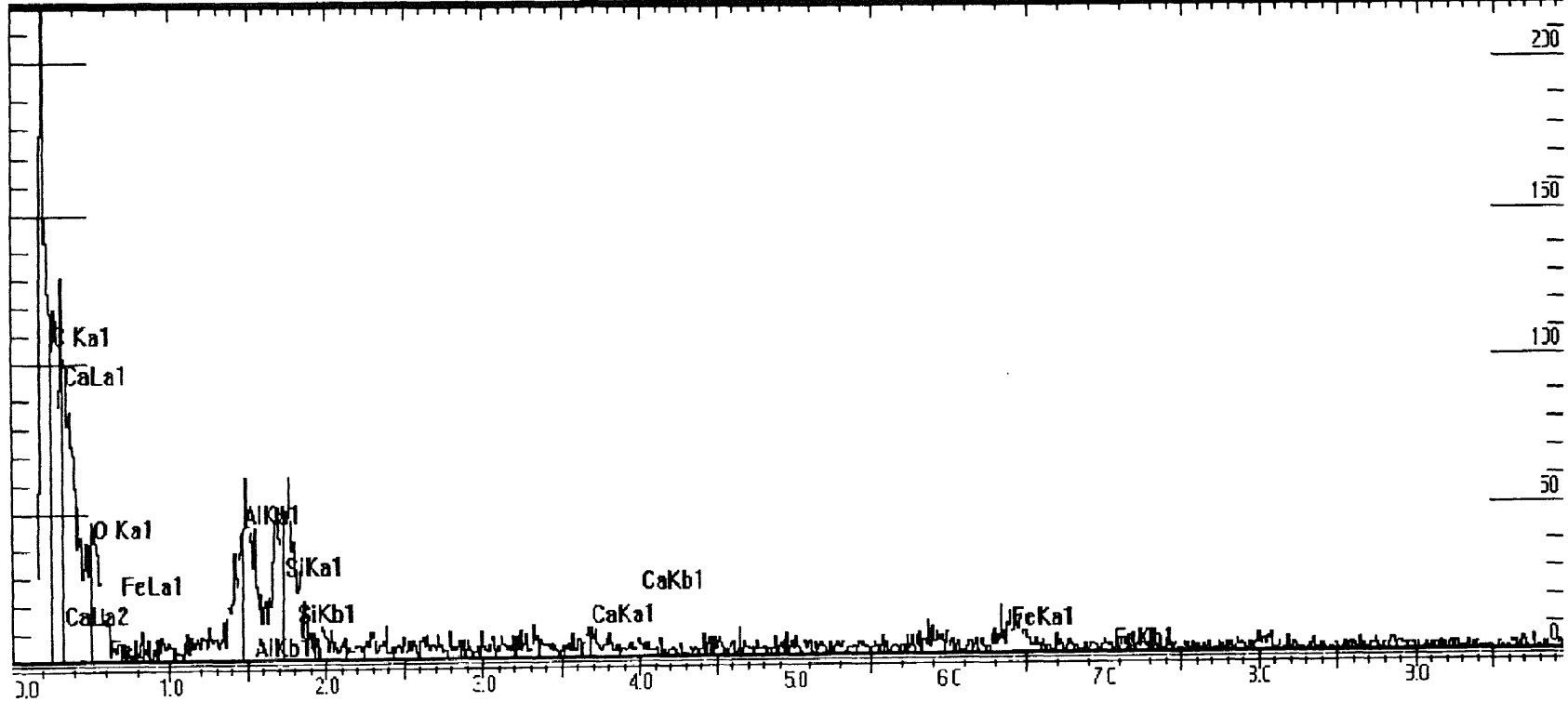


Figure 4.25 EDS Spectra for the Residual HWD

Spectrum: Spectrum1

Range:20 keV

Total Counts=10032, Linear, Auto-YS=126

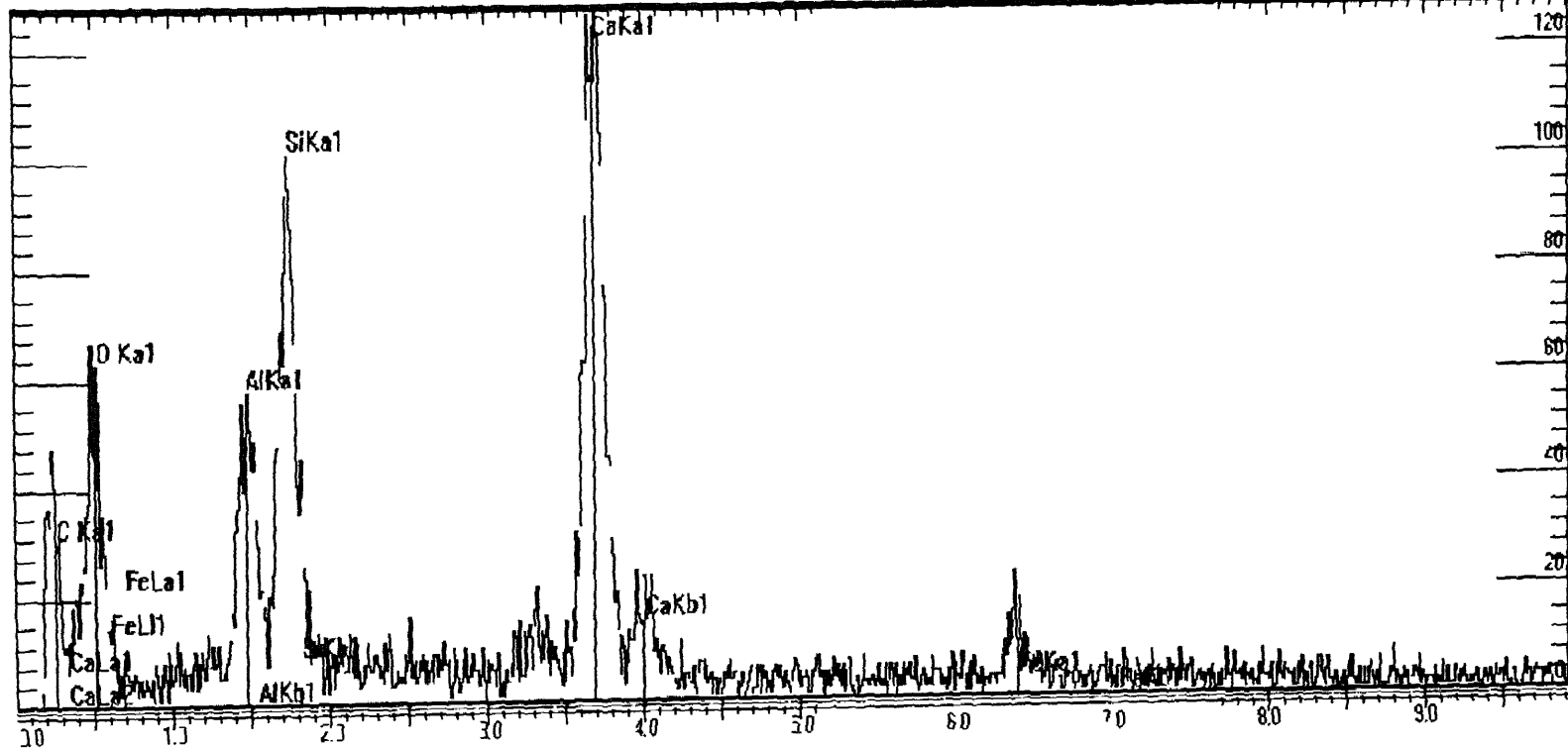


Figure 4.26 EDS Spectra for the Residual JCD

Spectrum: Spectrum1

Range:20 keV

Total Counts=9030, Linear Auto-VS=116

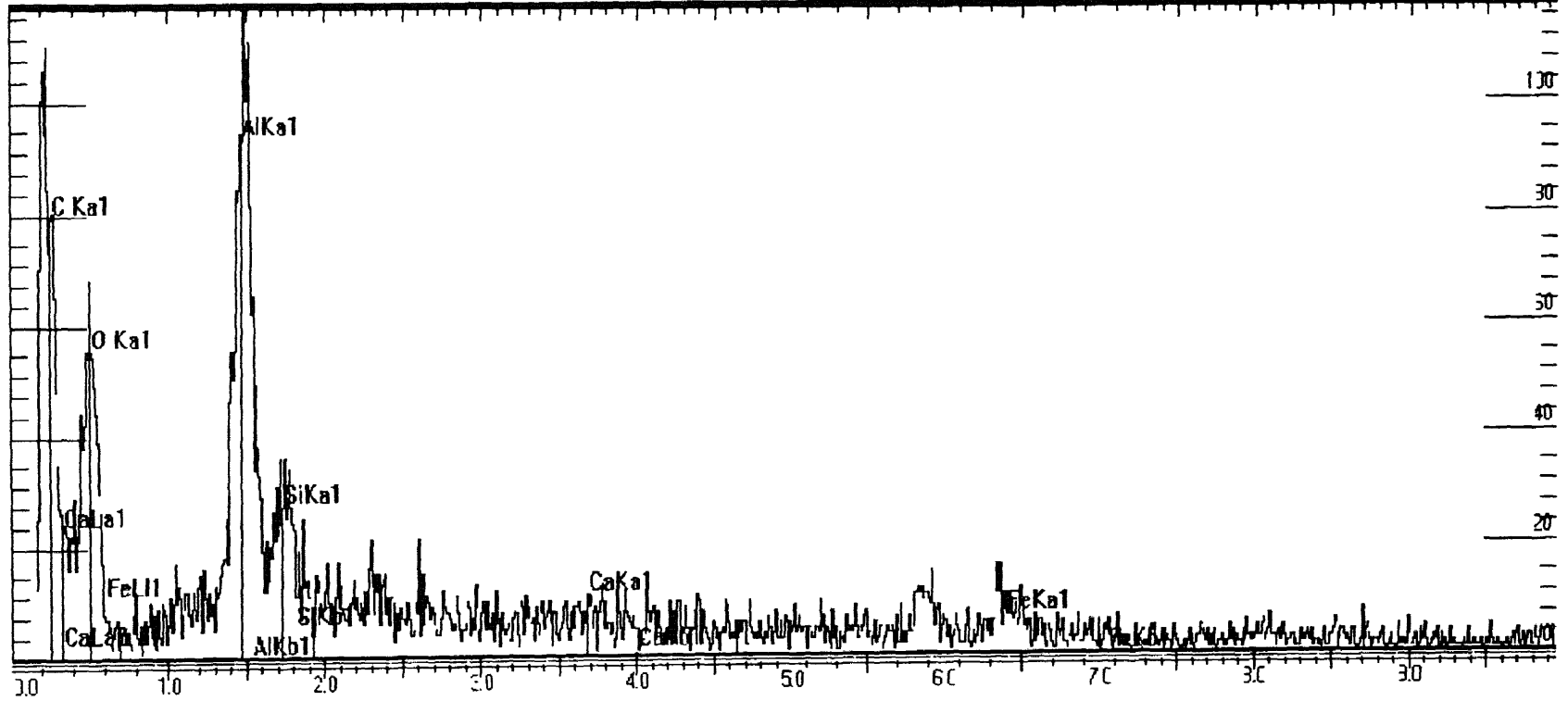


Figure 4.27 EDS Spectra for the Residual WQD

4.14 Elemental Mapping:

Determination of the Distribution of various elements over the area of the micrographs is possible with EDS (Goldstein., 1994). Figures, 4.28, 4.29 and 4.30 represent selected elemental maps of the residual samples. These maps show the presence of inorganic substances such as Ca, Al, Fe and Si. Presence of oxides of these elements has been indicated by the results of XRD and XRF analyses. The amorphous phases observed in electron micrographs may be attributed to the presence of these oxides.

4.15 Discussion on the Probable Causes and Mechanisms of Increase in Grain Size of Residuals due to Drying and Freeze-Thaw

The mechanisms responsible for growth in particle size are (1) Dehydration of residuals upon drying and (2) Change in plasticity due to change in the nature of organic matter. Van Schulenborgh, (1954), also noticed similar phenomenon which caused the increase in grain size of organic topsoil due to air-drying.

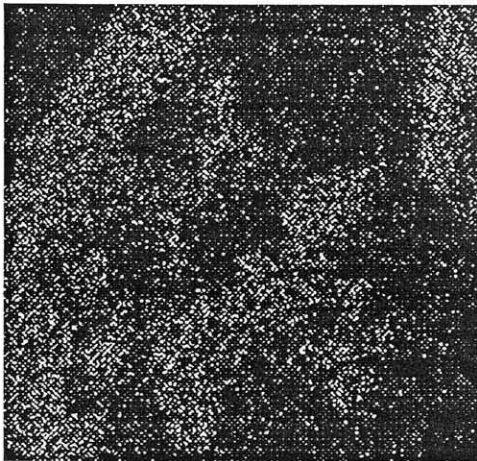
The dehydration of soil by drying: This may result in a vigorous cementing action of the colloids on the soil aggregate. The dispersion of such aggregates requires a rehydration of the colloidal particles and this rehydration may be very slow. WTP residuals contain humus, which possess gel-like properties, as stated in Chapter 1. During drying, the alteration of gel structure causes permanent reduction in volume. Moreover, air has entered the gel structure and this air can hardly be removed on re-wetting.

Schalsa and others (1965) investigated the influence of air-drying on volcanic soils from Frutillar and Santa Barbara regions of Chile. These soils were rich in organic matter. They have observed that the effect of air-drying on the sand and clay fractions was more pronounced than silt fraction. Maximum increase in sand fraction occurred in

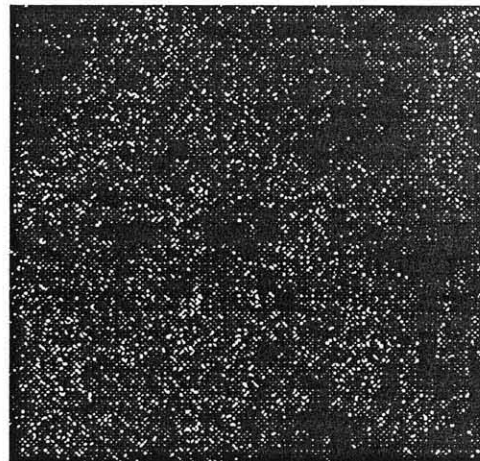
the B-horizon of the Frutillar soil and amounted to 93%. The clay fraction of the same sample decreased by 57%. On the other hand, the sand content of the A-horizon of the Santa Barbara was not significantly affected by air drying, whereas there was a 68% increase in sand fraction with the B-horizon. Air-drying decreased the silt fraction in the A-horizon of the Frutillar soil by 13%. In the Santa Barbara soil, air-drying increased the amount of silt by 10% in the A-horizon, but caused a 26% decrease in the B-horizon.

The change in plasticity may be due to a change in the nature of the organic matter. Organic matter can not be re-wetted upon drying, due to absorption of the air and polymerization of organic molecules under the influence of Al, Fe or Si compounds, so that a hydrophobic humate is formed. Both the above phenomena prevent the water from penetrating into the pores of the aggregates.

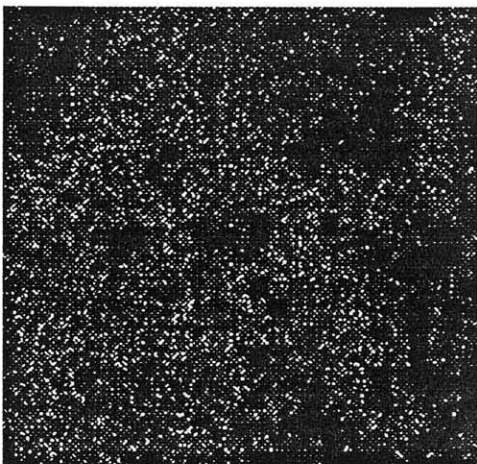
It is interesting to note that WTP residuals contain the necessary elements Al, Fe, and Si for these mechanisms stated above to have happened. Several references can be cited in which the bridging action of organic materials to form stable aggregates is indicated (Kohnke 1968, USDA Soil Survey Manual 1951). According to Berger (1965), soils with a good organic matter content and also those high in iron oxides have a good granular texture. Soils with fine texture acquire their granular structure because of the binding of the particles together by iron oxides and by gums and resins formed by the decomposition of organic matter. In this study, of the above two mechanisms cited, the binding due to iron oxide is possible, since all the three residual samples tested contained iron oxide.



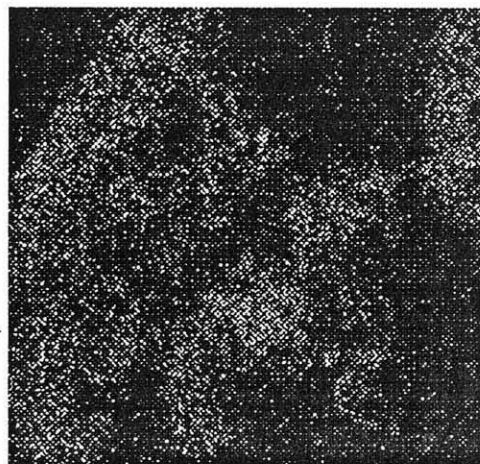
(a) Aluminum



(b) calcium

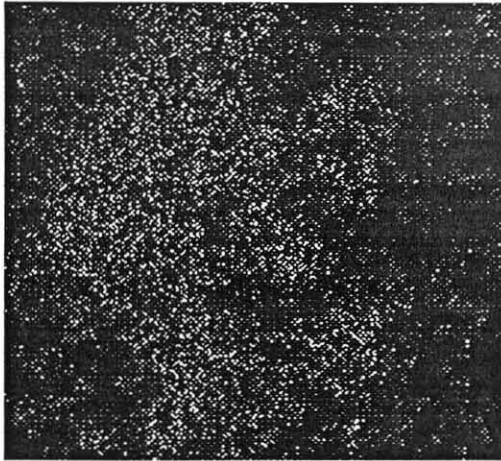


(c) Iron

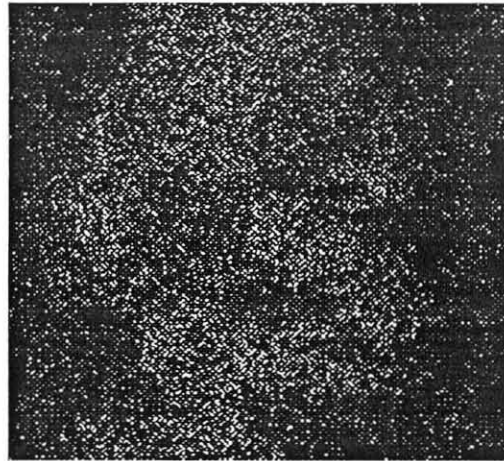


(d) Silica

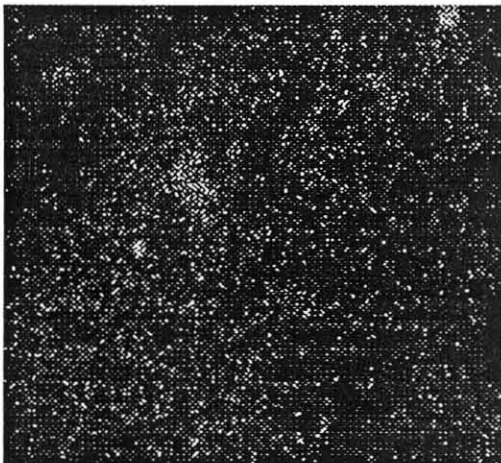
Figure 4.28 Elemental Map for the WTP Residual HWD



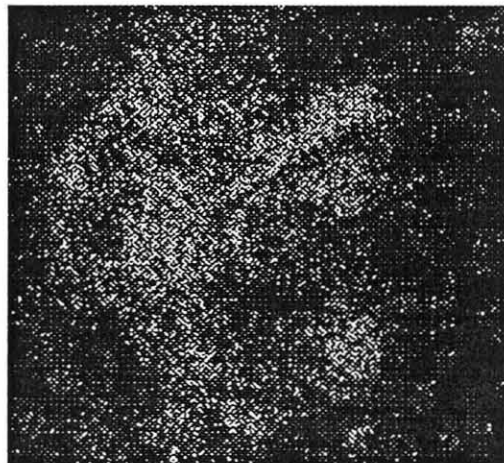
(a) Alumina



(b) Calcium

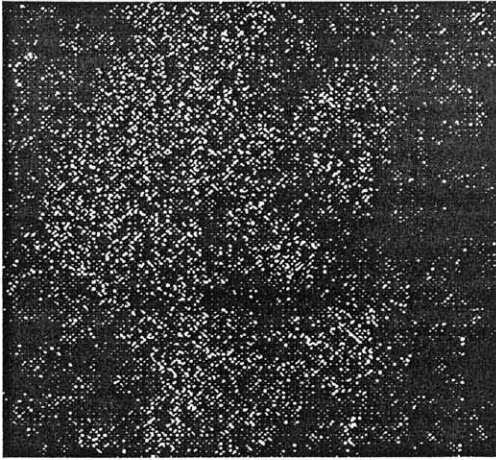


(c) Iron

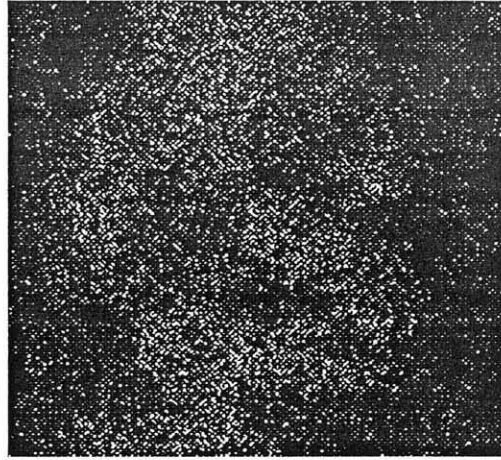


(d) Silica

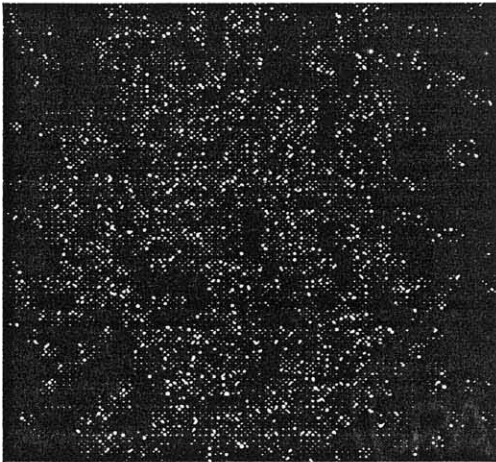
Figure 4.29 Elemental Map for the WTP Residual JCD



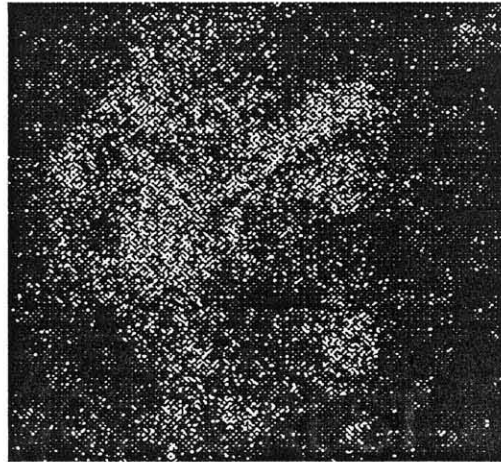
(a) Aluminum



(b) Calcium



(c) Iron



(d) Silica

Figure 4.28 Elemental Map for the WTP Residual WQD

Weil (1998) offers the following explanation for cementation which is the result of dehydration and loss of plasticity. During flocculation, individual colloidal particles coagulate together into tiny clumps or floccules. The floccules can then be bound together by cementing agents such as the microbial polysaccharides or iron oxides to form the stable aggregations in the topsoil. Once again, this mechanism is also possible for the three residual samples utilized for this study, since these samples contained iron oxide.

References regarding topsoil and organic matter have been cited in the above section to describe the phenomenon occurring in WTP residuals. The source of WTP residuals is the raw water in the reservoirs. This water is due to run-off from the catchment area of the reservoir. This run-off carries with it the topsoil, rich in organic matter and the erodible silt-sized particles. In order to understand the nature, composition and behavior of solids in the WTP results, it is quite logical to investigate the topsoil.

The mechanism of cementation due to organic matter can be utilized to explain the increase in particle sizes of the residuals HWD and WQD. The sample JCD has a significant amount of lime content. This compound causes cementation, similar to that of lime stabilization. Therefore the significant increase in grain size of JCD samples can be attributed to the presence of organic contents and calcium oxide. Other residuals HWD and WQD also contain metallic oxides in small quantities and hence the dominant cause for increase in grain sizes for these samples can be attributed to cementation by organic contents.

CHAPTER 5

CONCLUSIONS AND RECOMMENDATIONS FOR FURTHER STUDY

5.1 Conclusions

Based on the results of this study, the following conclusions have been drawn:

1. After the residuals are subjected to drying and freeze-thaw conditions, grain sizes of the WTP residuals increase. Plasticity of the residuals decrease and the materials become granular. Specific gravity of solids increases.

2. Effects observed under item 1 above can be attributed to cementation due partly to organic matter and partly due to oxides such as calcium oxide, aluminum oxide and ferric oxide present in the residuals.

3. The water content Vs dry unit weight curves for the residuals are bell shaped with a definite peak in the dry to wet tests, where as in the wet to dry tests these curves are of odd shape without a definite peak. In the dry to wet tests, the residuals attained higher dry unit weights at lower optimum moisture contents than those obtained in wet to dry tests.

4. Undrained shear strength of all residuals excepting JCD “wet to dry” conditions were greater than those obtained during “dry to wet” conditions.

5. Chemical composition of fresh residuals is almost the same as those for dry residuals and for those subjected to freeze-thaw conditions.

6. Organic contents of dry residuals are almost the same as those subjected to freeze-thawed conditions.

7. X-Ray Diffraction studies showed the presence of no clay minerals in the three residuals considered for this study.

9. Organic matter present in the residuals made it difficult to obtain X-ray diffractograms and Electron micrographs of fresh residual samples could not be obtained since samples of fresh residuals desiccated immediately upon placement inside the ESEM.

5.2 Suggestions for Further Study

Following are the suggestions for the study with WTP residuals.

1. In order to obtain information regarding the microstructure of fresh residuals, X-ray Absorption Fine Structure (XAFS) tests have to be performed on fresh, dry and freeze thaw residuals. The distribution of organic matter and the metal oxides will have to be observed.
2. Detailed investigations regarding the nature and composition of organic matter should be undertaken.
3. Techniques will have to be developed to look at the amount and distribution of water in the residuals subjected to different conditions.

REFERENCES

- Alvi, P. M., and K.H., Lewis. 1986. "Geotechnical Properties of Industrial Sludge". *International Symposium on Environmental Geotechnology*, 1 and 2: 57-76.
- ASTM. 1995. Annual Book of ASTM Standards, Philadelphia, PA.
- AWWA. 1978. Water Treatment Plant Sludges - An Update of the State of the Art: Part 1. Committee Report. *Jour. AWWA*, 70(9): 498-503.
- AWWA. 1981. Lime Softening Sludge Treatment and Disposal. Committee Report. *Jour. AWWA*, 71(11): 600-608.
- Berger, and Kermit C., 1965. *Sun, Soil and Survival – An Introduction to Soils*, University of Oklahoma Press, Norman, OK.
- Bohn, H. L., B.L. McNeal, and G.A. O'Connor. 1985. *Soil Chemistry*. 2nd Ed. A Wiley-Interscience Publication, and John Wiley & Sons. New York, NY.
- Cornwell, D. A., and H. M. M. Koppers. 1990 *Slib, Schlamm, Sludge*. AWWARF and KIWA Ltd. Denver, CO.
- Cornwell, D. A., C. Vandermeiden, and G. Dillow. 1992. *Landfilling of Water Treatment Plant Coagulant Sludges*. AWWARF, Denver, CO.
- Das, B. M., 1994. *Principles of Geotechnical Engineering*. 3rd Ed., PWS Publishing Company Boston. MA.
- Elliott, H. A., Dempsey, B.A., Hamilton, D.W., and deWolfe, J.R.,. 1990. *Land Application of Water Treatment Sludges: Impacts and management*. Denver, CO.: AWWARF.
- Farrell, J. B., J. E. Smith Jr., R. B. Dean, E. Grossman, and O. L. Grant., 1970. Natural Freezing for Dewatering of Aluminum Hydroxide Sludges. *Jour. AWWA*, 62(12): 787-791.
- George, D.B., Berk, S.G., Adams, V. D., Morgan, E.L., Roberts, R.O., Holloway, C.A., Lott, R.C., Holt, L.K., Ting, R. S., and Welch, A. W., 1991. *Alum Sludge in the Aquatic Environment*. AWWARF. Denver, CO.
- Goldstein, J.I., 1994. *Scanning Electron Microscopy and X-Ray Microanalysis*. 2nd Ed. Plenum Press, New-York, NY.

- Huang, J. C. 1979. *Sludge Characterization and Dewatering*. Ph. D Dissertation. University of Missouri-Columbia, MS.
- Judkins Jr, J. F, and R. H. Wynne Jr., 1983. Crystal-Seed Conditioning of Lime-Softening Sludge. *Jour. AWWA*, 75(10):485-540.
- Knocke, W. R., and D. L Wakeland., 1983. Fundamental Characteristics of Water Treatment Plant Sludges. *Jour. AWWA*, 75(10): 516-524.
- Kohnke, H. 1968. *Soil Physics*, McGraw Hill, Inc., New York, NY.
- Lambe, T. W., and R.V. Whitman. 1969. *Soil Mechanics*. John Wiley & Sons, New York, NY
- Logsdon, G. S. and E. Edgerley Jr., 1971. Sludge Dewatering by Freezing, *Jour. AWWA*, 63(11): 734-740.
- Marshall C.E. 1964. *The Physical Chemistry and Mineralogy of Soils*, Vol. 1: Soil Materials John Wiley & Sons, Inc. NY.
- Mitchell, J. K. 1993. *Fundamentals of Soil Behavior*, John Wiley & Sons, Inc. New York, NY.
- Moore, D. M and Reynolds, R.C., 1996. *X-Ray Diffraction and the Identification and Analysis of Clay Minerals*, Oxford University Press, New York, NY.
- Novak, J. T., and D. C. Calkins., 1975. Sludge Dewatering and Its Physical Properties. *Jour. AWWA*, 67(2): 42-45.
- Oades, J.M., 1989. "An Introduction to Organic Matter in Mineral Soils", Chap 3. In: J.B. Dixon and S.B. Weed (Eds). *Minerals in Soil Environments*, 2nd ed., Soil Science Society of America Book Series: 1, Madison, WI, pp 252-273.
- Odell, R.T., Thornburn, T. H., and McKenzie, L. 1960. Relationships of Atterberg limits to some other properties of Illinois soils. Proceedings of the Soil Science Society of America Vol. 24, No 5, pp 297-300
- Raghu, D., and H. N. Hsieh. 1987a. Water Treatment Plant Sludge as Landfill Liner, In *ASCE-GT Special Conference - Geotechnical Practice for Waster Disposal*, ASCE, pp. 744-758. Ann Arbor, MI.
- Raghu, D., and H. N. Hsieh. 1987b. Material Properties of Water Treatment Plant Sludge, *The International Journal of Civil Engineering for Practicing and Design Engineers*, 5(5): 927-941.

- Raghu, D., and Hsieh. H.N., 1997. Criteria Development for Water Treatment Plant Residual Monofills *AWWA Research Foundation and American Water Works Association*, Denver, CO.
- Raghu, D., Hsieh. H.N., Basim. S.C., and Tian. P., 1995 Effects of Aging on the Properties of Water Treatment Plant Residuals. *Proceedings of WEF/AWWA Joint Residuals/Biosolids Conference* Kansas City MI.
- Schalsa, E.B., Gonzalez, C., Vergara, I., Galindo, G., and Schatz, A., 1965. "Effect of Drying on Volcanic Ash Soils in Chile", *Proceedings of the Soil Science Society of America*, 29, 481.
- Singh. A., 1975. *Soil Engineering in Theory and Practice* Vol. 1, Asia Publishing House New Delhi. India
- Sparks. D. L., 1995. *Environmental Soil Chemistry* Academic Press, New-York, NY
- USDA, 1951. Soil Survey Manual, Handbook 18,
- USEPA, 1986. *Handbook For Stabilization/Solidification of Hazardous Waste*. EPA/540/2-86/001. Government Printing Office, Washington, D.C.
- Van Schuylenborgh, J., 1954. The Effect of Air-drying Of Soil Samples UPON Some Physical Soil Properties, *Netherlands Journal of Agricultural Society*, 2,50,
- Vesilind, P. A. and C. J. Martel. 1990. Freezing of Water and Wastewater Sludges, *Jour. Environmental Engineering, ASCE*, 116: 854-862.
- Wang, M. C. and W. Tseng. 1993. Permeability Behavior of a Water Treatment Sludge. *Jour. Geotechnical Engineering*, 119(10): 1672-1677.
- Wang, M. C., J.Q. Hull, and M. Jao., 1992a. Stabilization of Water Treatment Plant Sludge for Possible Use as Embankment Material. *Transportation Research Record*, 1345: 36-43.
- Wang, M. C., J.Q. Hull, B.A. Dempsey, and D.A. Cornwall., 1992b. Engineering Behavior of Water Treatment Sludge. *Jour. Environmental Engineering*, 118(6): 848-864.
- Weil, Ray R., 1998. *Laboratory Manual for Introductory Soils*, Sixth Edition, Kendall Hunt Publishing Company. Dubuque, IA.

Wilum Z and Starzewski K., 1972. *Soil Mechanics in Foundation Engineering*, Vol.1, John Wiley & Sons, New York NY.

Xia 1993, *Geotechnical Characterization of Water Treatment Plant Residuals*. M.S Thesis submitted to the Faculty of Civil and Environmental Engineering. New Jersey Institute of Technology, Newark, NJ.
